European Polymer Journal 197 (2023) 112343

Contents lists available at ScienceDirect

European Polymer Journal

journal homepage: www.elsevier.com/locate/europolj

Vitrimer chemistry for 4D printing formulation

Amirhossein Enayati Gerdroodbar [a,b], Hura Alihemmati [a,b], Mahdi Bodaghi [c], Mehdi Salami-Kalajahi [a,b,*], Ali Zolfagharian [d,*]

[a] Faculty of Polymer Engineering, Sahand University of Technology, P.O. Box 51335-1996, Tabriz, Iran
[b] Institute of Polymeric Materials, Sahand University of Technology, P.O. Box 51335-1996, Tabriz, Iran
[c] Department of Engineering, School of Science and Technology, Nottingham Trent University, Nottingham NG11 8NS, UK
[d] School of Engineering, Deakin University, Geelong, Victoria 3216, Australia

ARTICLE INFO

Keywords:
Chemistry
Vitrimer
Sustainable
3D printing
4D printing

ABSTRACT

Vitrimerization is one of the new methods under development to convert polymer wastes into high-value compounds. The chemistry of vitrimers is such that the presence of dynamic chemical bonds changes the permanent covalent bonds into covalent adaptable networks, which are reversible. This allows for recycling and reprocessing of polymers by maintaining their initial properties after several cycles, which is included in the preparation of polymer resins to convert polymer waste into materials that can be formulated for three-dimensional (3D) printing resins. Four-dimensional (4D) printing has also been recently introduced as sustainable 3D printing of responsive polymers with dynamic applications, such as soft robotics, medicine, and medicals. Therefore, the synthesis of polymers with dynamic chemistry based on vitrimers can add unique properties such as shape memory, shape recovery, self-healing, and flexibility to the 3D printed products. Vitrimerization chemistry could contribute to polymer waste by producing 4D-printed resins. This article presents the vitrimerization chemistry used in different polymers to produce 4D printing resins with the mentioned capabilities and

Abbreviations: 2D, Two-dimensional; 3D, Three-dimensional; 3DPRTs, 3D printing capabilities; 3D-RSMP, Recyclable shape memory polymer; 4-AFD, 4-aminophenyl disulfide; 4D, Four-dimensional; ABS, Poly(acrylonitrile-butadiene-styrene); AELO, Acrylated linseed oil; AIBN, Azobisisobutyronitrile; AM, Acrylamide; AUD, Aliphatic urethane diacrylate; BA, n-butyl acrylate; BAPO, Phenylbis (2,4,6-trimethylbenzoyl) phosphine oxide; BiTEMPS, Bis (2,2,6,6- prepared tetramethylpiperindin-1-yl) disulfide; CANs, Covalent adaptable networks; CLPs, Cross-linked polymers; CNTs, Carbon nanotubes; DABA, 3,5-diaminobenzoic acid; DBTDL, Dibutyltin dilaurate; DCBs, Dynamic chemical bonds; DCC, N, N-methanetetraylbiscyclohexanamine; DCM, Dichloromethane; DETDA, Diethyltoluenediamine; DGBEA, Diglycidyl ether of bisphenol A; DIW, Direct ink writing; DLP, Digital light processing; DMA, Dynamic mechanical analysis; DMAP, 4-Dimethylaminopyridine; DMEP, Bis (2-methacryloyloxy ethyl) phosphate; DMF, Dimethylformamide; DSC, Differential scanning calorimetry; EBT, 2,2′- (ethylenedioxy) diethanethiol; EC, Ethylene carbonate; ED, Ethylenediamine; EDDET, 2,2-(ethylenedioxy) diethanethiol; EGBT, Ethylene glycol bisthioglycolate; EGDA, Ethylene glycol diacetate; EGMP, Ethylene glycol bis-mercaptopropionate; ELO, Epoxidized linseed oil; EoL, End-of-life; Epikure 3253, 2, 4, 6-tris-dimethylaminomethyl phenol; EtOAc, Ethyl acetate; FDM™, Fused deposition modeling (Fused filament fabrication); GDGDA, Glycerol 1,3-diglycerolate diacrylate; GHG, Greenhouse gases; GMA, Glycidyl methacrylate; Gt, Gigaton; HDI, Hexamethylene diisocyanate; HDPE, High density polyethylene; HEMA, Hydroxyethyl methacrylate; HPPA, 2-Hydroxy-2-phenoxypropyl acrylate; HQ, Hydroquinone; HTPB, Telechelic polybutadiene; IBOMA, Isobornyl methacrylate; IPN, Interpenetrating polymer network; IR, Infrared; Irgacure 819, Bis(2,4,6-trimethylbenzoyl)-phenylphosphineoxide; K_2CO_3, Potassium carbonate; LDPE, Low density polyethylene; MALs, Multifunctional lightweight architectures; MIS, 2-amino-4-hydroxy-6-methylpyrimidine; MMA, Methacrylic anhydride; MMA, Methyl methacrylate; MMt, Million metric tons; MV, Methacrylated vanillin; NMP, Nmethyl-2-pyrrolidone; NVP, N-vinyl-2-pyrrolidone; ODA, 4,4′- (diaiminodiphenyl ether; PCL, Polycaprolactone; PDMS, Poly(dimethylsiloxane); PET, Poly(ethylene terephthalate); PETMP, Pentaerythritol tetra (3- mercaptopropionate); PFSE, Print flexible smart electronics; PI, Polyimide; POE, Poly(oxime-ester); PP, Polypropylene; PS, Polystyrene; PSA, Poly (styrene-coallyl alcohol); PU, Polyurethane; PVC, Poly(vinyl chloride); SA, Suberic acid; SH, Self-healing; SLA, Stereolithography; SM, Shape memory; SMPI, Shape memory polyimide; TAOE, Tetraallyloxyethane; TATAT, Hexylamine, and 1,3,5-tri-2-propenyl-1,3,5-triazine-2,4,6(1H,3H,5H)-trione; TBAB, Tetrabutylammonium bromide; TBD, 1,5,7-triazabicyclo [4.4.0] dec-5-ene; TBD, Triazabicyclodecene; TBP, Tri-n-butylphosphine; T_g, Glass transition temperature; THF, Tetrahydrofuran; THFA, Tetrahydro-furfuryl acrylate; TMP_3MP, Trimethylolpropane tri(3-mercaptopropionate); TMPTA, Trimethylolpropane triacrylate; TPO, Diphenyl (2,4,6-trimethylbenzoyl) phosphine oxide; TPOL, Ethyl(2,4,6-trimethylbenzoyl) phenylphosphinate; TPP, Triphenylphosphine; T_v, Topology freezing transition temperature; Ultraviolet, UV; UPCL, Urethane-networked PCL; UP_y, Ureidopyrimidinone; UPy-NCO, Isocyanatohexylaminocarbonylamino)-6-methyl-4[1H]-pyrim-idinone; V, Vanillin; VAM, Volumetric additive manufacturing; Zinc acetate, Zn $(Ac)_2$; Zn(acac)2, Zinc acetylacetonate.

* Corresponding authors at: Faculty of Polymer Engineering, Sahand University of Technology, P.O. Box 51335-1996, Tabriz, Iran (M. Salami-Kalajahi). School of Engineering, Deakin University, Geelong, 3216, VIC, Australia (A. Zolfagharian).

E-mail addresses: m.salami@sut.ac.ir (M. Salami-Kalajahi), a.zolfagharian@deakin.edu.au (A. Zolfagharian).

https://doi.org/10.1016/j.eurpolymj.2023.112343
Received 26 June 2023; Received in revised form 25 July 2023; Accepted 31 July 2023
Available online 6 August 2023

lists their recipes for the preparation of formulations used in 4D printing so that the researchers can use them in a practical way to possibly achieve simultaneous shape-programmable, self-healing, and recyclable features in printed structures.

1. Introduction

Polymers are now an essential part of contemporary life. These materials are deemed practical because of their low density, light weight, high absorption to weight ratio, good chemical resistance, electrical insulation, thermal insulation, durability, and processability. Some of the frequently utilized polymers are Poly(ethylene terephthalate) (PET), low density polyethylene (LDPE), high density polyethylene (HDPE), Poly(vinyl chloride) (PVC), polypropylene (PP), polyurethane (PU), and polystyrene (PS) [1]. Without accounting for any carbon credits from recycling, the global life cycle greenhouse gas (GHG) emissions of plastics were estimated to be 1.8 gigaton (Gt) of CO2-equivalent in 2015. The resin production stage produced the most emissions (61%) followed by the conversion stage (30%) and the end-of-life (EoL) stage (9%). We generated over 7500 million metric tons (MMt) of plastic waste by the year 2020, and by the year 2050, that number is projected to climb to 26,000 MMt [1]. Only 9% to 12% of plastic waste is now recycled, and the remaining 79% ends up in landfills, rivers, and seas, having a negative impact on our ecology and environment (Fig. 1) [1]. As a result, it is now challenging to manage and dispose of plastic waste internationally. Because of this, one of the key answers to reducing polymer waste and creating a workable way to get rid of plastics is to recycle and reuse these plastic wastes [2,3]. Therefore, recycling procedures and the reuse of recycled materials in various applications are two of the most efficient ways to reduce the growth of polymer waste. Traditional recycling methods fall into two primary categories: mechanical (physical) and chemical processes [4]. The mechanical recycling method's own drawbacks include the loss of characteristics upon recycling and the method's inapplicability for thermostats and network polymers [5]. The recovery of characteristics and processability will once more be constrained in chemical recycling because of the presence of persistent and irreversible covalent bonds [5–7].

In comparison to conventional carbon–carbon and carbon–nitrogen bonds, dynamic covalent bonds (DCBs) [8–10] have a lower bond energy and are also reversible covalent bonds [11]. These sorts of bonds, which include imine, silicon-oxygen, boron-oxygen, and disulfide bonds, can be broken and recombined in response to stimuli like heat, UV radiation, and pH [12]. As a result, the addition of these kinds of links will transform polymer networks that currently contain permanent covalent bonds into dynamic networks known as covalent adaptive networks (CANs). It's interesting to observe that while CANs are stable at operating temperatures comparable to those of thermoset materials, under the influence of external stimuli, reversible exchange processes of dynamic covalent bonds alter the network topology, allowing the recycling or reprocessing of such materials [13,14]. CANs can be classified as either dissociative covalent adaptive networks or associative covalent adaptive networks, depending on the mechanism of reversible chemical bond exchange [15]. Similar to a polymer network depolymerization, the dissociative covalent adaptive mechanism includes breaking and re-forming bonds [15,16]. With the increase in temperature, the rate of failure has outrun the development of the whole covalent adaptive network, and since the equilibrium has been progressively declining with the increase in temperature, an inverse decomposition has occurred. Due to the enhanced mobility of the polymer and decreased density of the crosslinking site, the material can now be processed and molded [17]. The crosslink density of dissociative CANs increases as the temperature decreases and eventually reaches the same

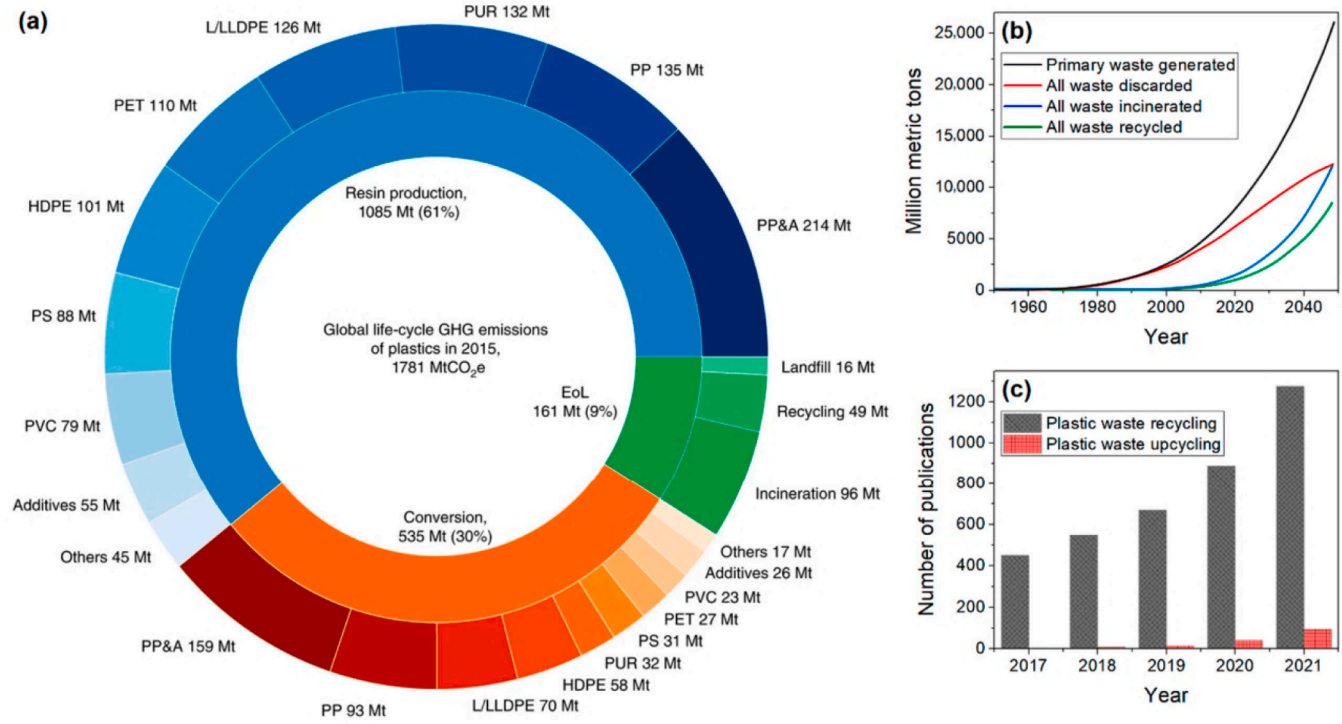

Fig. 1. (a) GHG Emissions of common plastics in the world, (b) Schematic of the production and disposal of plastic waste, (c) Image obtained from Web of Science data using the keywords "Plastic waste recycling" and "Plastic waste upcycling" (Reproduced from [1] under an open access Creative Commons license).

level as the initial condition, which results in the recovery of mechanical properties [14]. In contrast to dissociative CANs, associative CANs retain a constant crosslink density throughout the transition while simultaneously creating new bonds and rupturing old ones [14]. Leibler and colleagues identified this family of polymers in 2011 and gave them the name vitrimer, which translates to "glasslike polymer.".

The term vitrimer refers to a polymer with a dynamic cross-linked network that rapidly rearranges its topology at high temperatures, making the material fluid [18], malleable, and reprocessable (Fig. 2). In addition to high mechanical properties, these properties also induce chemical resistance, thermal stability, and plasticity, based on which polymers with reshaping, recyclability, high elasticity, shape memory, and shape recovery can be synthesized and processed. This concept is known as vitrimerization and has been used as a method that combines the properties of thermosets and thermoplastics to combine two methods of chemical and mechanical recycling.

In addition to the idea of vitrimerization, additive manufacturing (AM) has emerged in today's applications as a very effective and developing set of processes. Therefore, 3D printing, a specific technology within AM, allows for design flexibility, mass customization, waste reduction, and the production of complicated structures [19]. The process involves printing layers of materials that were successfully manufactured on top of one another. Other technologies have been introduced since then, such as stereolithography (SLA), powder bed fusion, fused deposition modeling (FDM™), inkjet printing, and contour crafting (CC) [19,20].

Numerous investigations have recently been conducted in this technology, with a focus on the creation of its tools and consumables. This method has been used in dentistry, civil engineering, transportation, electronics, decoration, jewelry production, and industrial moldings, to name a few. The use of 3D printing in the building industry has increased significantly. In less than a day, WinSun successfully mass-produced a set of moderately priced homes in China ($4800 USD each unit) [21]. Wohlers Associates predicted that one of the most significant uses of 3D printing will be in relation to personalized items, which is particularly apparent in medical applications. In this context, figures show that in 2020, 50% of 3D printing was concentrated on bespoke goods [22]. Medical professionals are interested in this method because it can be used to construct a variety of medical implants utilizing CT-imaged tissue replicas [23]. The idea of 3D printing evolved over time and was also applied to smart materials that react to stimuli; as a result of this study, a new method known as 4D printing [24] was introduced in 2013 [25]. A new design of a complex spontaneous structure that evolves over time as a result of interactions with the environment was given as the basis for the concept of 4D printing. 4D printing was first described using the formula "4D printing = 3D printing + time," which references to changes made to 3D printing through time [26–28]. To achieve self-assembly, deformation, and self-repair, it is an intentional evolution of a 3D-printed structure in terms of shape, organization, and purpose. The use of shape memory to achieve 4D materials has been practiced commonly. This is the reason that restoring the original shape can be important in various applications and has been investigated in several articles [29–32]. This property can be seen in polymers, ceramics, and alloys. However, the use of vitrimers and the prevailing chemistry in them has opened a new path for diversity in design. A summary of recent developments in vitrimers is also shown in Fig. 3a, which can be an introduction to the best possible preparation of printed parts with the characteristics of being given. As a result, the introduction of vitrimers to the world of 3D/4D printing may be one of the most interesting topics of the future.

The purpose of this review article is to connect the ideas of different vitrimerization chemistry and 3D/4D printing to create parts with unique features of simultaneous shape programming, self-healing, and recycling. As a result, a helpful and succinct taxonomy of the many types

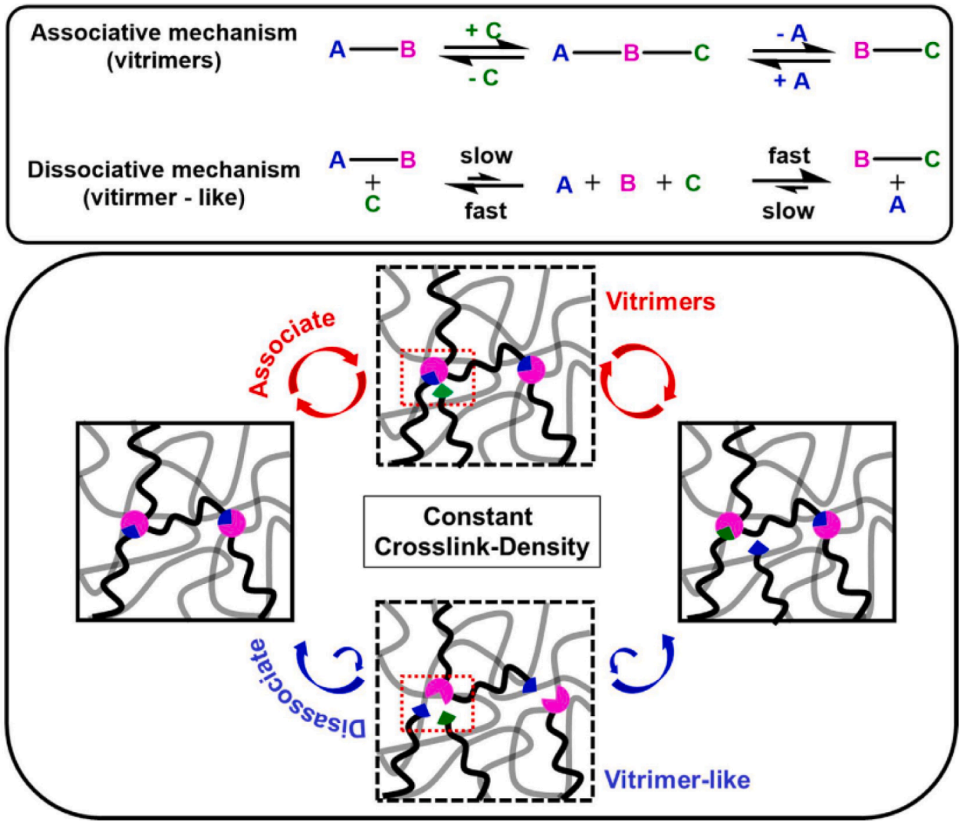

Fig. 2. Schematic of both dissociative covalent adaptive networks and associative covalent adaptive networks (Reproduced from [12] with permission from ELSEVIER).

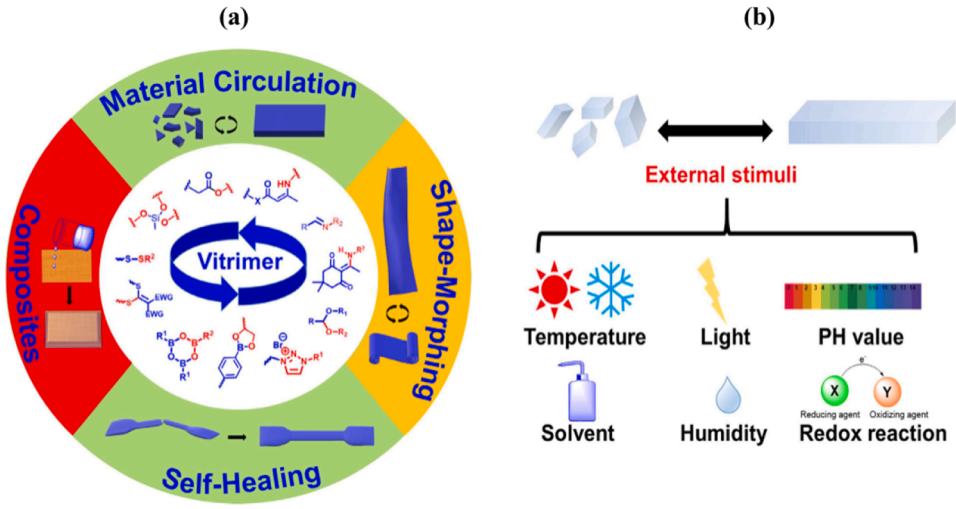

Fig. 3. (a) Recent virtimers common application, (b) Schematic of Stimuli for CANs (Reproduced from [12] with permission from ELSEVIER).

of vitrimerization chemistry has been provided at the beginning of the review paper. Then, related articles have recently undergone a thorough analysis. To accomplish 4D printing, formulations for 3D printing structures with shape-programmable, self-healing, and recyclable qualities have also been described, along with findings that demonstrate the resulting properties. After reading this article, it is intended that readers will have a fresh outlook on how thermoplastics, thermosets, and polymer elastomers should be reused, as well as a fresh approach to handling polymer waste to create products with higher added value. The primary goal of presenting these formulations was to enable 3D printing implementations of the formulations for usage in several future applications.

2. Dynamic covalent bonds and vitrimerization chemistry

2.1. Transition behavior

Two transition temperatures in vitrimers are crucial. The glass transition temperature (Tg), which is connected to the coordinated and extensive movements of the polymer segments, is the initial temperature. The polymer will transform from a rigid to a moldable condition once it reaches this temperature. The second is the topological freezing transition temperature (Tv), which is the temperature at which a substance undergoes a rapid bond exchange to transform from a viscoelastic solid to a viscoelastic liquid. The key distinction between these two temperatures is that the second temperature is chosen once the viscosity of 10^{12} (Pa.s) is attained [12], while the first temperature can be monitored using dynamic mechanical analysis (DMA) or differential scanning calorimetry (DSC). Another intriguing fact is that although being independent of one another, these two temperatures depend on the chemical structure as well. Since Tg is lower than Tv, the vitrimer typically changes from a rigid solid below Tg to an elastic solid between Tg and Tv to a viscoelastic liquid above Tv. On the other side, the Tv may occasionally be less than the Tg. Since there is no evidence of segmental motion or exchange responses in this range, unlike the previous range, the network can be thought of as stationary [33,34].

2.2. Stimuli response behavior

As said, applying an excimer will effectively give meaning to vitrimeric networks that feature excitable bands. This implies that the network will behave like a network with stable covalent bonds present at room temperature in the absence of stimulation. The repeated breaking and reformation of chemical bonds, as shown in Fig. 3b, provides the opportunity for movement between polymer chains and the reorganization of network topology, which ultimately leads to the shift in macrostructure when the correct stimulus is applied [12]. In this regard, it should be noted that the most prevalent stimulus is temperature, which might increase the frequency of reaction-inducing collisions. Newton also stated that temperature plays an important role in the balance of reactions, particularly in dissociative CANs. However, it should be emphasized that this activation temperature cannot go over a particular point because doing so may result in the destruction or breakdown of the polymer's backbone, which has unfavorable side effects. For this reason, many vitrimers have been activated at low temperature using a catalyst [12]. Besides this, light is also one of the most attractive stimuli in vitrimers, which are divided into three main categories [35–37]. The first class is the photo-induced cyclisation, such as [2 + 2] or [4 + 4] cycloadditions [38,39]. The incident light's wavelength can also control these processes because it tends to encourage cleavage and cycloadditions at various wavelengths [40]. The second group of these light reactions is referred to as photo reversible radical cleavages, and examples include allyl sulfides [41,42], disulfides [43], and dimethacrylates [44]. Finally, in more recent years, thioester-based thiol-ene elastomers have also been found to exhibit a third type of non-radical photo-cleavage in which ultraviolet (UV) irradiation in the presence of photo-bases promoted an anionic exchange [45,46]. In addition to these two stimuli, pH, which is a particular kind of catalyst, is one of the most alluring stimuli employed [47,48]. In addition to other crosslinks [49,50], pH has been shown to activate imines and acylhydrazone crosslinks. In this respect, it can be argued that imine production is accelerated at about pH = 4, and some of these activation methods have been used in drug delivery applications and hydrogels with self-healing properties.

2.3. CANs chemistry and vitrimer design

These compounds were previously mostly categorized as associative or dissociative by their response mechanisms in the last mini-review by Du Prez et al. (2016) [51]. Understanding their sort is essential to the production of vitrimers, but the problem is that this kind of link can contain a variety of chemistries [51]. Esters and related functional groups like carbamates, carbonates, and carbamides as well as acetals and imines exhibit the most common type of dynamic covalent exchange at a carbon-center. Thioethers and vinylogous urethanes both experience conjugate addition–elimination, a distinct type of exchange that is commonly observed. Transalkylation takes place at the nitrogen and sulfur centers of polyionic vitrimers, and heteroatom links are formed

and broken by cross-linkers like boronic esters, silyl ethers, and disulfide bonds [12].

2.3.1. Transesterification

An ester is swapped for an alcohol during the event known as transesterification. The study of Leibler and colleagues [18], which was done for a simple carboxylate, is one of the most significant cases. A catalyst made of zinc acetate [$Zn(Ac)_2$] has successfully controlled the transesterification process. Additionally, it has been demonstrated that the type, quantity, and application of a catalyst can influence certain characteristics, including the activation energy for bond exchange reactions as well as Tv and stress relaxation qualities [52,53]. Recently, catalyst-free vitrimers based on internal activation [54] have been discovered. Catalysts based on Lewis acids or potent organic bases have also recently been employed. 2019 saw the development of catalyst-free vitrimers by Du Prez based on phthalate monoester transesterification at 150 °C [55]. The nearby carboxylic acid group, which might attack the ester moiety to reversibly generate an activated phthalic anhydride, which is more vulnerable to attack by another alcohol, provided the mechanism for this internal catalyst. The oxime moiety and polyester were also combined to create poly(oxime-ester) (POE) [56], which can facilitate an oxime-transesterification exchange reaction without the requirement for a catalyst and with a simpler breakdown. The samples were illustrations of ester exchange in transesterification vitrimers that also investigated other stimuli like light and solvent. For example, light-activated vitrimers using carbon nanotubes (CNTs) [57] or gold nanospheres [58] in the polymer network are two of them. These nanoparticles could absorb light energy and convert it into heat through the photothermal effect, enabling localized healing of the vitrimers. In order to program two-dimensional (2D) flat epoxy-based vitrimer sheets into intricate 3D shapes at room temperature, Ji's team developed solvent-activated vitrimers [59]. Bio-based transesterification vitrimers have also garnered a lot of interest as a means of reducing reliance on non-renewable chemical feedstock. They consist of polylactide vitrimers [60], lignin derivative vitrimers [61,62], and poly-functional soybean oil epoxidized vitrimers [63–65]. According to the works of Hillmyer et al. [60] and their most recent work on networks with urethane links [66], carbamic acid esters were utilized in addition to the carboxylic ester bond to create dynamic bonds and transcarbomylation exchange reactions of vitrimers. The bond exchange between carbamide and urea falls within this group as well. An alternative functional component that can be utilized as a cross-linker is the urea moiety. According to Li et al. [67], free urea moieties were added to produce poly(urethane-urea).

2.3.2. Transacetalation and transimination

The key trades in this category include the exchanges of acetal and imide bonds. Meanwhile, subsequent efforts have employed acetal bond exchange as a method for the creation of intricate supramolecular structures [68,69]. Additionally, transacetalization and acetal metathesis are two mechanisms that can affect acetal exchange [12]. In the first instance, an acetal is said to be alcoholized when one of the free hydroxyl groups reacts with it. During this reaction, a certain portion of the acetal structure is chosen, and a new acetal is created as a result. However, it may be stated that the second mechanism merely involved an exchange reaction between two acetals and that alcohol was not present. Regarding this, Zhu et al. have created reshapable and recyclable polymer networks [70]. The number of free hydroxyl groups will have an impact on Tv and relaxation rate for these two mechanisms. Additionally, acetal-based polymer networks have demonstrated superior mechanical and recycling properties [12]. One of the most beneficial exchanges in this group is the Imine bond exchange, so to speak. It is pertinent for the preparation of polyimines with the ability to form dependent on water and ambient temperature when Zhang et al. process is used [71]. It is assumed that the imine/amine exchange was brought about by a little portion of the imine being hydrolyzed.

2.3.3. Exchange of conjugated systems

This class also includes exchanges such thiol ether conjugate addition-eliminations and ketoenamine bond exchanges. Transamination, in general, is a process in which an amino group is switched out for a ketoacid. It is also possible to study this reaction in vinylogous urethane vitrimers without the need for a non-reactive catalyst. However, the activation energy of the process can be significantly reduced by the presence of a catalyst, such as acid and alkaline base catalysts [12]. Du Prez used a non-catalytic method to exploit this mechanism [72]; additionally, vinylogous urethane (Vur-ethane) vitrimers were created by exchanging ketoenamines [72]; and finally, the usage of a conjugate and its removal were both researched [73]. Ishibashi and Kalow were able to create silicone vitrimers using thioetherification of Meldrum's acid alkylidene, which have properties like thio-functionalized PDMS [74,75], based on their discovery that Meldrum's acid derivatives can also form reversible covalent bonds with other nucleophilic agents.

2.3.4. Transalkylation

Different chemistries can also take place in this kind of exchange when salts are present. Typically, polyionic systems are where this kind of chemistry happens most frequently. This kind of exchange begins and concludes with a mutual anion and triazole nucleophilic attack on the alkyl halides, which results in attachment and detachment via dissociative exchange [12]. Transalkylation of N-centered salts is one sort of this exchange, and Drock-Enmuller was the person who first created this kind of ionic vitrimer. Poly(1,23-triazole) and a two-factor alkylating agent make up this network [76]. Guo et al. reported networks consisting of instances of C-N transalkylation of pyridinium salt in addition to this [77]. Sulfonium salts can be employed in bond exchange reaction design in a similar way to the earlier salts, with the reversibility of these systems having already been established by Goethals et al. [12]. Additionally, Vitrimeric networks of poly(thioether) networks and sulfide-sulfonium salts were made and studied without the need of a catalyst in recent research by Du Prez et al. [78]. Additionally, their molecular analyses have demonstrated that the SN_2-type reaction between sulfonium salts and thioether nucleophiles provides the basis for the exchange mechanism in this vitrimer [78]. Furthermore, according to the findings of Du Prez et al. and Zhang et al.'s studies, cross-linked rubbers with sulfur can be recycled by adding trimethyl-sulfonium iodide (TMSI) [79].

2.3.5. Heteroatom bond exchange

This category includes exchanges such the silyl ether (Si-O) exchange, disulfide (S-S) bond exchange, and boronic ester (B-O) exchange [12]. Guan and colleagues' use of boronic ester metathesis in solid state polymers has produced reversible cross-linked networks for the first time [80]. The chemistry of bis-dioxaborolane was used in this study to network polycyclooctene, which has 20% 1,2-diol groups. Additionally, small molecular studies on this chemistry have shown that the type of cross-linker and cross-linker using bis-dioxaborolane can be designed to adjust the speed of dynamic transesterification because the nitrogen atom in the area is five times faster in exchange than the atom of oxygen has been [12,80]. Additionally, Leibler et al. used dioxaborolane cross-linkers in typical polymers to create vitrimers without catalysis. [81] It was applied. Additionally, Guan et al. [82] have explored the creation of boroxines, which can engage in B-O exchange processes, as a result of the dehydration of boronic acids. The ability to recover monomers from these compounds by boiling them in water in addition to their pure processing has allowed for the further creation of N-coordinated boroxine vitrimer networks, including imine-coordinated boroxines [83,84]. Besides, Si-O bonds, like the previous hetero atom, are crucial to the chemistry of vitrimers. Guan exploited this kind of link when creating silyl ether exchange-based vitrimers [34]. Additionally, a procedure intended to generate vitrimers by direct silyl ether metathesis has been documented [85]. In addition to his studies, Lu has created vitrimers with the highest glass transition temperature recorded in vitrimers

to date by employing the silyl ether motif [86]. Disulfide bonds and the self-healing vitrimeric structures they produce are another type that plays a significant role in this group [12]. According to the research findings, self-healing characteristics of vitrimeric networks with aromatic disulfide bonds generally follow radical-mediated processes rather than metathesis [87]. The results of spectroscopic investigations carried out by Nevejans support this dynamic chemistry. As a result, it has been claimed that aromatic disulfide exchange employs a spontaneous process, with sulfur-containing radicals being transported after the disulfide link has been homolytically destroyed [88]. Additionally, in the case of disulfide dynamic chemistry, it can be added that the mechanism of thiolate anions will also be activated by adding nucleophilic substances as a catalyst, such as triethylamine or tri-n-butylphosphine (TBP), in which case the exchange reaction of both radical-mediated and thiol-mediated exchange reaction will follow. The main thing to note here is that using compounds with a more powerful bidentate nucleus will aid in the thiolate anion mechanism's ability to dominate by producing more and more potent anions of this kind [88]. Additionally, utilizing the typical and affordable 4-aminophenyl disulfide (4-AFD) crosslinker and this aromatic disulfide chemistry, Odriozola et al. [89] created vitrimers based on diglycidyl ether of bisphenol A (DGEBA) and diethyltoluenediamine (DETDA). Since it is also feasible to employ non-aromatic disulfur compounds in vitrimers, Yan et al. created an inverse vulcanized sulfur-polymer network that could be molded and reprocessed using the same chemistry [90]. By fusing two heterogeneous cross-linked polymers (CLPs) in different mixing ratios and using bis (2,2,6,6-prepared tetramethylpiperindin-1-yl)disulfide (BiTEMPS) as a crosslinker, Tsuruoka et al. were also able to produce vitrimers with the ability to precisely adjust mechanical properties and self-healing [91]. Dynamic metathesis, which involves the reversible light-driven exchange of disulfides and diselenides (Se-Se) to create Se-S bonds, is also crucial for controlling the composition of the mixture of light-sensitive vitrimers at various wavelengths [92]. Having introduced these dynamic covalent bonds, for a deeper understanding of the type of exchange reaction, a general schematic has been drawn and classified in Table 1.

Table 1
A general schematic of CANs and BERs in vitrimers (Reproduced from [12] with permission from ELSEVIER).

Dynamic bond	Schematic of exchange reaction
Ester	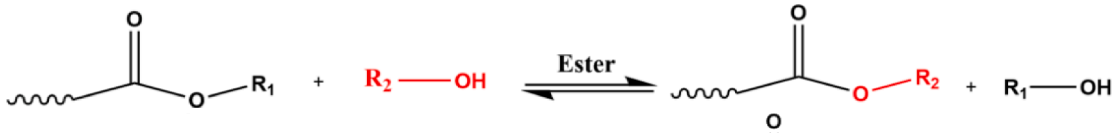
Carbamate	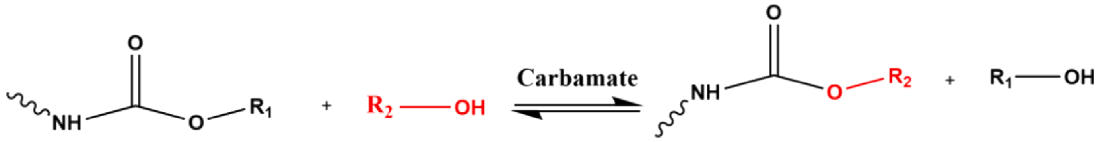
Carbonate	
Acetal	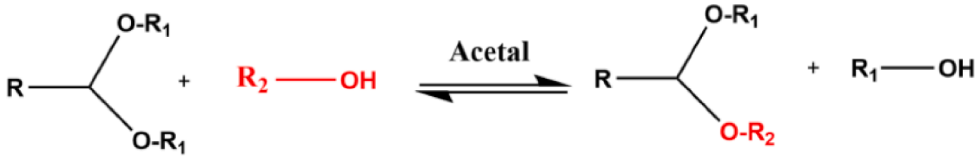
Imine	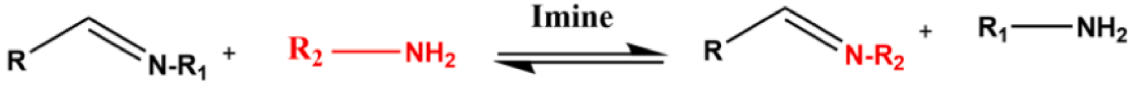
Vinylogous Urethane	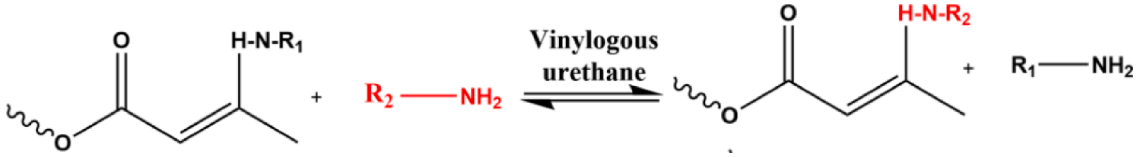
Thioether	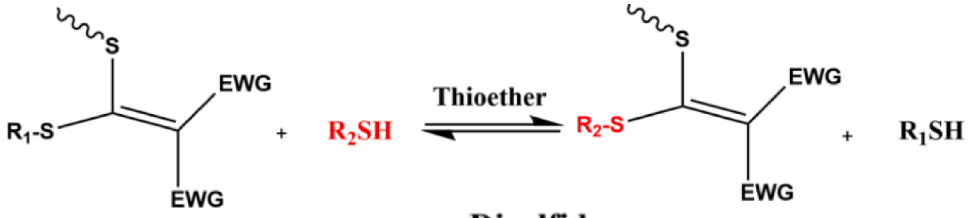
Disulfide	
Silyl ether	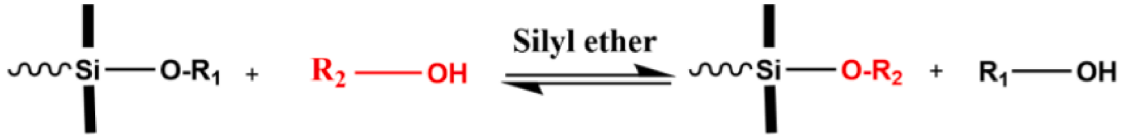

3. Vitrimers chemistry in advanced 3D/4D printing formulation

It is possible to enter the formulation for 4D printing from two perspectives. According to the desired qualities, various polymerization and modification techniques will be used in the first approach to synthesis all materials, including monomers, polymers, multifunctional crosslinkers, and other materials. The intended remolding will next be completed by combining exact proportions of the synthesized components with additional required materials. In the second viewpoint, these materials are bought already manufactured, and there are no recent developments regarding polymer synthesis or various functionalization techniques. We'll delve deeper into these two areas for various polymer classifications.

3.1. Synthesized-based formulation

3.1.1. Acrylate and methacrylate-based vitrimer

Due to their good mechanical strength, adequate solvent resistance, and ease of fabrication, printed thermostats have been evaluated for numerous technical applications [93]. However, the presence of permanent transverse connections and their non-recyclability has grown to be a concerning issue [94]. As a result, creating an acrylate vitrimeric network would be a good option for printing thermostats that can be recycled and reused [93]. However, the problem with these vitrimers is that they can reduce mechanical characteristics, a problem that could previously be fixed by adding fillers [95–97]. However, using these particles increases viscosity, which has the unfavorable effect of decreasing UV light penetration depth during printing [98–100]. This is because of significant shrinkage and dimensional instability. Therefore, the inclusion of hydrogen bonds in the structure of the resin formulation is one of the suggested environmental solutions to address the decline in the mechanical properties of printable acrylate vitrimers [101–103]. Additionally, the presence of hydrogen bonds won't prevent bond exchange reactions from occurring in vitrimer for reprocessability and recycling because this bond vanishes with an increase in process temperature and reappears when the temperature is reduced, which increases the mechanical properties of the printed part [104,105]. In order to execute exchange reactions, we will first combine hydrogen bonding with the utilization of hydroxyl esters that are present in the acrylate vitrimeric network. According to Fig. 4, first, glycidyl methacrylate (GMA) and suberic acid (SA), two monomers, were combined to create a diacrylate prepolymer for this purpose. With regard to this prepolymer, it can be argued that engineering the end functional groups is the only way to easily produce cross-linked vitrimers. Since the hydroxy ester structure has been introduced to this prepolymer or oligomer, there is no longer any restriction on the creation of vitrimer, which will be produced by the reaction between epoxy and carboxyl groups. The second phase involves creating a 3D printing formulation made of vitrimeric diacrylate and acrylamide (AM) prepolymer, which will be used to create the hypothetical thermostat using UV light radiation. Finally, this formulation's dynamic ester exchange reactions between esters and hydroxyl groups, won't stop even after heating, which will result in the

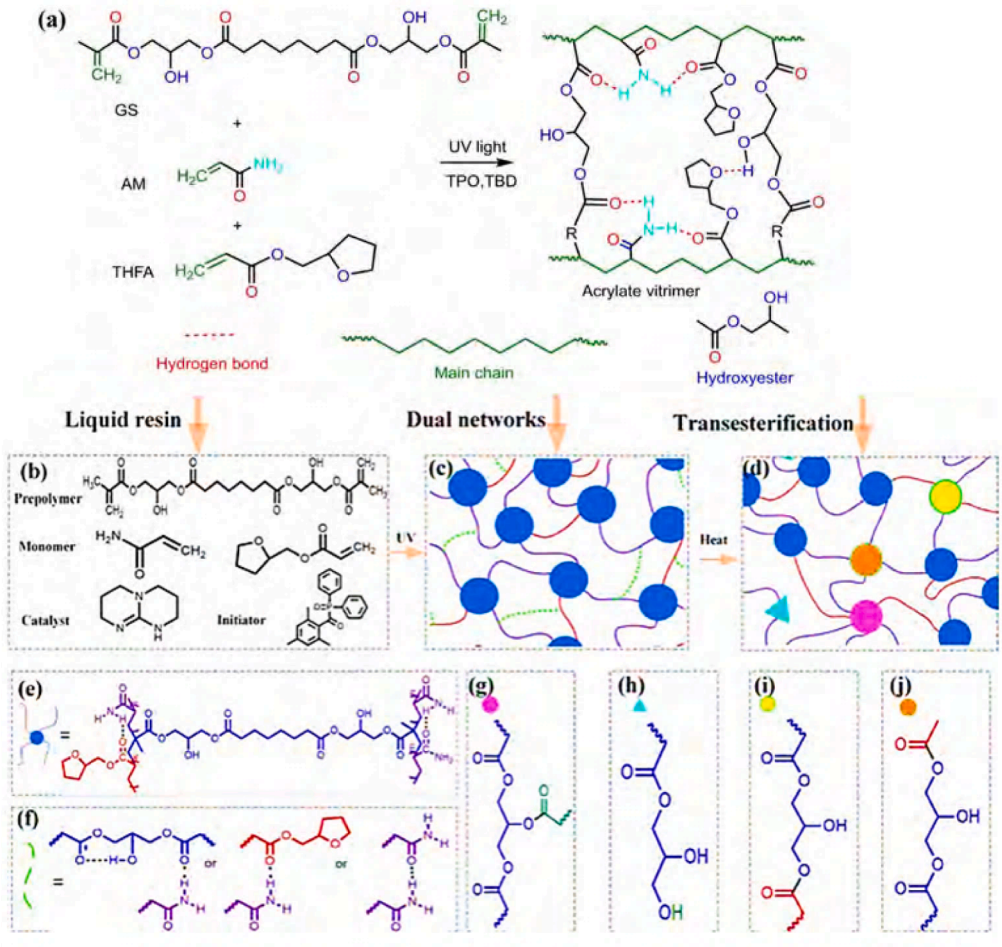

Fig. 4. (a) Acrylate vitrimer preparation, (b) Reactants chemical structure, (c,d) Photo crosslinked network (blue dots) and hydrogen bonds (green dotted line) and recombination of dynamic covalent bonds (purple,yellow, orange, and green dots), (e,f) Dual cross-linked networks structure, (g-j) CANs after heating (Reproduced from [93] with permission from American Chemical Society).

reprocessing of printed thermostats, in which as the temperature rises, the hydrogen bonds that are already present are broken and the printed piece retains its vitrimeric ability [93].

The reagents required for the synthesis of vitrimeric diacrylate prepolymer and the preparation of resin formulations with the ability to be reprocessed and recycled are: Glycidyl methacrylate (GMA), suberic acid (SA), tetrabutylammonium bromide (TBAB) as a catalyst, 1,5,7-triazabicyclo[4.4.0]dec-5-ene (TBD), tetrahydro-furfuryl acrylate (THFA), acrylamide (AM), ethylene glycol (EG), and diphenyl (2,4,6-trimethylbenzoyl) phosphine oxide (TPO) as a photoinitiator. Initial attempts at creating acrylate prepolymer (GS) involved the reaction of stoichiometric quantities of GMA and SSA. In order to do this, a three-necked balloon was filled with 28.43 g of GMA monomer, 17.42 g of SA monomer, and TBAB catalyst (at a rate of one percent by weight of the total weight of the two monomers). The mixture was then agitated for three hours at 105 °C. The reaction's output, which is an acrylate prepolymer, was washed three to five times with deionized water before the product was separated using a funnel in order to remove the catalyst from it. Finally, deionized water was removed by 24 h of freeze-drying in a freeze dryer. Now, to make the photocurable resin formulation, GS and THFA were put into a beaker and thoroughly mixed while being agitated at room temperature. Next, monomer AM was added as a hydrogen bonding agent, and the temperature was raised to 70° C. Rapid mixing was taking place. Also, 60% of the formulation's weight is made up of total monomers (GS, AM, and THFA), and the remaining 40% is made up of AM, THFA, and TBD (5 mol% to the "COO" groups). After thoroughly mixing the entire mixture, one percent of it by weight was added to the photoinitiator to finish off the formulation. The mixture was then held under vacuum at room temperature for around 30 min to produce a resin that was bubble-free. The prepared resin was poured into a 75 mm × 5 mm × 2 mm mold and degassed for half an hour. Then, cross-linked acrylate vitrimers (GS-xAM) were prepared by irradiating for two minutes with an ultraviolet mercury lamp with an intensity of 20 mW/cm^2. Finally, a desktop-grade SLA high-precision printer with a precision of 0.025 mm/layer was used for 3D printing [93]. Examining the test data revealed that the average tensile strength and Young's modulus increased by 4.4 and 3.85 times, respectively, and reached 40.1 and 871 MPa when 20% by weight of AM was added to the formulation. Additionally, diverse shapes were printed and could be remolded after being dissolved in ethylene glycol [93] (Fig. 5).

3.1.2. Vanillin-based vitrimer

As we move on to 3D printing resins with chemical/mechanical recycling and self-healing capabilities, we will continue our previous section's work [106]. For this reason, photocurable polymers with functional groups for vinyl and ethylenediamine that are coupled with a vanillin block have been proposed. This section's introduction explains how the imine can promote reprocessability and self-healing. In addition to all, the resin itself will become 3D-printable due to the existence of vinyl bonds. According to the chemistry of this resin, these imine interactions are produced by the Schiff-base reaction between the ethylene diamine's amino group and the aldehyde function of vanillin. They are also produced by the combination of a short aliphatic part that is produced by the reaction of vanillin with the ethylene carbonate that results [106]. Vanillin (V), ethylene carbonate (EC), potassium carbonate (K_2CO_3), methacrylic anhydride (MAA) as a methacrylate agent, ethylenediamine (ED), sodium sulfate, and phenylbis (2,4,6-trimethylbenzoyl) phosphine oxide (BAPO) as a photoinitiator are the main materials used to synthesize precursors and prepare 3D printing resin [106]. Extended vanillin (ExtV) has first been created synthetically. In order to achieve this, a solution made up of 10 g of vanillin (V), 6.38 g of ethylene carbonate, and 11 g of potassium carbonate should be transferred to a 250 ml round-bottomed three-necked flask along with 100 ml of DMF. Additionally, it should be noted that the reaction mixture needs to be stirred under reflux at 110 °C under a nitrogen environment. The reaction mixture must be cooled to room temperature and diluted in 150 ml of distilled water in order to cleanse the end result. After that, 150 ml of ethyl acetate (EtOAc) was added. The organic phase is then dried using sodium sulfate, concentrated under decreased pressure, and then dried once more in a vacuum oven at 60 °C for 12 h to produce a white powder. Methacrylated extended vanillin (M−ExtV) should then be synthesized in the second stage and added to the methacrylated vanillin (MV). In order to do this, 10.13 g of vanillin, 11.30 g of MAA, and 0.056 g of DMAP were introduced to a flask with a magnetic stirrer and reacted for 24 h at 60 °C in a nitrogen atmosphere. The output of the reaction was diluted with 150 ml of dichloromethane (DCM) and washed with saturated aqueous solution of sodium bicarbonate and 0.5 M sodium hydroxide. Again, the eluate phase was dried over sodium sulfate and dried for 2 days at 30∘C under vacuum until powder [107,108]. Therefore, M−ExtV was also synthesized in a similar way and for this purpose, 5 g of ExtV together with 4.29 g of MMA and 0.019 DMAP in a round-bottomed flask under nitrogen under reflux at 60 °C for They were stirred for 24 h. After washing the reaction product as in the prior process, a pale-yellow powder was produced. In addition to the aforementioned precursors, two Schiff-base resins with the names SB1 and SB2 were also created utilizing MV and M−ExtV combined with ED. In order to do this, 50 ml of DCM was mixed with 0.41 g of ED and 3.60 g of M−ExtV before being agitated at room temperature for five hours. Finally, white powder SB2 and yellow powder SB1 were created through synthesis. Two thermoset photocurable synthetic materials with self-healing capabilities based on Schiff chemistry, designated X-SB1 and X-SB2, were created from SB1 and SB2 in DCM at a concentration of 70%

Fig. 5. Printed vitrimeric samples (Reproduced from [93] with permission from American Chemical Society).

w/v. Then, 10% by weight of BAPO photoinitiator was added to the mixture after combining Kama resins with DCM, and the mixture was agitated for 30 min. A UV curing lamp with 36 W intensity (385 nm wavelength) was used to photopolymerize the mixture containing the photoinitiator for 10 min to cure it. To let the DCM solvent drain, the produced films were left at room temperature for three days.

Examining the test results reveals that the glass transition temperature for printed parts is relatively high, at roughly 75 °C. Additionally, good thermal stability has been discovered, with the degradation's initiation temperature rising above 300 °C. The most significant outcome of developing this vitrimeric network, however, is the resin with self-healing capabilities, reprocessing and flexibility, mechanical and chemical recycling that their paths showed in Fig. 6(a-g), despite the imine linkages, as mentioned. The malleability property is further confirmed by looking at the shape memory results of printed vitrimeric thermostats. Also, the results showed that X-SB2 resin got its first shape after ten seconds. It can be added that, heating the resin over the glass transition temperature, which started transimination, can give it a temporary shape. Finally, it was demonstrated that this resin could be used to make parts utilizing the digital light processing (DLP) technique [106].

Glycerol has also been utilized to create vitrimeric based on vanillin-glycerol UV cure resin as part of the inquiry into thermostats and vanillin compounds. The important finding in this work is that the entire vitrimer synthesis method is an environmentally friendly method that is produced by combining monomers in different ratios with a photoinitiator and a transesterification catalyst without the use of solvents [109]. Here, the monofunctional monomer 2-Hydroxy-2-phenoxypropyl acrylate (HPPA) is selected for the synthesis of vitrimer by transesterification reactions. Another very interesting point is that the use of this monomer due to the presence of glycerol (main component of triglycerides) in its structure can help in the preparation of degradable oleic acid vitrimers [110–112]. Also in the project, the cross-linker 2-Hydroxy-3-[[4-[2-hydroxy-3-[(2-methyl-1-oxo-2-propen-1-yl) oxy] propoxy]-3 -methoxyphenyl] methoxy] propyl 2-methyl-2-propenoate (DGEVA dimetha crylate, DGEVADMA) has been used due to the presence of hydroxyl and ester functional groups, which has been reported for the first time in UV curing resins [109]. Because of its high swelling and heat stability due to the presence of vanillin fragments, this crosslinker is noteworthy in terms of interaction chemistry and can be a very excellent substitute for cross-linkers with bisphenol A fragment [113]. The antibacterial and antifungal capabilities of vinyl-based polymers [114] and V DGEVA dimethacrylate can also give UV cure resin [115] shape memory and antimicrobial qualities are additional features that make this crosslinker appealing.

The reagents used for the preparation of 3D printing Vitrimer formulation are reported in the text above and it should only be mentioned that in order to obtain a transparent piece and due to its optical properties, Ethyl(2,4,6-trimethylbenzoyl) phenylphosphinate (TPOL) is used as photoinitiator (Fig. 7a). To prepare the UV cure resin, at first, the catalyst of the transesterification bond exchange reaction, i.e., zinc acetate ($Zn(acac)_2$) was dissolved in HPPA at a temperature of 70 °C at a rate of 5 mol%. After cooling, different amounts of DGEVADMA and 3 mol % of TPOL were added and stirred at room temperature until complete mixing. For resin curing, the mixture was poured into teflon molds and cured by 500 W Helios Italquartz GR.E UV lamp at a wavelength of 250–450 nm and intensity of 310 mW·cm-2 for 2 min. Now, the 3D printing process was done using DLP technique and Phrozen Sonic Mini 4 K 3D printer (desktop LCD/LED, Hsinchu, Taiwan)

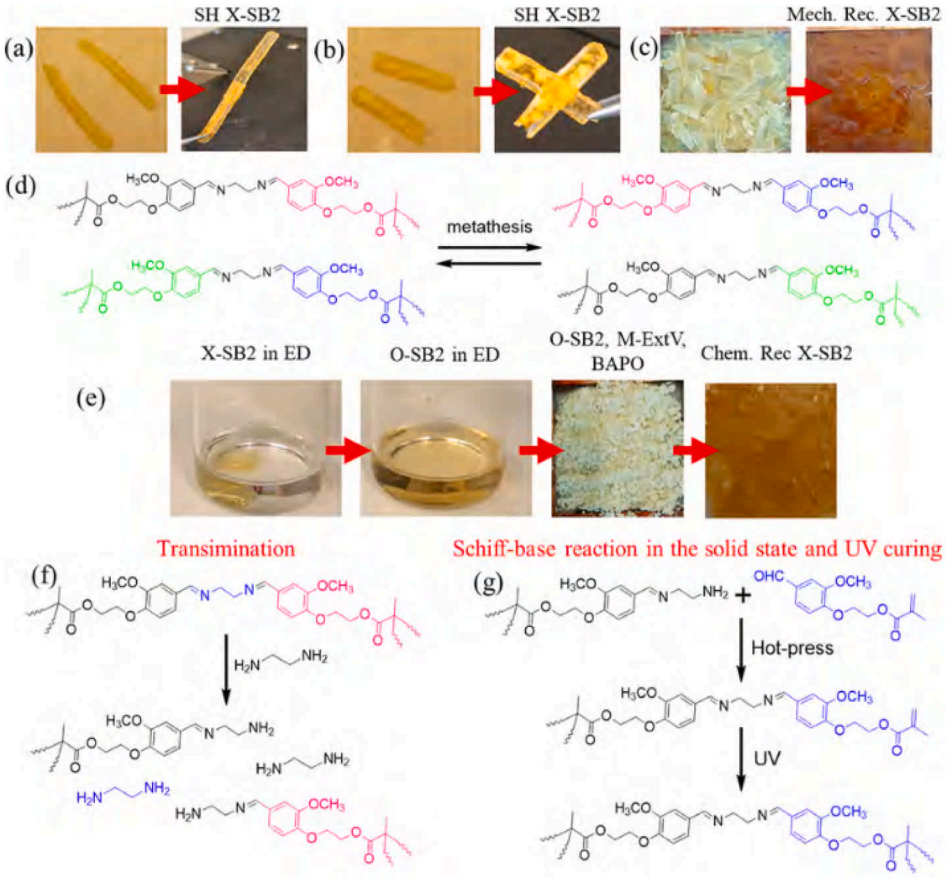

Fig. 6. (a,b) Printed sample after the self-healing, (c) Mechanical recycled of X-SB2 with hot-press, (d) Schematic of metathesis pathway leading to the self-healing and mechanical recyclability of X-SB, (e) Chemical recycling of X-SB2 in ED, (f) Mechanism of transimination pathway leading to the solubilization of X-SB2 in ED, (g) Proposed reactions during the hot-press and UV curing [106] (Reproduced from [106] under an open access Creative Commons license).

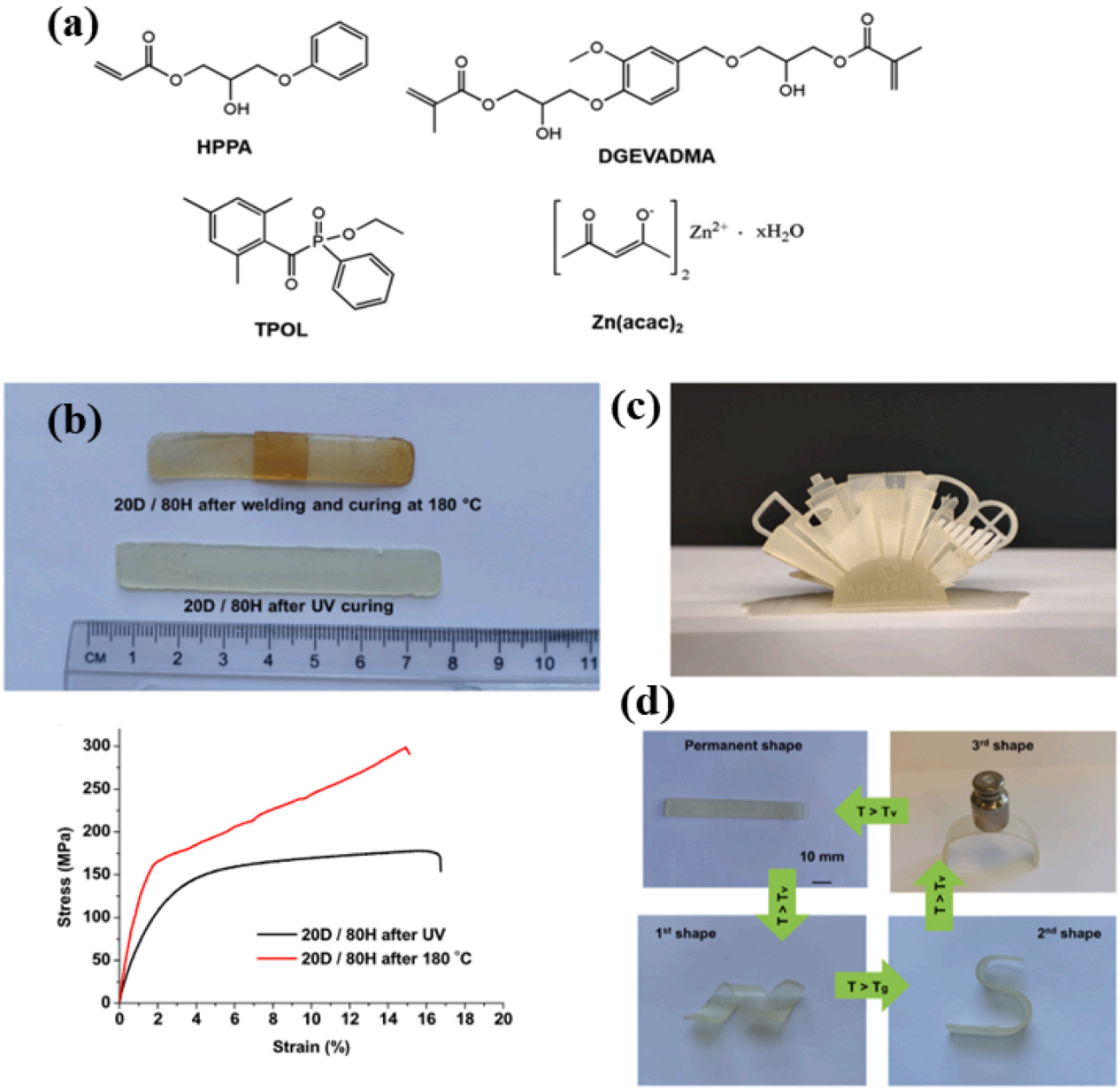

Fig. 7. (a) Chemical structure of used materials, (b) Self-healing test of 3D printed vitrimer, (c) DLP printed vitrimer, (d) Shape memory analysis of 3D oriented vitrimer (Reproduced from [109] under an open access Creative Commons license).

at a wavelength of 405 nm and a substrate curing time of 12 s, which is used to check accuracy and quality. Print, the structure of "City" and to check the shape memory properties, a rectangle is printed [109].

Examining the results of vitrimer with a weight ratio of 8:2 of glycerol- and vanillin-based monomers (20D/80H) indicates a high welding efficiency of 114.12% for tensile strength and a recovery rate of 75% after alkalization in addition to shape memory properties in high temperature furnaces Glass and bottom transitions are achieved. To check the self-healing properties of this printed vitrimer, sample cutting and rejoining at 180 °C for 1 h have been used. The results of this test for the repaired specimen showed a higher Young's modulus and tensile strength than the sample, which confirms the self-healing property of these printed parts (Fig. 7b). To analyze this property, it can be said that the mentioned transesterification reactions exist in this system, and the remaining carboxyl groups due to the lack of complete curing will cause the intensity of these exchange reactions to increase at higher temperatures due to the presence of hydroxyl and carboxyl groups. Also, to prove the ability of this prepared resin in DLP printing, the structure of "City" was used, which is sufficiently detailed (Fig. 7c). The smoothness of the surface after printing and the success in printing details have been a sign of the quality of the synthetic resin. By heating the printed sample up to Tg or Tv, it was shown that a temporary shape was created and fixed by applying an external force. After reheating, the permanent shape is obtained, which is due to the presence of free hydroxyl groups in the chemical structure, which can make the synthetic structure flexible and induce shape memory properties (Fig. 7d). These structures can be used in the construction of artificial muscles and actuators due to these reversible properties [109].

3.1.3. Acrylate-cyanate-based vitrimer

A lot of research has been focused on this area so far so that polymer networks with this property can be created with various solutions

[116–118]. In addition to all these refined properties added to the printed parts using vitrimers, the preparation of reconfigurable polymer networks is also of interest, and the reconfigurable property is one of the most important properties in the design of 4D printable parts [119–121]. Utilizing photothermal dual-curing resin to create a network of two orthogonal polymerization mechanisms has been suggested as one approach for the creation of such components [119,120]. Among these approaches, three-dimensional parts made from acrylate-cyanate resin might be considered [119]. Utilizing active groups, such as hydroxyl groups, on the side chains or the main chains is another method for generating these networks [122]. In this case, the printed component will develop an extra cross network because of a transesterification reaction between the hydroxyl and ester functional groups upon heating [119]. The resin formulation that is used to create the 3D printed item using the DLP process will be shown in this section. After heat treatment, the ester reaction amidation is used to create the aforementioned networks [123]. The main monomers and other materials used in the synthesis and formulation of the 3D printing resin used are Ethylene glycol bisthioglycolate (EGBT), Tetraallyloxyethane (TAOE), 2,2′- (ethylenedioxy)diethanethiol (EBT), Pentaerythritol tetra (3- mercaptopropionate) (PETMP), and the photoinitiator bis(2,4,6-trimethylbenzoyl)-phenylphosphineoxide (Irgacure 819). Ethylene glycol diacetate (EGDA), hexylamine, and 1,3,5-tri-2-propenyl-1,3,5-triazine-2,4,6 (1H,3H,5H)-trione (TATAT) are also used. At the beginning of the work, hexylamine and ethylene glycol diacetate (EGDA) reacted stoichiometrically at 140 °C. To prepare the precursor of the 3D printing resin formulation, a mixture called TE1 with molar ratios of 5:7:3 of the three monomers was prepared from the mixture of three acrylate and thiol monomers TAOE, EGBT, and EBT. Then TE2 mixture was obtained by adding TATAT and PETMP with a molar ratio of 4:3, and finally TE3 was obtained from a mixture of TATAT and EGBT with a molar ratio of 2:3. In this final mixture, 3% by weight of Irgacure 819 along with 0.03% of Sudan III was added as a photoabsorber and the mixture was stirred in a dark environment until complete homogenization (Fig. 8a). In the following, a printer with a commercial projector (DELL 1609WX) with a lamp intensity of 10 mW/cm^2 was used for the 3D printing process. Also, exposure time and the replenishment time for each layer of the print are 5 and 8 s, respectively. Finally, a UV box with an intensity of 955 mW/cm^2 and a wavelength of 265–700 nm was used for 60 s.

The usage of post-thermal treatment because of the amidation of ester's presence can vary and adjust the properties as needed [123], which is one of the intriguing results of these adjustable networks. This idea has been put into practice to the point where a rigid printed part can be transformed into a liquid with low viscosity since the modulus of this network created utilizing amidation of ester has been reduced by 50 times [123]. To put it another way, this can be used as a novel tactic to distinguish between the printing process and the finished properties. It may be concluded from further examination of the findings that the

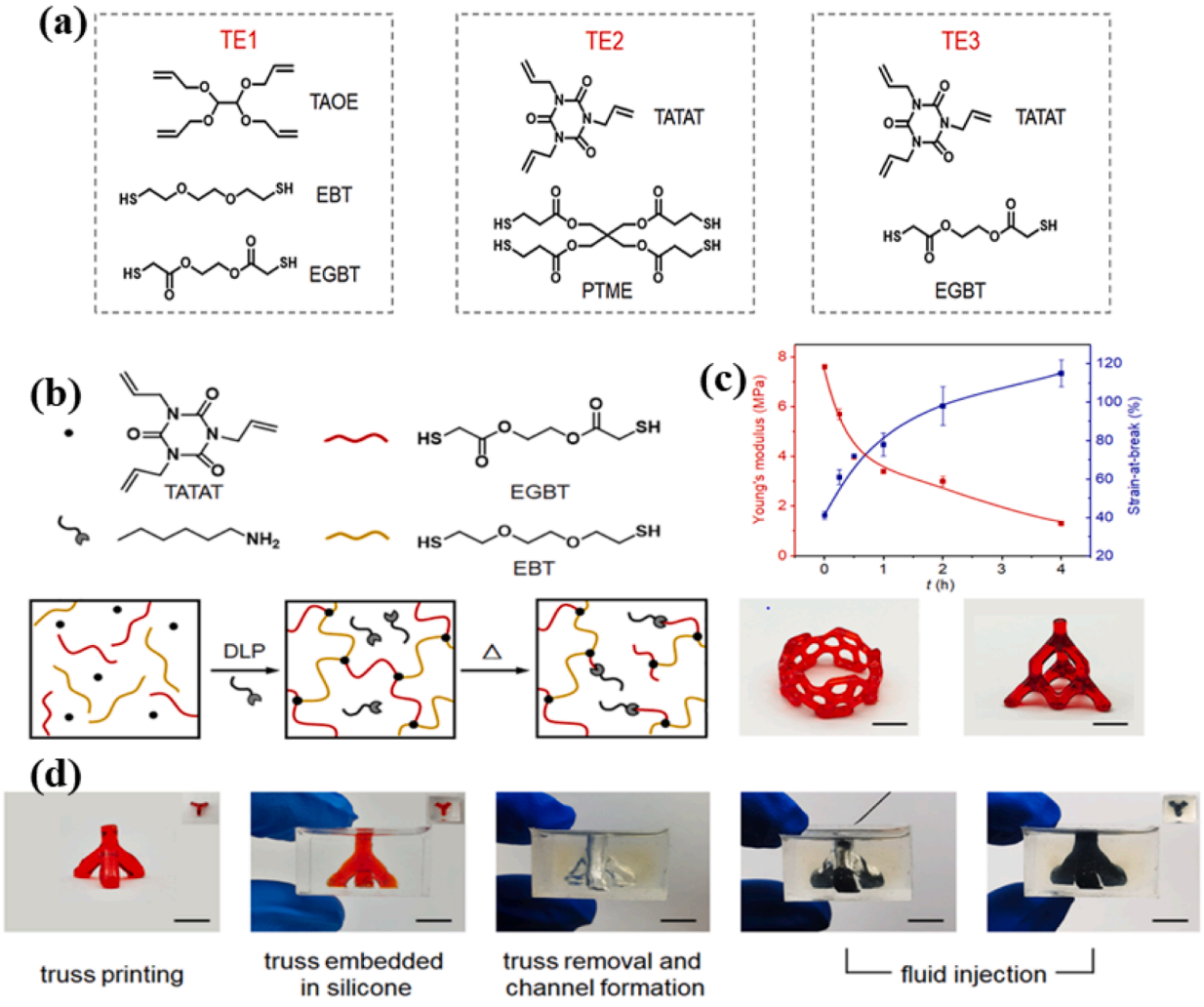

Fig. 8. (a) Chemical structure of monomers used DLP printing, (b) Schematic of reconfiguration mechanism and 3D printing results, (c) Results of mechanical evaluation of printed samples, (d) TE3 application in microfluidic device (Reproduced from [123] with permission from American Chemical Society).

chemistry in the formulation that has been provided is a result of a photoinduced thiol-ene click reaction [123]. Following, the amine component will be introduced to the structure, and as a result of heating, the ester bonds will be attacked, allowing the ester bond and amine reaction to be largely controlled in order to regulate the density of connections [121,125]. The advantage of employing thiol-ene chemistry over the photoinitiated acrylate system is that it will result in the formation of steric connections between the primary chains of the polymer network, altering its overall structure and allowing for network rearrangement [126,127]. Another interesting feature of this system based on thiol-ene (VTE) photochemistry is that the density of the ester bond may be altered and regulated by varying the proportion of the two thiols utilized. Additionally, it may be inferred from Fig. 8b that VTE50% and VTE100% transform into liquids, but other samples appear to remain intact. The amidation process also took place during the post-treatment, as shown by Fig. 8c, which resulted in a reduction in the density of the connections. As a result, the modulus decreased, and the strain-at-break increased [123]. Fabricated 3D channels (Fig. 8d) for microfluidics have been listed as one of this synthetic resin's purported appealing applications. By eliminating the amine under a nitrogen environment and utilizing non-printable Poly(dimethylsiloxane) (PDMS) at 140 °C (much below the temperature at which PDMS degrades), the truss is made here using the TE3 formula [123].

3.1.4. Linseed-based vitrimer

Research related to the field of recycling polymers, vitrimers and the using them in the process of 3D printing has been developed to the point that today plant derivatives such as vegetable oils, rosin, or carbohydrates are considered as bio monomers [128–130]. Meanwhile, the use of vegetable oils has made them an attractive choice due to their unsaturated triglyceride structures, easy availability, biodegradability, and bio-friendliness [131–133]. The point is that to use these monomers in the process of 3D printing or photocuring resins, existing unsaturated bonds can be converted into epoxy groups during the oxidation reaction, and finally, by using compounds such as carboxylic acid, acrylate monomers are opened as a result Synthesized epoxy ring [134–136]. Using acrylate systems and free radical photopolymerization in these monomers can create heterogeneous networks, low conversion percentage and low toughness [137,138]. In addition to this problem, the introduction of thiols is not only a positive step for hand weaving to a uniform network, but it will also improve the mechanical properties and toughness of the entire reed network. But it should be noted that at high concentrations of thiol, the curing mechanism changes from a chain growth to a step growth reaction, which is called thiol-click chemistry [139,140]. In this part, we will examine one of the resins prepared with this chemistry with vitrimeric properties. For this purpose, acrylated linseed oil (AELO) has been used in the project, and the resulting network will have dynamic hydroxyl ester bonds. Also, to activate chemical transesterification and achieve properties such as healing and shaping memory at high temperature in printed vitrimers, organic phosphate ester has been used as a catalyst [141].

Epoxidized linseed oil, acrylic acid, phenyl bis(2,4,6-trimethylbenzoyl) phosphine oxide (BAPO) photoinitiator, bis (2-methacryloyloxy ethyl) phosphate (DMEP) as the catalyst, and ethylene glycol bis-mercaptopropionate (EGMP) are among the monomers and other consumables [141]. Epoxidized linseed oil (ELO), 0.33 g of butylated hydroxytoluene, and 23.076 g of acrylic acid have been added to a three-necked flask as an acrylate agent in the first step of the production of acrylated linseed oil (AELO). After mixing for 20 min at 60 °C, 8.12 g of triphenylphosphine was used as a catalyst to substitute acrylate groups in place of epoxy. After mixing for a further hour at 60 °C, 22.055 g of acrylic acid were added, and the combination was then left to mix at that temperature for the remainder of the night. The completed mask was cooled, then the excess acrylic acid was washed out three times in saturated sodium bicarbonate solution and once in salt water. The mask was then dissolved in ethyl acetate. A yellow liquid has been extracted as the primary product after drying the eluate phase over sodium sulfate and removing the solvent. As an exchange reaction paper, 70 wt% of AELO has now been blended with 2 wt% BAPO and 8 wt% DMEP for 30 min at 40 °C until completely homogenized. Sudan II, a photoabsorber, has also been added to the aforesaid formulation in the amount of 0.05 wt% in order to prevent excessive polymerization and guarantee resolution throughout the 3D printing process. Also,20 wt% of the two chosen thiols were added and mixed in a dark area after cooling and thorough mixing. The resin containing TMP_3MP is separated with the code AELO-TMP_3MP, while the formulation including the thiol crosslinker EGMP is isolated with the code AELO-EGMP. Anycubic Photon Zero, a DLP printer with a wavelength of 405 nm and a layer thickness of 50 μm, was chosen [141].

From the results of this thiol-acrylate dynamic network, we can mention the 3D printing of structures with a size of 550 μm with a high baking speed. As shown in Fig. 9 a,b, a comb-like structure consisting of holes of different sizes has been designed and printed to demonstrate the DLP printing capability of synthetic vitrimers, and it has been shown that it is possible to print holes with a size of 250 μm with resolution. Also, due to the dynamic nature of the printed networks, it shows triple shape memory, and this ability is created in them to control these changes and the ability of macroscopic deformation during heating [141]. Fig. 9 c shows that upon heating up to Tv by applying an external force, the permanent shape of the flower printed by the DLP process, thermally annealed, can be seen. This illustrates the potential use of these thiol acrylate networks in actuator, biomedical, and soft robotics applications by showing that the reported time to regain the first temporary shape is 30 s [141]. Fig. 9 d, in which rectangular bar-shaped samples with and without defects were printed, and the printed disc was positioned in the defect area, also illustrates the self-healing capabilities of these networks. Fig. 9 d, which depicts the mechanical results of the repaired sample, indicates that the mechanical properties of the damaged sample have improved after repair. The results of the tests indicate repair and welding for 4 h at a temperature of 180 °C. Additionally, this network was able to relax 63% of its initial tension at 180 °C for 22 min thanks to the presence of dynamic linkages, and following thermal annealing, it showed increased durability [141].

3.1.5. Polyurea-poly(dimethylsiloxane)-based vitrimer

Along with all these examined cases, should note that elastomeric vitrimer have been attended. So, in a case, polyurea elastic vitrimer was also synthesized and studied [142]. In the continuation of this part, we will examine these synthetic vitrimeric networks in more detail. To prepare the final resin, three synthesis steps were used includes: PDMS-based linear elastomer, a carbonyl cross-linker, and a polyurea vitrimer, which is shown in Fig. 10 a-c [142]. For the synthesis of PDMS-based linear elastomer, 30 g of aminopropyl terminated Poly(dimethylsiloxane) polymer with a molecular weight of 3000 g/mol was added in 140 ml of tetrahydrofuran (THF) solvent. Then, 1.25 g of 4,4′-methylenebis (phenyl isocyanate) monomer was slowly added to the mixture under nitrogen atmosphere. The mixture was allowed to react for 24 h at room temperature and then the solvent was removed under vacuum to obtain the final product [142]. Also, for the synthesis of carbonyl cross-linker, 2-(methacryloyloxy)ethyl acetoacetate monomer was first purified by a column to remove the inhibitor. Then, the amount of 10.71 g of the purified monomer was dissolved with 410.5 mg of the thermal initiator azobis-(isobutyronitrile) in 50 ml of anhydrous dimethylformamide solvent in a flask, and after half an hour, it was purged with nitrogen at 68 °C for 24 h was reacted. Finally, after purification and removal of the solvent, a viscous yellowish liquid has been extracted as the main product [142]. After these two syntheses, 15.6 g of PDMS-based linear elastomer synthetic polymer along with 803.3 mg of carbonyl cross-linker were added to THF to prepare polyurea vitrimer. After 15 nitrogen purges, the reaction continued for one night at 30 °C and finally, the final product was prepared by removing the solvent [142]. Also, for the 3D printing process, FDM™ printing process was performed using a

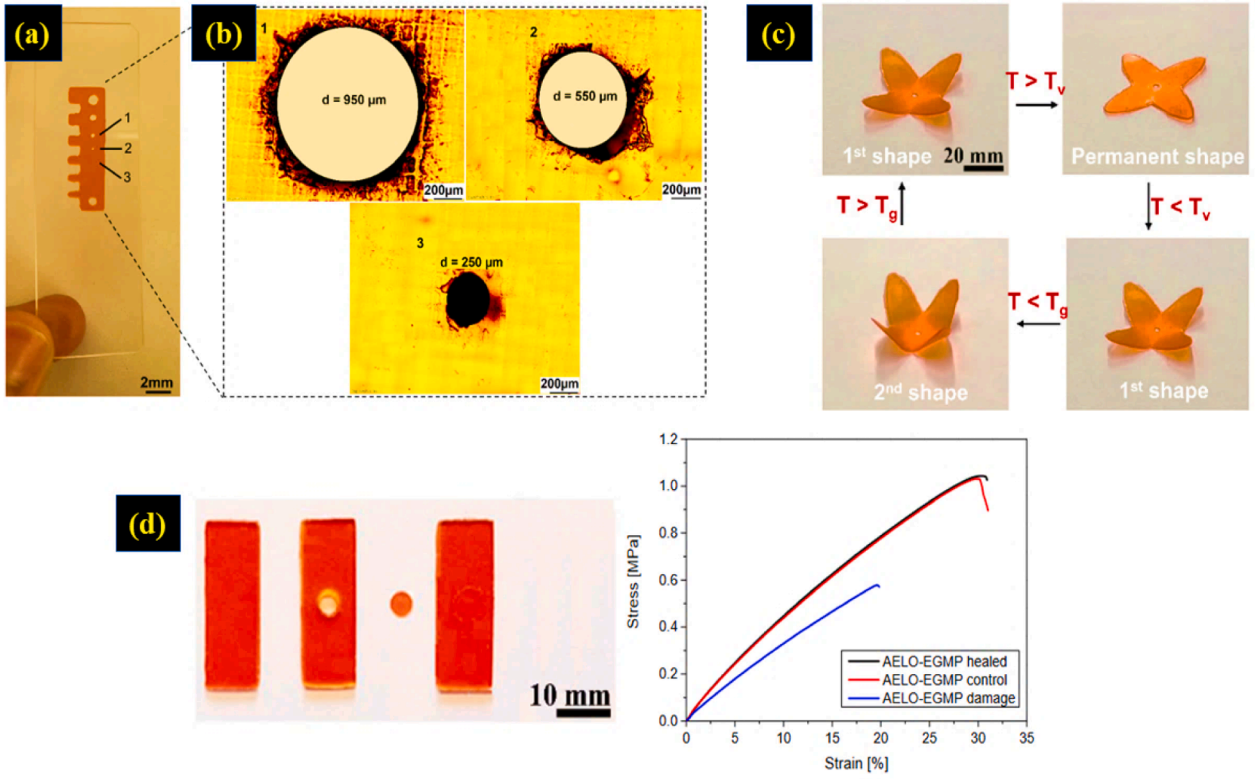

Fig. 9. (a,b) DLP-printed comb-like structure and cavity microscopic inspection designed to achieve maximum resolution, (c) Analysis of triple shape memory of flower DLP 3D-printed, (d) DLP Printed rectangular bar with defect and without defect and mechanical results for healing analysis (Reproduced from [141] under an open access Creative Commons license).

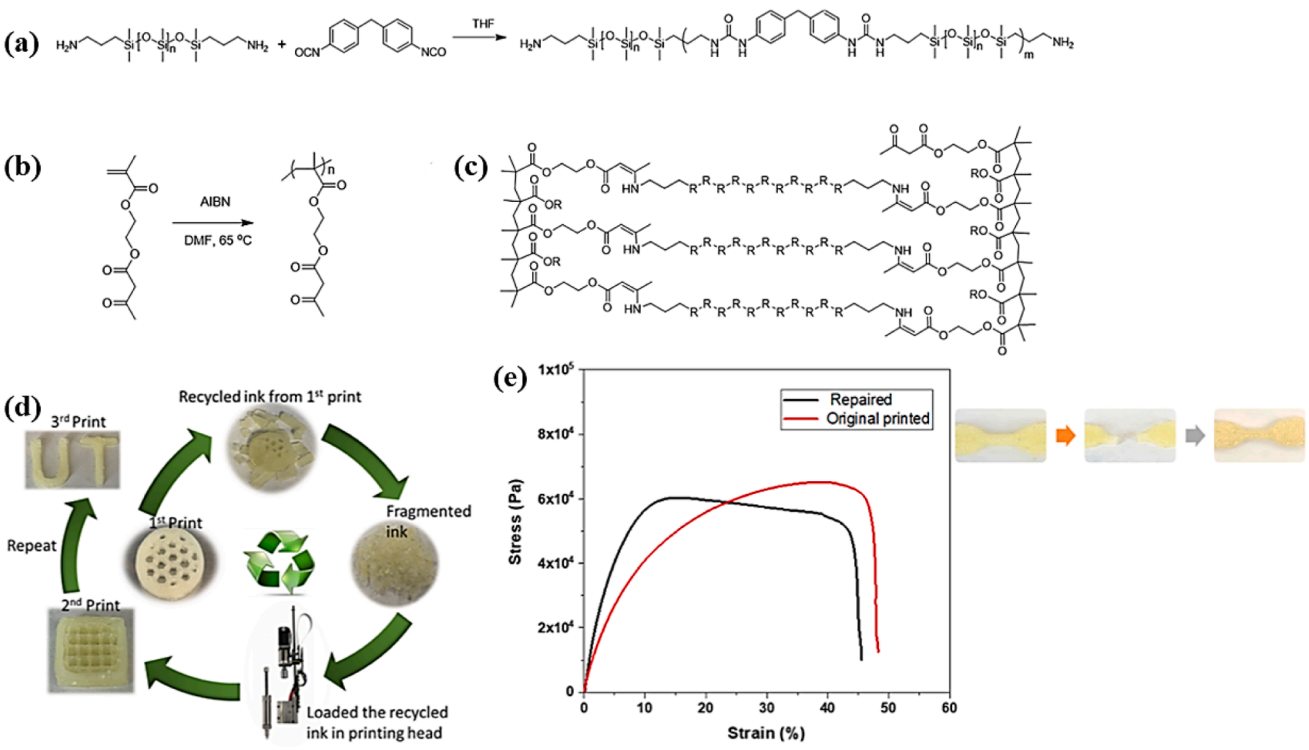

Fig. 10. (a) PDMS-based linear elastomer synthesis path, (b) Carbonyl cross-linker synthesis path, (c) Polyurea vitrimer synthesis path, (d) Printability and recyclability of Polyurea vitrimer, (e) Repairing of Polyurea vitrimer and mechanical analysis of healed sample (Reproduced from [142] with permission from American Chemical Society).

Hyrel Engine SR 3D printer. Regarding the printing conditions, it can be said that the first layer was printed at a speed of 8 mm/s and the other layers after this layer were printed at a speed of 12 mm/s [142].

As mentioned briefly at the beginning, vinylogous urethane cross-links have been used to prepare this elastomeric vitrimer [142]. In this case, it should be said that this type of cross-link chemistry has been used recently and it has been shown that the bond exchange reaction is possible with the rapid addition and removal of terminal free amino groups [72,143]. From the results obtained about this type of chemistry used, it can be said that compared to transesterification exchange reactions, they have better thermal and chemical stability and are less sensitive to decomposition such as hydrolysis [72,144]. Based on Fig. 10d, it can be said that the resins prepared from synthetic vitrimers have recyclability and printability. Also, this result should be mentioned that these resins have maintained this ability up to three times and after that they suffered from a decrease in mechanical properties [142]. This drop in mechanical properties can be related to side reactions at high temperature during the reprocessing process. In addition to this crown, we can also mention the properties of Repairability, which can be clearly seen in Fig. 10e. The interesting thing is that the results of the mechanical tests showed that the Young's modulus was 1.14 MPa for the repaired sample and 0.9 MPa for the original sample, which is a significant increase. This increase in Young's modulus can be ascribed to the additional heating processes during the repairing steps, such as longer annealing time in an oven [142].

3.1.6. Polybutadiene-based vitrimer

During the analyzed study, we also go into Volumetric Additive Manufacturing (VAM) and Vitrimers. This method has a high speed and can quickly change a photopolymer liquid into a polymer solid [145]. This approach was first introduced by Wang et al. [146] and is intended for quick AM in any setting. The hydrogen bond appears to be dynamic in this section after research on vitrimers containing ureidopyrimidinone (UPy) was conducted. As a result, the unique network can experience self-healing and shape memory when UPy groups are present in the polymer's structure [147–149]. This polymer chemistry will be dynamic because the quadruple hydrogen bonding of UPy results in the production of a flexible structure [150,151], which is broken and reformed by the solvent's temperature and results in the formation of vitrimer [152,153]. Additionally, telechelic polybutadiene (HTPB) contains unsaturated bonds that can form cross-linked networks, it is sensitive to radical photopolymerization. Additionally, HTPB with UPy functionality is one of the UV-curable vitrimers that can crosslink at room temperature and is appropriate for 3D printing. This network can feature dynamic chemistry in addition to the permanent link because of the chemistry produced from UPy [154]. As a result, telechelic HTPB that has been functionalized with UPy has been used in this study [154]. The coupling of 2(6-isocyanatohexylaminocarbonylamino)-6-methyl-4 [1H]-pyrim-idinone (UPy-NCO) monomer with hydroxy-functionalized polybutadiene (HTPB) has been exploited in this way for the synthesis of UPy-HTPB-UPy [154]. Polybutadiene (HTPB), dibutyltin dilaurate (DBTDL), hexamethylene diisocyanate (HDI), and 2-amino-4-hydroxy-6-methylpyrimidine (MIS) are monomers as well as other essential components of this synthesis [154].

A first stage of synthesis was required to create this resin, which involved creating isocyanato-terminated pyrimidone (UPy-NCO), UPy-HTPB-Upy, and C-UPy-HTPB-UPy. It is sufficient to transfer 4.48 g of MIS together with HDI to a three-necked flask and agitate it at 100C for 24 h while under a nitrogen environment in the first phase to create UPy-NCO. After cooling, all that is needed to dry under vacuum for one day at 50 °C is to make a white precipitate by washing it eight or nine times with petroleum ether [154]. We'll now go on to the UPy-HTPB-Upy synthesis. For this, 50 ml of chloroform and 0.781 g of Upy-NCO and 3 g of HTPB were weighed, added, and then two drops of DBTDL catalyst were added and heated to 60 °C for 16 h. After 16 h of the process, 200 ml of chloroform were combined with 5 g of 200–300 mesh silica gel to dilute the mixture [154]. The silica gel was then removed using suction filtering, yielding a clear, viscous liquid. After extracting some of this solvent, a tiny amount of methanol was then added, resulting in a milky white, sticky precipitate. After repeating this procedure multiple times, the transparent elastomer was finally dried for a day in that vacuum. However, 0.5 g of the earlier product was added to chloroform in the last phase of the synthesis of C-UPy-HTPB-UPy in various weight ratios (2% to 5%) of photoinitiator (DMPA), and the required rosette was produced. The mixture was molded in Teflon containers, and then the piece was cured by exposing it to 25 W of 365 nm UV radiation (Fig. 11a) [154]. One of the most obvious outcomes of this study is that even without the addition of a photoinitiator and cross-linking, UPy-HTPB-UPy synthesis has demonstrated good promise for 3D printing procedures (Fig. 11 b,c). Due to the initiator and unsaturated links present, these polymers are vitrimers prior to the development of these transverse connections and can also be printed using the FDM™ method [154]. However, research has indicated that the creation of long-lasting connections close to the vitrimeric network can improve the printed object's stickiness and mechanical strength. Since UPy-HTPB-UPy is soluble in chloroform due to the existence of hydrogen bonds, it is a good resin for direct ink writing (DIW). Similar to Bell's argument, the UV radiation used in the DIW method boosted the strength between the layers by creating cross-linking. Additionally, the heating-responsive shape memory effect of two flowers printed with two distinct formulations in the amount of initiator is good (Fig. 11 b,c) [154].

3.1.7. Polycaprolactone-based vitrimer

As another case study, we investigated the vitrimeric resin for 3D/4D printing based on polycaprolactone vitrimer (PCL) [155]. Until now, this polymer is known as one of the materials used in FDM™ printing technique [156,157]. In general, for the formation of this vitrimer, PCL with the end hydroxyl group (PCL-diol) is covalently linked with poly (hexamethylene diisocyanate) (PHMDI) using zinc acetylacetonate (Zn $(acac)_2$) catalyst. This process produced urethane-networked PCL (UPCL), which can enhance the mechanical and shape memory capabilities of thermoplastic PCL. The network is then modified to become a U-PCL-based vitrimer (U-PCL vitrimer) by adding a low-molecular-weight poly (styrene-coallyl alcohol) (PSA) as a dynamic crosslinker to react with PCL's ester functionalities via transesterification at a high temperature. Due to its ability to prevent chain length fragmentation during the network marketing process, this polymer has been used to improve network connections. It has also been observed in other studies that can be related to the use of small molecules with three hydroxyl groups, such as glycerol [158]. Preserving the crystallinity of PCL polymer is another objective of this design [155].

These monomers and other components, which can be listed as follows, were employed to create this vitrimer: zinc acetylacetonate hydrate (Zn(acac)2), with a molecular weight of 1200 g/mol, PCL-diol with a molecular weight of 2000 g/mol, commercial PCL filament, and PHMDI with NCO concentration of 22.6–23.7% [155]. We shall deal with the synthesis of the U-PCL Network in the first step. Ua-PCLs were the name given to poly(-caprolactone) networks constructed of urethane, where "a" represented the molar ratio of [NCO] to [OH] [155]. According to the conventional procedure for U1.7-PCL synthesis, a 20 ml scintillation vial was filled with 2.5 g (1.25 mmol) PCL, 0.118 g (0.448 mmol) Zn(acac), and 5 ml THF. Then, after stirring the mixture for an hour at 25 °C, 0.791 g (1.453 mmol) of PHMDI diluted in mL THF was gradually added to form the U-PCL network. By placing the completed product in a vacuum oven at 60 °C for two hours, THF was removed [155]. We shall now discuss the synthesis of U-PCL Vitrimer in the second stage. The U1.7-PCL-PSAb vitrimer was named after the molar ratio of PSA's hydroxyl groups to the total moles of ester groups from PCL and PSA, and "b" stood for the molar ratio of PCL and PSA's ester groups. The molar ratio of [NCO]/[OH] for the initial UPCL network preparation was set at 1.7. In reference to the total molar content of Zn $(acac)_2$ molecules and ester linkages in PCL, it should be noted that the

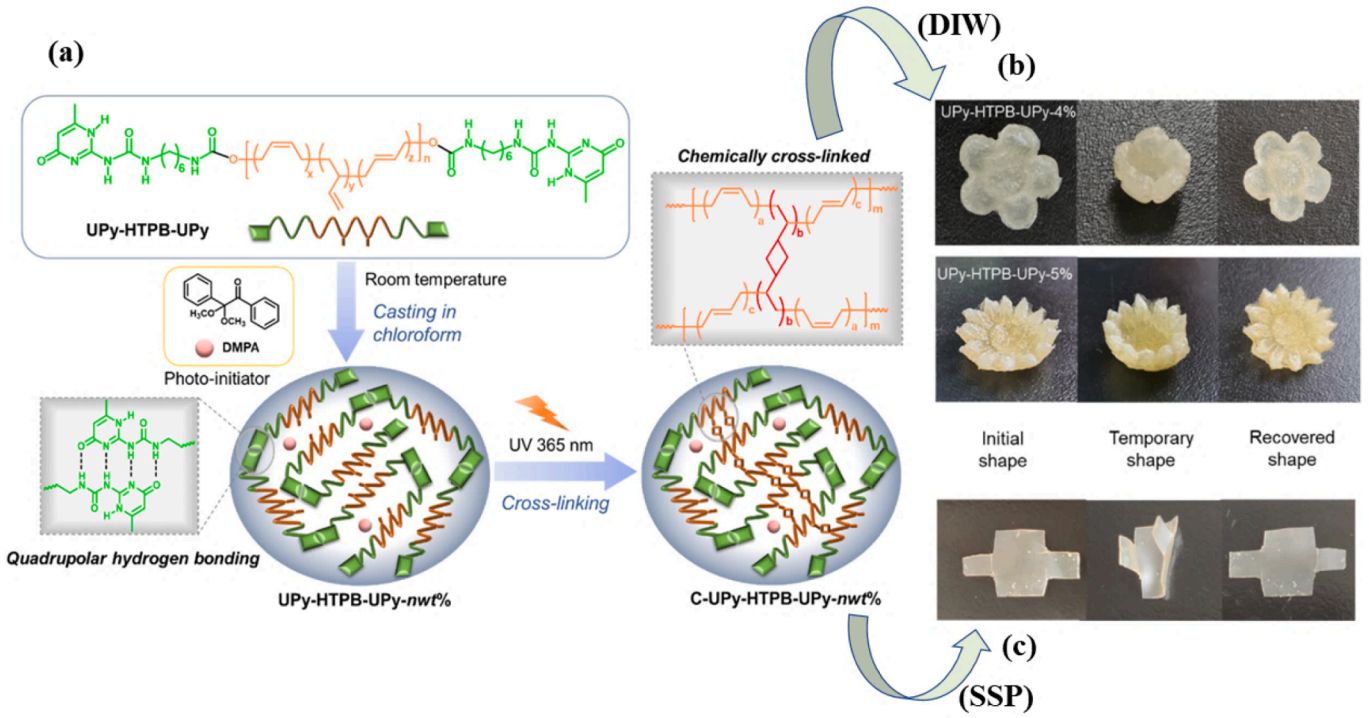

Fig. 11. (a) Schematic of synthesis (n show the photoinitiator fraction), (b) Direct ink writing of vitrimer, (c) Solid state printing of vitrimer (Reproduced from [154] under an open access Creative Commons license).

initial Zn(acac)2 M feed% was set to 2. To synthesize U1.7-PCL-PSA6, 2.5 g (1.25 mmol) PCL, 0.118 g (0.118 mmol) Zn(acac), and 5 ml THF were combined in a 20 ml scintillation vial. After that, PHMDI (0.791 g, 1.453 mmol) dissolved in THF (2 ml) was progressively added to the mixture. One hour into the reaction time, 0.26 g (0.217 mmol) PSA that had been dissolved in 2 ml THF was added to the mixture. The mixture was then placed in a vacuum oven at 60 °C for two hours to remove the THF solvent (Fig. 12a). Finally, by increasing the temperature to 120 °C over the course of the next 24 h, transesterification was triggered. Synthetic vitrimers were utilized in selective manufacturing methods to make films or filaments. U-PCL vitrimer film production: Polymers were deposited in a stainless-steel spacer mold and a 30 mm (L) × 30 mm (W) × 0.3 mm (T) Kapton polyimide mold to produce U-PCL vitrimer films. After that, the polymers were put through a 10-MPa, 30-minute press at 170 °C. For reprocessing, U-PCL vitrimer films were cut into small pieces. Then, using the same procedure, the pieces were pressed back into the original mold. All of the films underwent a 12-hour vacuum drying process at 70 °C before to analysis [155]. The small pieces of U-PCL vitrimer that had been manufactured were fed into a filament extruder (Filibot H303, Fordentech), which was then heated to 200 °C [155].

The results of the tests taken from this vitrimer have confirmed the memory chip's ability. This heat-activated property is necessary and essential for the application of these resins in 4D printing. The point here is that in this vitrimer, due to the presence of crystalline PCL, several shape memory behaviors caused by the crystalline phase will be

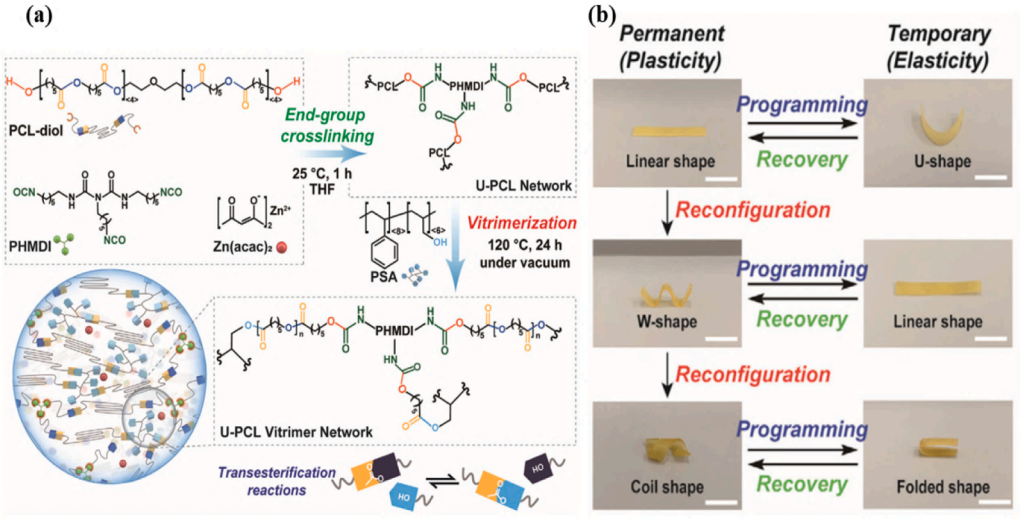

Fig. 12. (a) Schematic of monomer's chemical structure, crosslinking and vitrimerizatin mechanism, (b) U1.7-PCL-PSA6-Zn4 vitrimer can be complexly shaped by using elasticity- and plasticity-based cumulative shape reconfiguration (Reproduced from [155] under an open access Creative Commons license).

obtained, and for this reason, it was mentioned in the first that the crystallinity was maintained during the synthesis process. In addition to this reason, this vitrimeric network can also produce a shape memory property under the reconfiguration of the network at a temperature higher than the plasticity temperature (Tp), which network rearrangement is induced by dynamic transesterification reactions. The results of the shape memory properties of these synthetic vitrimers are shown in Fig. 12 b. Based on the figure, it can be said that, initially, U1.7-PCL-PSA 6-Zn4 vitrimer was changed to the desired shape at 60 °C, allowed by cooling to − 20 °C for fixing the temporary shape. Shape reconfiguration was done at 160 °C for 10 min, then the structure was fixed by cooling it down [155]. Also, in Fig. 13a, 3D printed mobile bridge is shown to prove the capability of this vitrimeric resin again. This bridge based on synthesized vitrimer containing PCL has advanced properties such as programmable shape, weldability, reprocessability, reprintability, recyclable properties, shape recovery and self-healing (Fig. 13 a-m) [155]. Also, formed 3D-printed vitrimer items exhibit greater heat resistance than commercial PCL prints and are reprocessable or reprintable frequently using filament extrusion and a portable fused deposition modeling (FDM™)-based 3D printing technique [155].

3.1.8. Polyimide-based vitrimer

Another instance involves the investigation of synthetic new shape memory polyimide (SMPI) ink [159]. This ink has demonstrated compatibility with both photopolymerization- and extruder-based 3D printing methods [159]. The primary chemicals used in the synthesis and processing of resin are as follows: 4,4′-(4,4′-isopropylidenediphenoxy) diphthalic anhydride (DABA), 4,4′-(diaminodiphenyl ether (ODA), 3,5-diaminobenzoic acid (DABA), 4-dimethylaminopyridine (DMAP), N-N-methanetetracyclohexanamine (DCC), and photoinitiator Irgacure 2100. There is also a need for solvents such N-vinyl-2-pyrrolidone (NVP) and N-methyl-2-pyrrolidone (NMP), isobornyl methacrylate (IBOMA), and hydroquinone (HQ) [159]. It will be expressed for the production of polyimide (PI) in the first step. For the polycondensation of dianhydride (BPADA) with the two types of diamines (ODA and DABA), the molar ratio of DABA and ODA was fixed to 1:1 for the synthesis of copolyimide. In conclusion, it can be claimed that 0.746 g (5 mmol) of DABA and 28 ml of NMP solvents were transferred to a three-necked flask and well mixed while being agitated under nitrogen at room temperature. Following the addition of 5.2 g (10 mmol) of BPADA, the reaction was allowed to proceed for 24 h at room temperature [159]. Following this, 1.001 g (5 mmol) of ODA was added to the reaction, which was then permitted 24 h to finish at room temperature. The solution was stirred for 5 h at 290 °C to complete the imidization, after which the product was precipitated in ethanol and filtered. It should be noted that the esterification of hydroxyl groups on HEMA and carboxyl groups on DABA forms the basis of the second step in the production of photo-crosslinkable poly(acrylate-g-polyimide). This was accomplished by dissolving 6.905 g (5.1 mol) of synthetic copolyimide in NMP solvent at normal temperature [159]. The NMP solvent in the container was then supplemented with 0.663 g (5.1 mol) of HEMA monomer, 1.052 g (5.1 mol) of DCC, and 0.062 g (0.51 mol) of DMAP. At room temperature, the other was moved and stirred. We then slowly combined these two solutions and kept them at room temperature for 24 h (sedimentation occurred during this phase) to execute Steglich esterification. The product was then created by removing the solvent after it was precipitated in ethanol. A small amount of synthetic poly(acrylate-g-polyimide) was dissolved in NVP solvent in the third step after this compound was created. Next, the methyl acrylate monomer IBOMA, inhibitor HQ, and photoinitiator Irgacure 2100 were added, and everything was thoroughly mixed to create the 3D printing resin based on polyimide. 420 nm wavelength utilized in the printing process with the DLP technology [159]. The exposure time and layer thickness for each layer were both set at 30 s. The printed objects were dried in a vacuum oven for a full night at 200 °C after being post-cured for 30 min in a UV-light environment

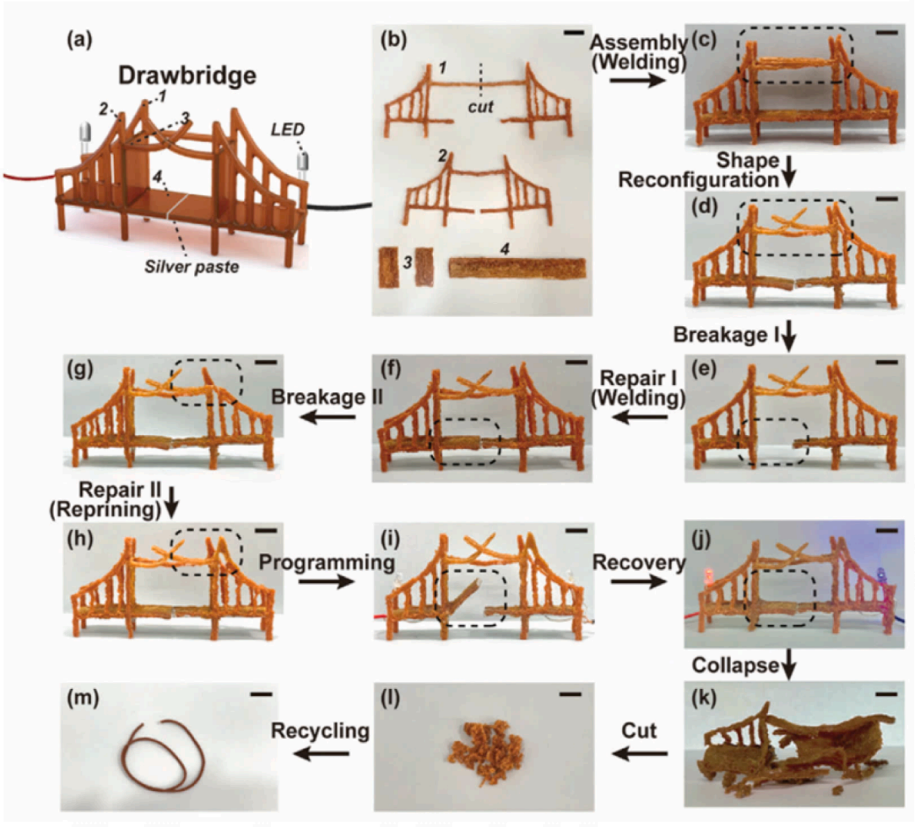

Fig. 13. Pictures of the multifunctional 3D printing capability of synthetic vitrimers: (a) mobile bridge printed with handheld FDM™-based 3D printing and welding technique, (b) assembly schematic of printed mobile bridge components, (c) mobile bridge assembled with welding technique, (d) Reconfiguration of the movable bridge, (e) Schematic of the broken bridge, (f) Repaired bridge through welding, (g) Reconfiguration of the broken movable bridge, (h) Repaired bridge through reprinting, (i) Shape programming, (j) Shape recovery, (k) Collapsed vitrimer bridge, (l) Cut bridge pieces for recycling, (m) Reprocessed vitrimer filament for reprinting (Reproduced from [155] under an open access Creative Commons license).

(Fig. 14) [159]. Additionally, Table 2 [159] reports all formulations that were taken into consideration. One of the important results observed is the printing ability of these synthetic resins, which can be seen in Fig. 15a. With varying degrees of complexity, the three geometries of an airplane, stator, and pagoda have been 3D printed, and the prints are of high quality. After processing, the printed plane in Fig. 15a(i) did not emit any shrinkage (Fig. 15a(ii)). Fig. 15a(v) [159] depicts the stator of an ultrasonic motor as another model. After processing, there was no shrinkage in the geometry of the two concentric circles, the outer circle of which had the designated motor teeth. The distance between Fig. 15a (vi) and the layerstacking trapezoid teeth is 400 μm. It should also be mentioned in relation to 3D printing that a superb pagoda with great complexity can be broken down into three parts, as illustrated in Fig. 15a (ix), which includes the body of the six-layer tower, the broad base, and the top of the tower. This illustration demonstrates that complicated geometries may be printed using synthetic resins on polyamide. Additionally, Fig. 15a (ii-iv) demonstrates the usefulness of resin in 4D printing and makes evident the safe shape memory characteristics of industrial resins. The plane's wings are temporarily curved upward and exhibit a "bird-like" shape, but after heating, they have assumed their final configuration [159]. The self-rolling tendency, among the other findings, suggests the usage of these synthetic resins as actuators. Here, six pieces of PI film are connected using five pieces of equal-thickness SMPI hinges. Due to the strong driving force of the SMPI hinges, as shown in Fig. 15b, the formed planar structure may self-fold into a 3D box as the temperature climbs to 160 °C. In addition, four pieces of homogeneously thickened SMPI material are alternately joined at a 90° angle and employed as clamps, as shown in Fig. 15b [159]. A summary of the results extracted from the studies of synthetic vitrimers is reported in Table 3.

Table 2
Different prepared 3D printing resin formulation (based on wt%) (Reproduced from [159] with permission from ELSEVIER).

Material	SMPI-1	SMPI-2	SMPI-3	SMPI-4	SMPI-5
PI-g-HEMA	20	20	20	20	20
NVP	78	24	70	66	62
IBOMA	0	4	8	12	16
Irgacure 2100	1.9	1.9	1.9	1.9	1.9
HQ	0.1	0.1	0.1	0.1	0.1

3.2. Off the shelf material-based formulation

3.2.1. Acrylate-based vitrimer

The usage of transesterification band exchange processes has also been investigated [116], continuing the investigation into the reprocessability of thermostats via vitrimeric networks. Thermostats with 3D printing capabilities (3DPRTs) based on UV curing methods have been produced in this instance, claim the article's authors, using a two-step polymerization process [116]. Because acrylate resins are employed, this thermostat may be printed with intricate lines and used with processes like digital light processing (DLP), mask projection

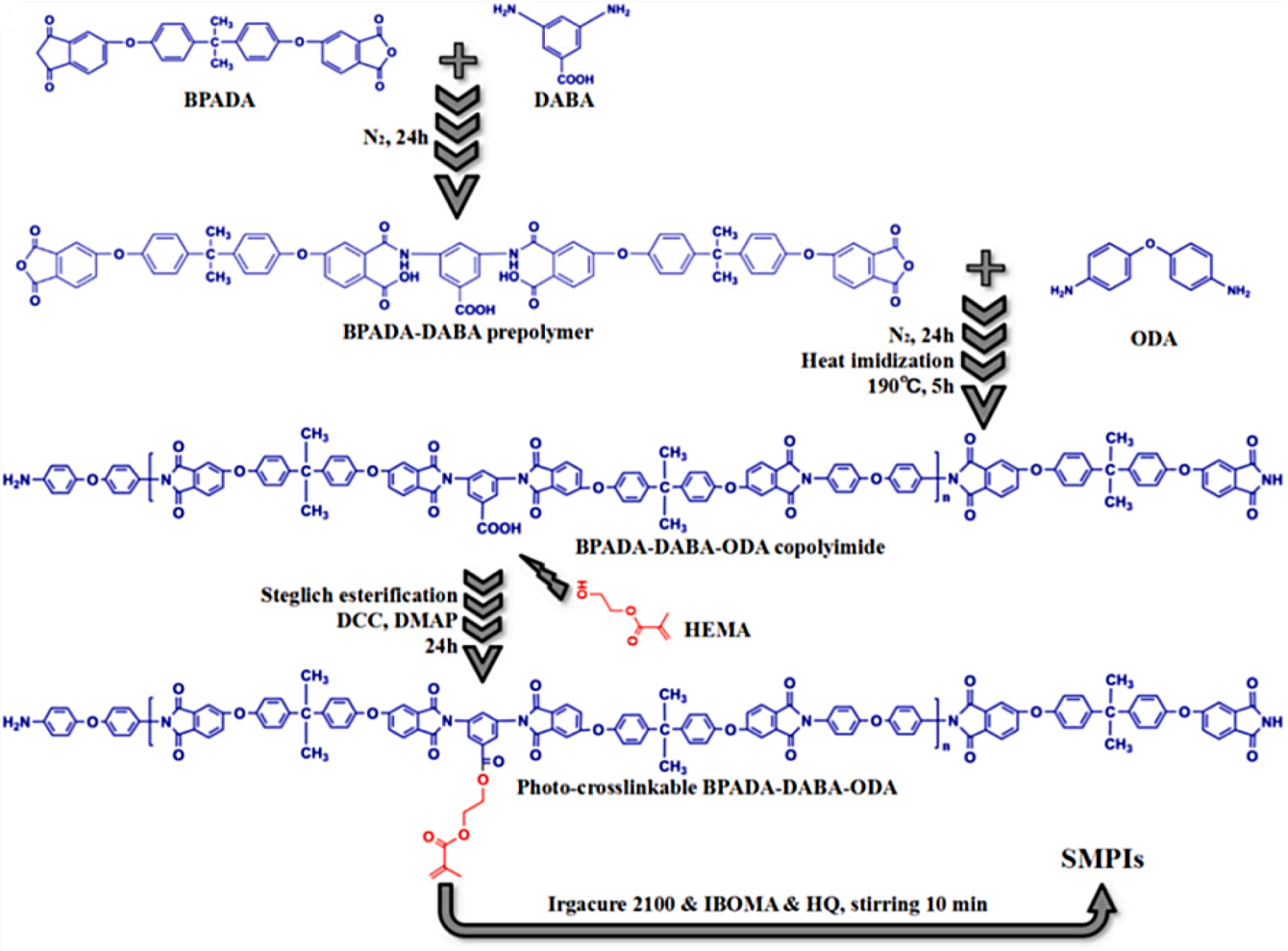

Fig. 14. Schematic for Synthesis of SMPI (Reproduced from [159] with permission from ELSEVIER).

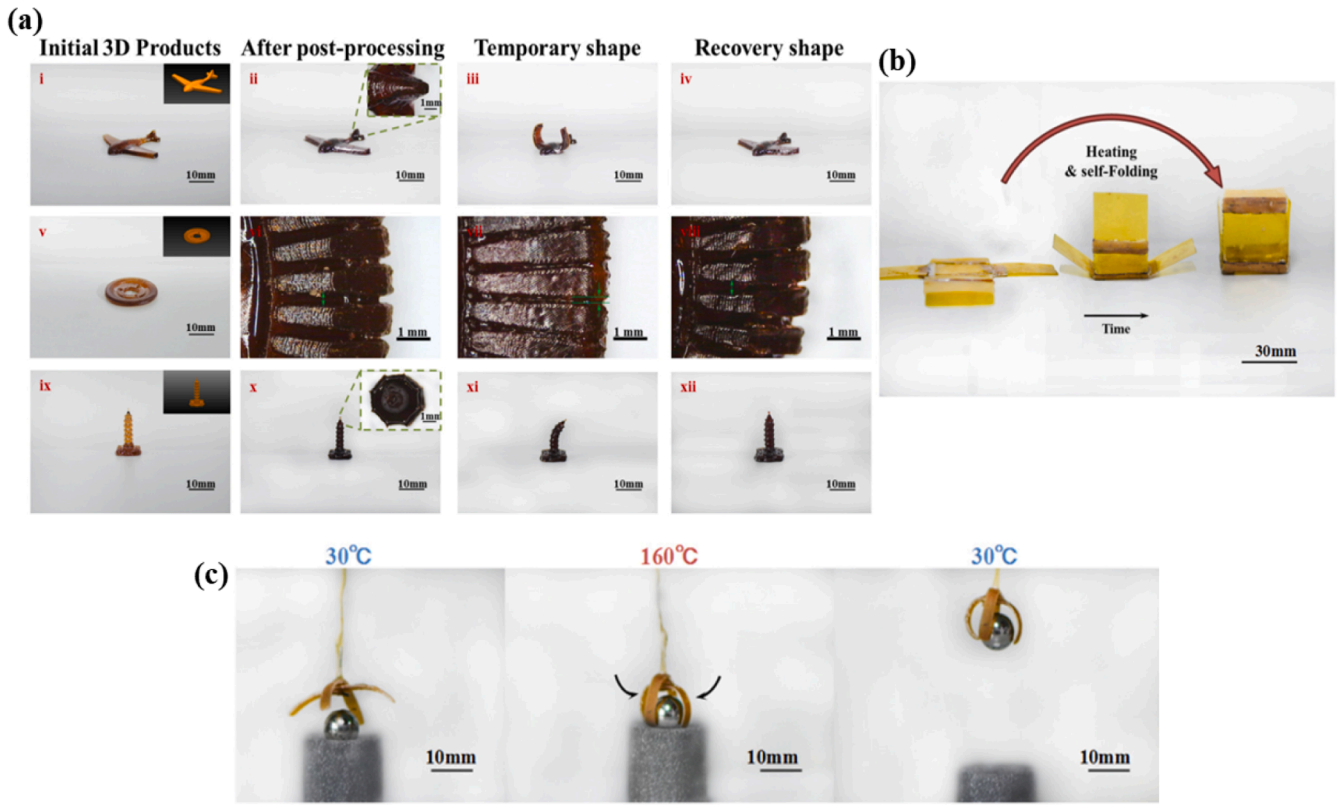

Fig. 15. (a) DLP-based 4D printed complicate products of SMPIs: airplane (i), stator of ultrasonic motor (v), and exquisite pagoda (ix); the initial shape of printed products after postprocessing: airplane (ii), stator (vi) and pagoda (x); the temporary shape of printed products: airplane (iii), stator (vii), and pagoda (xi); the recovery shape of printed products: airplane(iv), stator (viii) and pagoda (xii), (b) self-folding box, (c) stimuli-response gripper (Reproduced from [159] with permission from ELSEVIER).

stereolithography, and two-photon lithography (Fig. 16a) [116]. The printed thermostat is also reprocessed (Fig. 16a) [116] as a result of heat activating a transesterification reaction between the ester and hydroxyl functional groups designed in the printed polymer network. Fig. 16c also shows the crosslinks produced by the UV-induced opening of acrylate groups during the 3D printing process in the presence of the photo-initiator. These crosslinks are truly long-lasting covalent connections with distinctive blue spots [116]. But as was discussed earlier, heating the sample to 180 °C will start the band exchange reaction in this network, resulting in the formation of dynamic covalent bands (DCBs), which are indicated in Fig. 16d by red dots. As a result of the bonds between ester and hydroxyl groups breaking and re-forming during DCB formation, the total density of linkages is kept constant (Fig. 16f, g) [116]. Fig. 16b shows that 3 g of zinc acetylacetone hydrate (Zn(acac)2) and 45 g of 2-hydroxy-3-phenoxypropyl acrylate monomer were initially added to a 100 ml container. At a temperature of 70 °C, the mixture was stirred after the catalyst had been well combined. The selective photoinitiator diphenyl(2,4,6-trimethylbenzoly) phosphine oxide was then added to the vessel and agitated at room temperature along with 2% of the combined weight of the monomer and crosslinker. Then, 5 g of bisphenol A glycerolate monomer, the catalyst, was added. It is important to keep in mind that this photopolymer resin is produced with a 9:1 wt ratio of monomer to crosslinker, a 1:1 M ratio of ester groups to hydroxyl groups, and a 5 mol% catalyst concentration to OH groups. In order to improve print resolution and control photo-polymerization, 0.02 wt% of the total weight of Sudan I was used as a photoabsorber during 3D printing. A high-resolution 3D printer based on DLP was used for the printing process, and each 50-μm layer received 2 s of irradiation [116].

In order to show the healing capabilities of the developed formulations, the lack of a 3D printed rabbit ear is considered a defect [116]. After the surface of the fault has been polished, Fig. 17a amply demonstrates that the repair has been carried out completely and expertly [116]. It should be mentioned that the rabbit's mechanical function was restored by heating it to 180 °C for four hours after printing. Fig. 17b illustrates the regeneration mechanism, which may be summarized as follows: upon heating, the bond exchange reaction is initiated, the nearby hydroxyl group attacks and breaks the existing dynamic bonds, and the new dynamic bonds are produced by bonding to the nearby ester group [116]. The original and restored areas of the surface are connected and homogenized as a result of this happening throughout the entire network. Fig. 17c also looks at the mechanical properties of the repaired base, which were fixed by UV irradiation and heating [116]. It's crucial to keep in mind that during the exchange reaction, the balance between fracture and re-formation will stabilize the density of cross-linking, which will restore the mechanical properties lost as a result of the defect, in this case 93% of the strength and 100% of the basilar stiffness [116]. Fig. 17d illustrates how 3DPRTs have proven to be capable of recycling, enabling the 3D printing of objects with acceptable mechanical properties after being ground into a powder and pressed into a mold with an SUTD pattern [116].

Today's engineering users place a significant emphasis on light structures and the architectural methods employed to create them. We can cite items like pressure vessels, pipes, bridge decks, cars, trains, airplanes, ships, and even wind turbine blades as examples of these. One of the key factors for this structure's popularity is its high specific strength and stiffness, tailorability, and resistance to corrosion. Sandwich structures are among the most prevalent and have a core that is crucial for maintaining flexibility and portability. Polymer cores with three-dimensional structures and polymer foam have been the focus in

Table 3
Summary of the studies and results from synthetic vitrimer based 3D/4D printing formulations.

Category of vitrimer	Material	Type of Printing	Result	Application
Acrylate and Methacrylate-Based [93]	GMA, SA, TBAB, TBD, THFA, AM, EG, TPO [93]	SLA [93]	The average tensile strength and Young's modulus were 4.4 and 3.85 times respectively and reached 40.1 and 871 MPa. Also, different shapes were printed and dissolved in ethylene glycol could be remolded again [93]	3D/4D printing of remolded and recyclable structures [93]
Vanillin-Based [106]	V, EC, K_2CO_3, MAA, ED, BAPO [106]	DLP [106]	relatively high glass transition temperature for printed parts, good thermal stability, self-healing properties, reprocessing and flexibility, mechanical and chemical recycling [106]	3D/4D printing of Structures with good thermal stability, self-healing properties, reprocessing and flexibility, mechanical and chemical recycling [106]
Vanillin-Based [109]	HPPA, DGEVA, DGEVADMA, $Zn(acac)_2$, TPOL [109]	DLP [109]	high welding efficiency of 114.12% for tensile strength and also a recovery rate of 75% after alkalization in addition to shape memory properties, self-healing properties [109]	Soft robotics and actuators [109]
Acrylate-Cyanate-Based [123]	EGBT, TAOE, PETMP, EGDA, Irgacure 819, TATAT [123]	DLP [124]	Single homogeneous network using active groups such as hydroxyl groups [123]	fabricated 3D channels for microfluidics [123], 4D printing
Linseed-Based [141]	EGMP, TMP_3MP. epoxidized linseed oil, acrylic acid, BAPO, DMEP [141]	DLP [141]	Triple shape memory and this ability is created in them to control these changes and the ability of macroscopic deformation during heating, possible to print holes with a size of 250 μm with resolution, self-healing properties [141]	actuator, biomedical and soft robotics [141]
Polyurea-Poly (dimethylsiloxane)-Based [142]	4,4′-methylenebis (phenyl isocyanate), aminopropyl terminated Poly (dimethylsiloxane), 2-(methacryloyloxy) ethyl acetoacetate, azobis-(isobutyronitrile) [142]	FDM™ [142]	Proper thermal and chemical stability and are less sensitive to decomposition such as hydrolysis, Repairability, Young's modulus was 1.14 MPa for the repaired sample and 0.9 MPa for the original sample, which is a significant increase [142]	3D/4D printing formulation for Repairable or self-healable structures [142]
Polybutadiene-Based [154]	HTPB, DBTDL, HDI, MIS, DMPA [154].	FDM™, DIW [154]	Good potential for 3D printing processes, increase the adhesion and mechanical strength of the printed piece, presence of hydrogen bonds caused the solubility of the polymer, so UPy-HTPB-UPy is soluble in chloroform and this resin is suitable for DIW, good heating-responsive shape memory effect [154]	Volumetric Additive Manufacturing (VAM) [154]
Polycaprolactone-Based [155]	PCL-diol (2000 g/mol), commercial PCL filament, PHMDI with NCO content of 22.6–23.7%, $Zn(acac)_2$ [155]	FDM™ [155]	Programmable shape, weldability, reprocessability, reprintability, recyclable properties, shape recovery and self-healing [155]	3D/4D printing of structures with Programmable shape, weldability, reprocessability, reprintability, recyclable properties, shape recovery and self-healing properties [155]
Polyimide-Based [159]	DABA, ODA, DABA, HEMA, DMAP, DCC, IBOMA, HQ [159]	DLP [159]	Good print quality, any shrinkage after processing, Shape memory properties [159]	4D Printing of shape memory and low shrinkage structures [159]

the meantime. Due to its simpler and more affordable processing as well as a wider range of features, printable polymers with shape memory capabilities have eclipsed other materials such as metal alloys in the meantime. Now that vitrimers can be recycled and reprocessed, they are being used in this work to build multifunctional lightweight architectures (MLAs) [160]. The objective of this research is to develop a thermoset polymer with high strength, stiffness, shape recovery ratio, recovery stress, and good recycleability that can be printed in three dimensions [160].

To prepare 3D printable and recyclable shape memory polymer (3D-RSMP) resin, 3.5 wt% of 2-hydroxy-2-methylpropiophenone monomer with 20 wt% of 1,4-butanediol dimethacrylate monomer along with 1 wt % of bis photoinitiator (2,4,6-trimethylbenzoyl)-phenylphosphineoxide and 0.5 wt% of triethylamine were added in 200 g of bisphenol A glycerolate dimethacrylate, which was continued to mix at 72 °C for 4 h [160]. For the 3D printing process, an Asiga Pico 239 SLA 3D printer was used with a regulated light intensity of 28 mW/cm^2 and a radiation wavelength of 385 nm for a layer thickness of 0.15 mm [160]. Fig. 23 a report the first outcome of the target structures. Images of two printed lightweight microlattice series can be seen in these formats. In the first series, a Kelvin unit cell, a cubic unit cell, and an octet unit cell were selected as illustrations of the bending-dominated geometry and stretching-dominated geometry, respectively. These samples have been successfully printed. Additionally, the second series' architecture is based on well-known patterns like foams, which are constructed from first- and second-order octet microlattices. The prints' lack of waves or opposing portions are another noteworthy feature. Additionally, the vertical wall of the cubic microlattice had a layer thickness of 0.15 mm when printed vertically only, which was consistent with the printing parameter and indicated high-quality and high-resolution DLP 3D printing with the 3D-RSMP resin [160]. The first programming for these constructions consisted of four steps: heating, putting load at rubbery temperature, cooling under steady stress to glass temperature, and removing load. From the significant findings of this test, it can be concluded that the microlattice changed from its initial structure to one that was shorter and wider during the four-stage planning process. Additionally, it has been claimed that a free shape recovery test at 100 °C resulted in a shape recovery rate of 83%. The recovery rate has risen to 95% by raising the temperature to 150 °C, which is above the glass transition point. Also, appropriate and desirable mechanical strength has been recorded for these printed parts following recovery and these testing. It should be mentioned that a spring that was programmed for both compression and tension was printed using 3D-RSMP resin. After one minute of heating, the spring's ability to recover from compression under pressure was able to eliminate 20% of the strain. Moreover, the tension type of this characteristic was examined, and the

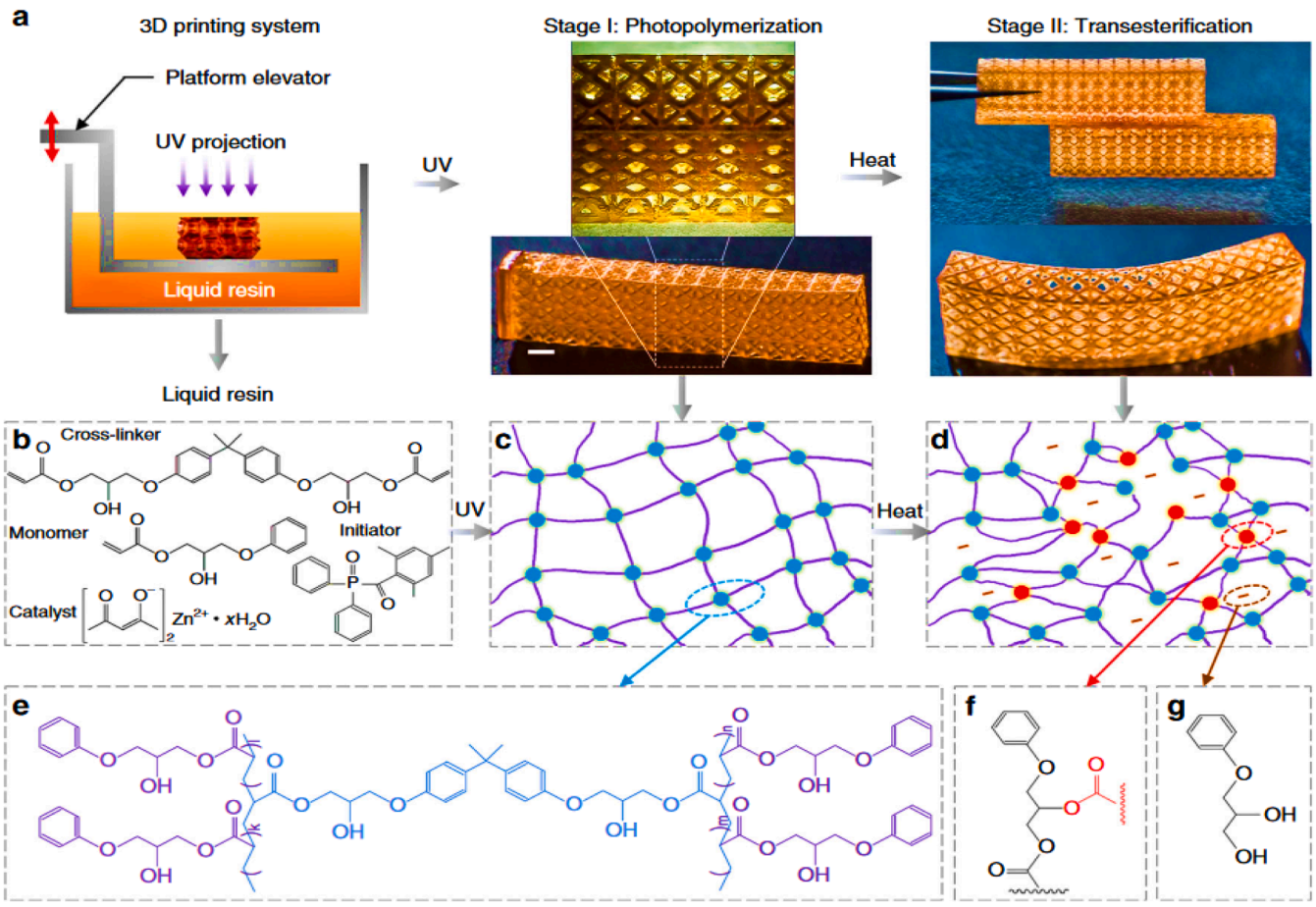

Fig. 16. (a) An overview of synthetic formulation 3D printing and two-step polymerization, (b) Chemical structure of monomer and other materials, (c) A schematic of permanent links formation, (d) Formation of DCBs via transesterification chemistry, (e) Chemical structure of permanent links formed during 3D printing, (f, g) Chemical structure of links after heating (Reproduced from [116] under an open access Creative Commons license).

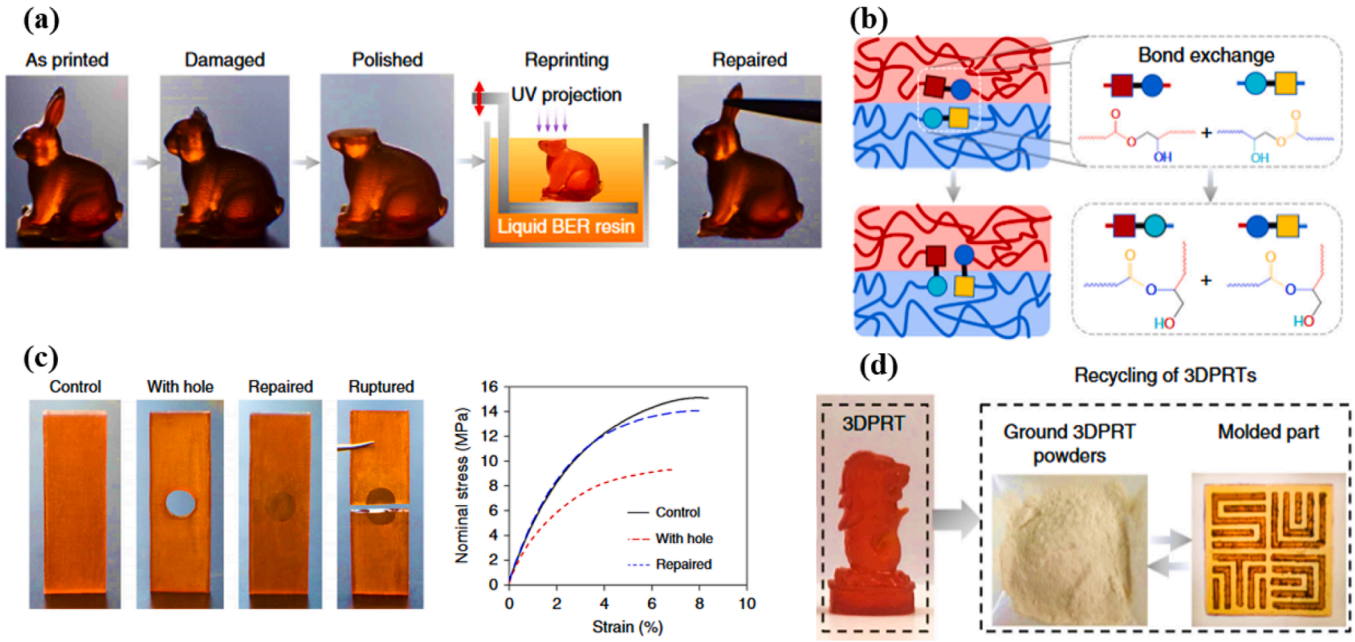

Fig. 17. (a) Repairability of 3D printing formulation, (b) Mechanism of bond exchange reaction during the repairing, (c) Analysis of mechanical properties after repairing, (d) Recyclability of 3D printed thermoset (Reproduced from [116] under an open access Creative Commons license).

spring was able to regain 20% of its initial strain after heating for one minute. In addition, the recyclability of this formulation and printed parts has also been confirmed. Following recycling and reprocessing, good mechanical properties are also documented [160].

3.2.2. Epoxy-based vitrimer

We can highlight the multi-stimuli-responsive vitrimer (m-vitrimer), which has thermal and photo-reversible disulfide bonds, as a follow-up study on shape-programmable polymer networks. Finally, flexible smart electronics (PFSE) with self-healing and programmable shape were created using two-dimensional (2D) vitrimer structures and printed conductive wires [161]. Bisphenol A diglycidyl ether epoxy oligomer (DEGBA), in combination with 2,2-(ethylenedioxy) diethanethiol (EDDET) and polysulfide oligomer (Thioplast G44), has been used to create m-vitrimer [161]. In addition to these substances, 2, 4, 6-tris-dimethylaminomethyl phenol (Epikure 3253) has also been utilized as a catalyst at 0.5 or 1.0 wt%. The mixture was transferred to the aluminum side and cured at 60 °C for 2 h before being post-cured at 90 °C for 1 h in a convection oven after complete hand mixing and degassing. In this study, the Vitrimer sample containing 40% molar thiol from G44 and 0.5 wt% of Epikure 3253 was selected. To print inks containing silver nanoparticles, direct ink writing (DIW) printing was used with a nozzle with an inner diameter of 0.61 mm at a pressure of 15 psi and a speed of 3 mm s^{-1} (Fig. 18a).

Fig. 18a shows that after bending, vitrimer has reverted to its original shape without any further bending when exposed to light or heat. The polymer network formed by the epoxy oligomer's curing between thiol and epoxide, which comprises dynamic thiol bands, is the cause of this phenomenon [46]. Direct heating can be used to train the printed part to change its structure from 2D to 3D configurations, from flat sheets to Sine, helical, and semi-sphere shapes. This is made possible by the existence of stimuli-induced plasticity in the m-vitrimer. Additionally, it can be deduced from Fig. 18b that UV light can be used to program 2D films into 3D shapes to create vitrimeric structures [46]. Since it is obvious that the glass slide caused the two-dimensional circuit to bend with UV light in two minutes, removing the slide caused the circuit to reverse itself and change into a free-standing bending shape. The printed circuit with conductive silver wire on the m-vitrimer elastomer displayed a resistance of 2.91 ± 0.07 according to Fig. 18c, however after breaking the circuit, the resistance became infinite. It was repaired and revealed when the slices were combined and IPL exposure for 30 s twice, with a cooling step in between cycles [46].

Additionally, high-performance 3D printed parts based on thermoset epoxy resin have been produced using the UV assisted DIW approach via a two-stage cure [162]. This manufactured resin combines epoxy oligomer thermal cure photopolymer resin with fumed SiO2 for reinforcement. Another aspect of this network's construction is its flexibility, which allows it to exhibit good dimensional and thermal stability while still maintaining the part's shape at high temperatures [162]. The printed piece can also be placed in a furnace to continue curing under heat, much like a thermal-curing epoxy resin, to complete the baking process [162]. Therefore, it can be argued that interpenetrating polymer network (IPN) epoxy composites can be created by adopting a two-stage curing procedure. Additionally, it will be demonstrated that this printed composite possesses shape memory, form recovery ratio, cycle stability, and high shape constant ratio features [162]. In order to create this photopolymer resin, acrylate and epoxy were employed in a weight ratio of 4/6 (wt/wt), or a molar ratio of 17.6/18.2 [162]. This photopolymer's acrylate component is made up of a blend of n-butyl acrylate (BA) and aliphatic urethane diacrylate (Ebecryl 8402), which amounts to 1/1 (wt/wt) or roughly 15.6/2.0 (mol/mol) [162]. Additionally, the acrylate component is combined with the epoxy base component of this formulation, Bisphenol A diglycidyl ether (DGEBA) epoxy oligomer (Epon resin 862) at the ratio specified [162]. This mixture, which contains 1.5 wt% of 2, 4, 6-tris-dimethylaminomethyl phenol, also includes baking powder. Additionally, the combination contained 1.0 wt% of phenylbis

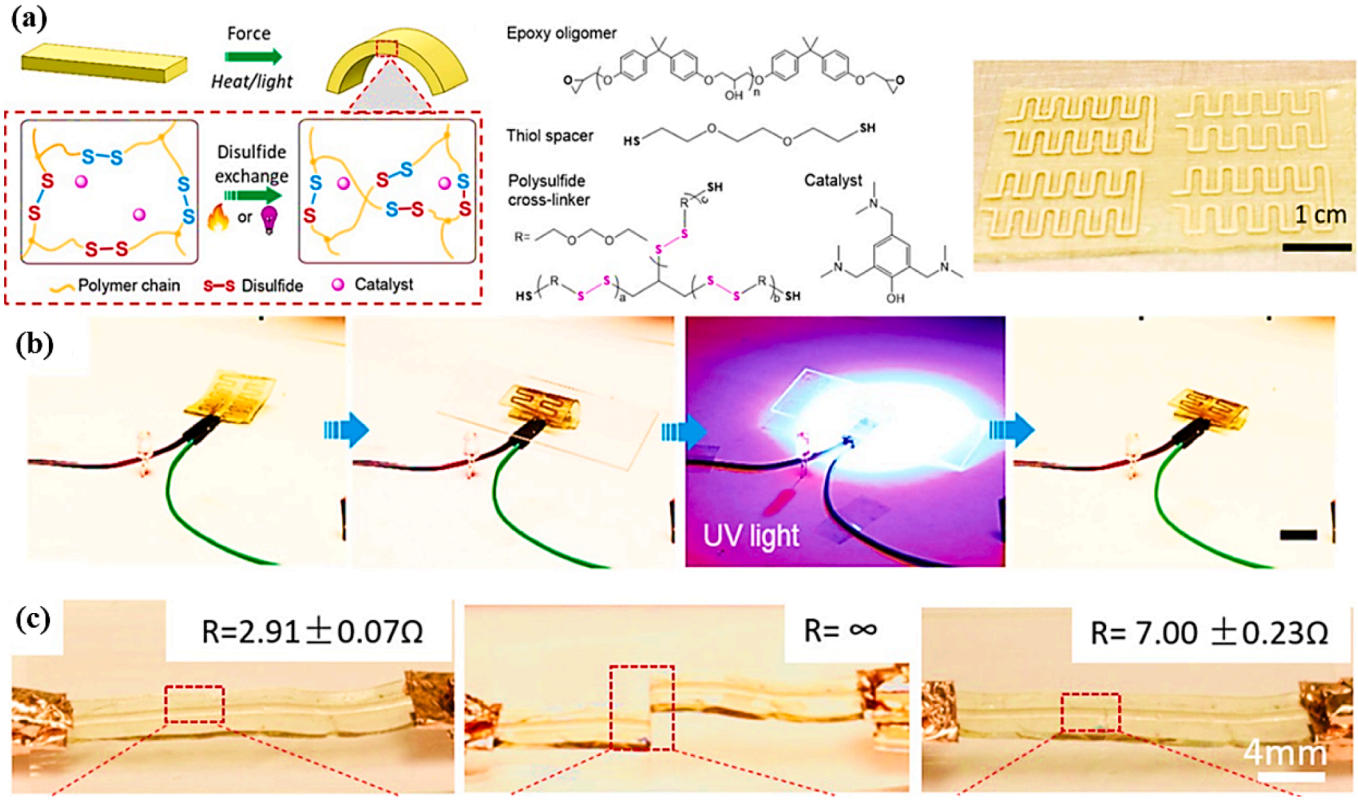

Fig. 18. (a) Schematic of reactants chemical structure and shape programmable mechanism via disulfide-based CANs chemistry, (b) Shape programmed printed circuit, (c) Self healed 3D printed circuit (Reproduced from ref [46] under an open access Creative Commons license).

(2,4,6-trimethylbenzoyl) phosphine oxide photoinitiator. Five minutes were spent blending this combination [162]. It was vortexed and then fumed silica nanoparticle (8 wt% as a strengthening agent) was slowly added to the mixture and mixed by hand for 15 min [162]. It should also be said in connection with the printer that the syringe was controlled using a pressure controller which moved in the x- and z-directions, while the printing platform moved in the y-direction. Also, a nozzle with an inner diameter of 0.41 mm is connected to the end of the syringe, and during printing, a pressure of 33 psi and a speed of 10 mm/s were applied, and the highest resolution was achieved by choosing an inner diameter of 250 um [162]. The results of these parts, which were printed using a nozzle with an inner diameter of 0.41 mm, and the suitability of the formulation created for this method were confirmed by the points discussed before creating the formulation. In the figure, the images below the dashed line relate to the heat treatment of the printed components, and the shapes above the dashed line relate to the parts after printing [162]. The print quality was further examined using a scanning electron microscope (SEM) test that the filament with a diameter of around 400 m was clear and sag-free. Additionally, the filaments' homogeneity will be visible. Additionally, thermal curing also promotes polymerization in the surface regions and causes the filaments to adhere, which results in the adherence of the layers [162]. Additionally, Fig. 19a,b [162] depicts the shape change behavior of this vitreous composite created over time.

Today, using elastomers that respond to magnetism is one of the factors taken into account while designing soft robots that can be controlled remotely. The tiny excitation strain in this system, which stops it from spreading, is one issue it has. Magnetic vitrimer (MV) has been suggested as one approach to designing such devices with quick reaction and proper cure [163]. By combining magnetic particles with a polymer that contains dynamic covalent bonds, these kinds of resins can be created. At room temperature, the behavior of MV is comparable to that of a typical magneto-responsive elastomer. However, as the temperature rises up to the activation temperature of the bond exchange reaction, large shape changes may take place because the behavior of MV switches from that of a typical elastomer to that of a viscous fluid [163]. In addition to this property, the presence of magnetic particles will result in the development of self-healing properties since a dynamic network exists [163]. In other words, in this section, we'll look at the soft composite material that is magnetically responsive and has disulfide linkages that are packed with magnetic particles [163]. The key idea here is that the exchange reaction of disulfide bonds occurs under heat or infrared (IR) irradiation, leading to a rearrangement of the network's dynamics, an increase in the movements of the matrix's polymer segments, and ultimately a change in shape [164,165].

This Vitrimer formulation is first materialized by curing the epoxy monomer with two different sulfhydryls. To do this, a specified quantity of EPS25 monomer is combined with stoichiometric amounts of the two curing substances 2,2-(ethylenedioxy) diethanethiol (EDDET) and pentaerythritol tetrakis (3-mercaptopropionate) (PETMP) [160]. Then, 10 wt% of iron oxide micro-particles (Fe3O4) and 1 wt% of 4-DMAP as a catalyst were added to this mixture (Figure 27 a) [163]. It should be noted that the chemistry governing the formation of this network was a thiol-epoxy reaction type, in which EPS25 and EDDET, both of which contain two thiol groups, form the polymer chains, and PETMP, which contains four thiol groups, crosslinks the chains into a network. Another point is that (dimethylamino)pyridine (DMAP) was utilized as the catalyst, and the molar ratio of thiols can be adjusted to influence the thermodynamic properties brought on by the density of crosslinks [163]. The vitrimer's fluid-like characteristics result from the disulfide bonds' simplicity in being destroyed and then rebuilt by an oxidation process and a reduction reaction, respectively [163,166], as shown in Fig. 20 a. Fig. 20a depicts the reconfiguration method and how the magnetic particles are incorporated in the vitrimeric matrix to create magneto-responsive vitrimer. The flowability of the composite has also improved as a result of the temperature rise and activation of the bond exchange reaction. This phenomenon leads to the controlled induction of a drastic and irreversible shape change in magnetic vitrimer by a magnetic gradient. As shown in Fig. 20b, the constructed vitrimer will be used in soft robotics applications. The MV may switch between a disk-shaped configuration and a soft robotic gripper by utilizing a local temperature field and magnetic gradient. Fig. 20a also shows the findings in relation to the self-healing characteristics brought on by magnetically led self-healing. The magnetic gradient-induced pulling force allowed the shattered "arms" to move towards the main "body" without actual physical touch. The interaction of a soft robotic gripper with a moving object using magnetic control (Fig. 20a) is another outcome that might be noted [163].

3.2.3. *Thiol-based vitrimer*

Because the type of catalyst can affect the pace of bond exchange reactions, it is clear from the thiol-acrylate chemistry section that recent attention has been paid to it. Therefore, a new catalyst for transesterification in thiol-click in photopolymer resin was used here, a mono-functional methacrylic phosphate [167]. The fact that this catalyst is liquid in contrast to other traditional catalysts means that it can be dissolved in a variety of acrylate monomers, which is one of its benefits. Because of this, the network across its methacrylate group is covalently incorporated, and the cure kinetics of dramatically triggered photopolymerization events are not compromised. Based on the same dynamic chemistry, this catalyst has also been utilized to create 3D printable vitrimers [168].These components are utilized in this formulation: Fig. 21b also depicts trimethylolpropane triacrylate, Miramer A99 acting as a catalyst for the transesterification bond exchange reaction, and other consumables. Zinc acetate catalyst ($Zn(acac)_2$) was first dissolved in 2-hydroxy-3-phenoxypropyl acrylate (HPPA) at a temperature of 70 °C to generate the vitrimeric 3D printing resin composition. After cooling, phenylbis(2,4,6-trimethylbenzoyl) phosphine oxide (BAPO), Sudan II, and the bifunctional acrylate monomer glycerol 1,3-diglycerolate diacrylate (GDGDA) were added to the mixture and mixed until fully combined. Another vitrimeric formulation was created using triphenylphosphine (TPP) catalyst, which was added to the

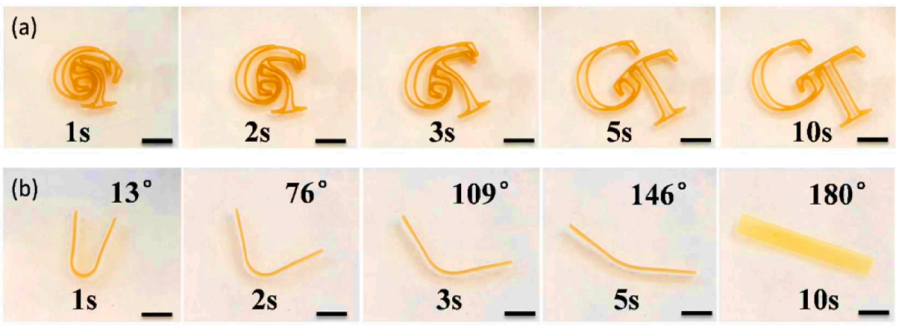

Fig. 19. Shape memory behavior of vitrimeric composites: (a) GT logo, (b) strip sample (Reproduced from [162] with permission from Royal Society of Chemistry).

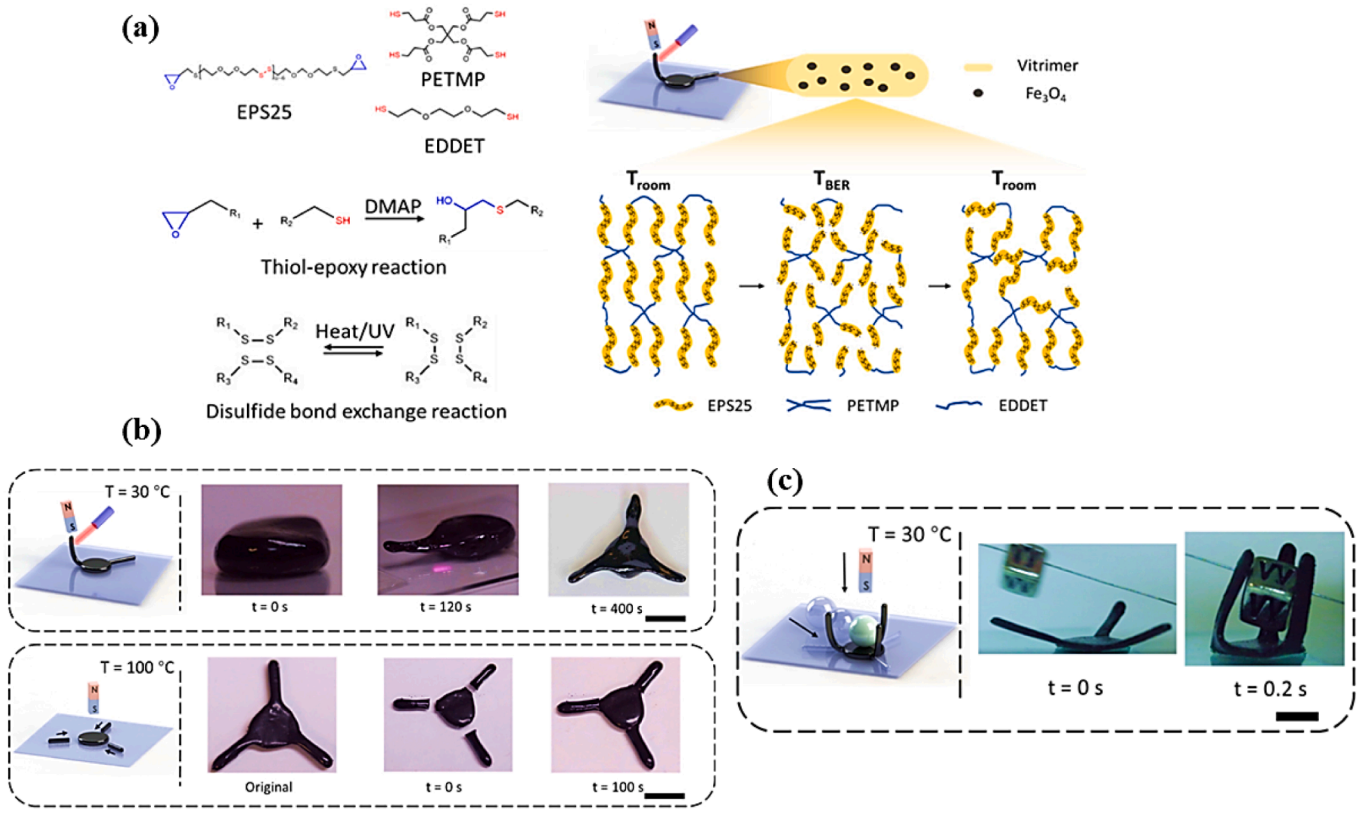

Fig. 20. (a) chemical structure of used monomers and mechanism of crosslinking creation and bond exchange reaction mechanism of vitrimer network, (b) An MV disk can transform into a soft gripper by applying local heating with a laser beam and a magnetic field by a permanent magnet and self-healing properties, (c) The soft robotic gripper can catch a moving object through fast actuation (Reproduced from [163] by permission from Royal Society of Chemistry).

mixture of HPPA and GDGDA after being first dissolved in Sudan II and BAPO in acetone. Additionally, this monomer was dissolved in dichloromethane together with BAPO and Sudan II and added to the mixture of HPPA and GDGDA acrylates in order to prepare the formulation comprising 1,5,7-triazabicyclo (4.4.0) dec-5-ene (TBD). The formulation containing the Miramer A99 catalyst is then created by combining Sudan II, HPPA, and GDGDA with the catalyst itself. Trimethylolpropane triacrylate (TMPTA) is also used. The Anycubic Photon Z printer was used to do DLP 3D printing of these compositions at a wavelength of 405 nm. The first two substrates were baked for 1001 s, and the remaining substrates were baked for 10 s per layer [168].

According to the examination of the data, the planned network is based on catalyzed transesterifications of hydroxyl ester linkages (Fig. 21a–c). Utilizing acrylate monomers with free hydroxyl groups, this dynamic chemistry penetrated the network of UV-cured resins and offered vitrimeric qualities based on the chemistry indicated. With regards to this synthesized network, it can be stated that the primary justification for selecting GDGDA and HPPA acrylate monomers was their ability to make a significant amount of hydroxyl groups available to the network to aid in transesterification exchange reaction [169]. In addition, catalysts including triazabicyclodecene (TBD), triphenylphosphine (TPP), and zinc acetyl acetonate have been utilized to build this network in order to accelerate bond exchange, which will speed up relaxing at high temperatures [170]. Because it exhibits greater activity in thiol-acrylate systems and can aid in the facilitation of exchange and dynamic reactions in this type of chemistry, an allylic phosphate such as Miramer A99 is used in the synthesis of the network [167]. According to the findings of the aforementioned explanation of the chemistry of the manufactured vitrimeric network, the relaxation speed has greatly risen as catalyst concentration in the network has increased. Thus, in 102 min, this network has successfully lowered 63% of its initial stress [169]. Fig. 21d illustrates the print quality and capabilities of vitrimers created using 3D printing and having a size less than 50 μm. Additionally, the form memory property of this resin can be proven based on Fig. 21e. The boundaries between the two faults were seen to be welded at a temperature of 180 °C for a duration of 4 h during the self-healing test. Additionally, the findings show that 99% of the bar's strength is restored after restoration without any flaws, while the strain has barely changed (Fig. 21f) [168].

3.2.4. *Poly(acrylonitrile-butadiene-styrene)-based vitrimer*

Additionally, as part of the ongoing investigations, we have looked into the production of vitrimers from commercial plastics because doing so is an excellent way to cut waste [171–173]. In one of the studies, poly (acrylonitrile–butadiene–styrene) (ABS) has been changed into a recyclable [18,174,175] ABS-vitrimer with an adaptive dynamic covalent network that can be replicated using the FDM™ technique. Thus, to build a vitrimer network from recycled ABS, the associative imine exchange mechanism has been employed [55,71,176]. Another feature of this network's design is the inclusion of an exchange reaction with a high activation energy, which may benefit FDM™ printability under high heating [177]. Because this thermoplastic contains butadiene segments, its structure contains unsaturated bonds. By using cysteamine and thiol-ene "click" chemistry to functionalize butadiene segments, which was developed using this chemistry, and then reacting with a short-chain dialdehyde like glutaraldehyde, ABS-vitrimer is created [172]. The two monomers cysteamine and glutaraldehyde are not poisonous and are safe in this system, which is another intriguing aspect of it (Fig. 22a,b) [172].

ABS, Cysteamine, Azobisisobutyronitrile (AIBN), Glutaraldehyde, and Octylamine were the substances employed in this study [172]. First, ABS pellets were dissolved in THF solvent to create ABS-vitrimers. The

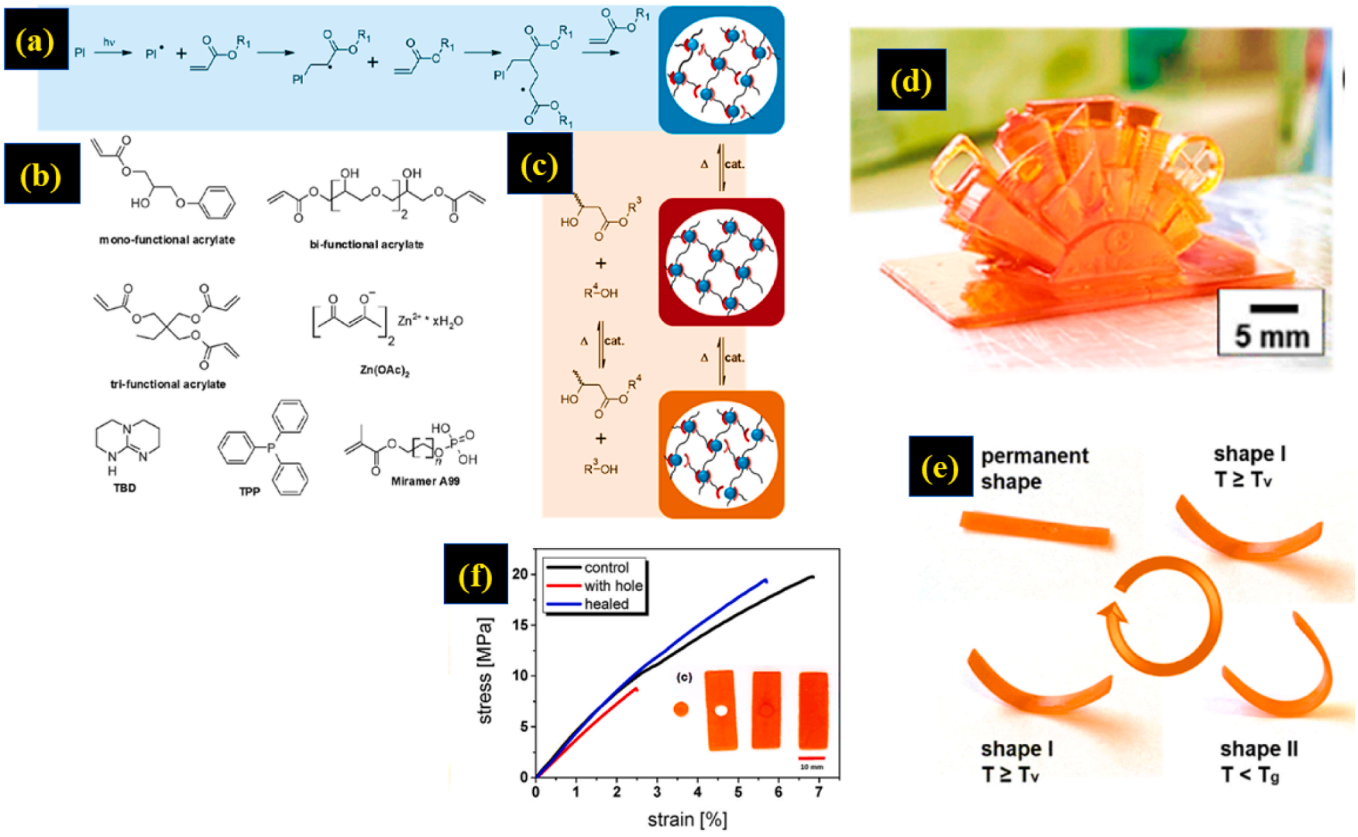

Fig. 21. (a) Schematic of photopolymerization mechanism, (b) Monomer and material's chemical structure used in vitrimer synthesis, (c) Schematic of exchange reaction of acrylate based vitrimer, (d) DLP printed acrylate based vitrimer, (e) Shape memory ability of acrylate based vitrimer, (f) Analysis of self-healing behavior of acrylate based vitrimer (Reproduced from [168] with permission of ELSEVIER).

structure was then expanded by adding butadiene components with amine groups via a thiol-ene reaction, and the reaction was maintained at 60 °C for 18 h with the addition of an AIBN thermal initiator. The combination was purified three times in ethanol after cooling and removing the solvent, and the precipitates were filtered and dried as the main product. Additionally, FDM™ printing is done with the Hyrel 3D System 30 M printer. In order to extrude the 1.75-mm polymer at the normal ABS extrusion temperature of 230 °C through a 0.5-mm hothead nozzle and deposit the polymer onto the hotbed stage, a dog-bone mold was employed [172]. Based on Fig. 22d, it is possible to verify that the manufactured vitrimers are capable of being reprocessed if the thermosets without dynamic bands do not exhibit this characteristic. Additionally, it has been noted based on Fig. 22c that the combination of these vitrimers made using Neat-ABS has also demonstrated reprintability [172].

3.2.5. *Polycaprolactone-urethane acrylate-based vitrimer*

Additionally, the notions of self-healing (SH) and shape memory (SM) in combination with the capacity for extensive crack healing have been revisited in subsequent investigations [178,179]. Here, semi-interpenetrating polymer network elastomers were created using 3D printed resins created from an ink containing urethane diacrylate and a linear semicrystalline polymer [180]. Thus, using the direct-ink-write (DIW) method, a highly stretchy semi-interpenetrating polymer network (semi-IPN) elastomer has ultimately been created [178]. Semicrystalline thermoplastic can have a dual role in this formulation, acting as both a switching phase for SM and a healer for SH behavior. The semi-IPN elastomer composite resin, also known as 3D printing ink, was created by mixing photocurable resin EBECRYL 8413, N-butyl acrylate (BA), with a mass ratio of 1/1.5 at 70 °C, polycaprolactone (PCL), with Mn = 70 000 to 90 000, and N-butyl acrylate. After that, 4 wt% of fumed SiO2 powder with 0.2–0.3 m particle size was added to the aforementioned resin. Then, phenylbis(2,4,6-trimethylbenzoyl)-phosphine oxide (Irgacure 819) was added as the photoinitiator at 1.5 wt% to the whole material after thorough mixing (Fig. 23) [180]. It should be noted that the syringe should be inserted on the 16th which moves solely in the z-direction and positioned on a screen in order to print DIW with this ink. Additionally, a nozzle with an inner diameter of 600 μm is attached to the end of the syringe in order to modify the diameter of the threads. A thermal component with a temperature about 70 °C was attached to the syringe, and ink was deposited at a pressure of 14 psi and a printing speed of 10 mm/s. The sample was exposed to UV radiation with approximately 50 mW/cm2 after printing one layer [180].

Fig. 24a–d shows the print quality and the resin's suitability for usage in additive manufacturing procedures. With the use of this photopolymer resin, geometric shapes like the Archimedean spiral, honeycomb, hollow vase, and Gumby toys may be printed off in one piece. The printed pieces are substantially stretched, which is another outcome of this resin, as seen in Fig. 24e, where the printed Archimedean spiral was stretched to more than 300% of strain. Another aspect of the printing of these sections is that, following the deposition, UV light connects the nearby filaments, increasing the adhesion between the layers [180]. Additionally, the usage of urethane frameworks that contain hydrogen bonds can aid in fortifying the interfacial bond. The elastomeric printed network has undergone significant stress and strain at room temperature due to the tiny PCL crystals' strong reinforcement phase performance [180]. The key point is that while there was initially some plastic deformation due to the crystals' presence, when the temperature rose over their melting point, the behavior changed to become

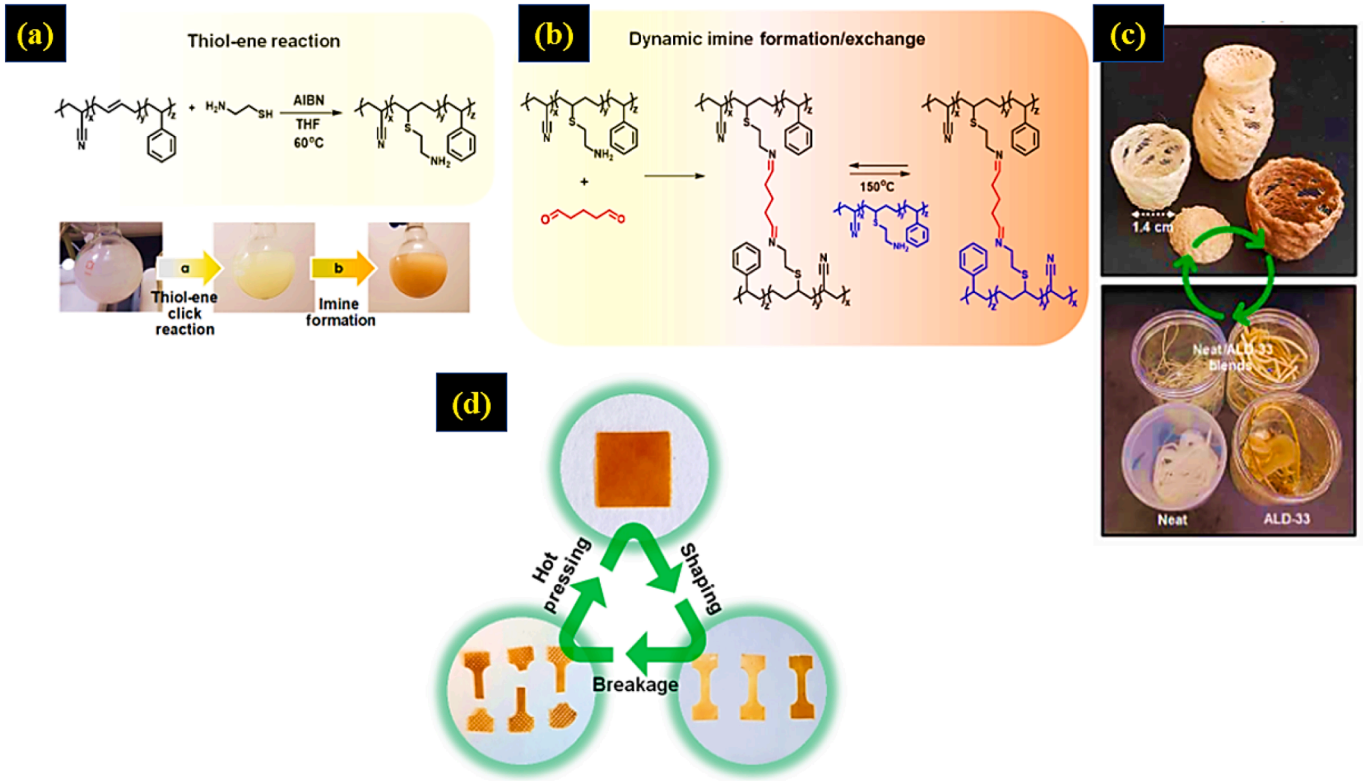

Fig. 22. (a) Thiol-ene click reaction mechanism of prepared ABS-vitrimer, (b) Mechanism of dynamic imine exchange of prepared ABS-vitrimer, (c) Reprinability of ABS-vitrimer mixed with pure ABS, (d) Reprocessability of prepared ABS-vitrimer (Reproduced from [172] under an open access Creative Commons license).

elastic, and after the crystals were removed, the sections displayed up to 400% strain [180]. The chip memory and chip recovery qualities for the printed parts based on Fig. 24g-o are also readily discernible based on the chemistry of the cured network. For further clarification, it should be noted that a 36 mm tall empty printed vase was heated before being flattened in a plate, resulting in the formation of a temporary shape with a 3 mm height (Fig. 24 g-k) [180]. The crystal will now melt at a specific temperature when the pot is heated and compacted, and the entropic elasticity of the elastomer will help the network regain its previous shape. It should be emphasized that other printed geometries also possess this property of memory shape, as demonstrated by the use of a heat gun to momentarily compress the honeycomb structure into a cylinder before allowing it to gradually revert to its original shape after around a minute [180]. To further highlight the highly malleable SM properties, the printed Gumby toy was twisted and stretched into a lengthy string as a temporary shape (Fig. 24 l-o). After being heated, the twisted string shape rolls, contracts, and then gradually takes on its original shape [180]. In addition to this characteristic, it has also been noted that these printed parts exhibit self-healing qualities, which come from the characteristics of chip memory (Fig. 24f). The figure indicates that the crack caused by cutting has been mended after heating without the addition of any foreign material for 50% of the breadth of the printed geometry of the virgin Archimedean spiral [180]. Following good contact between the fracture interfaces during the heating phase, which was aided by the SM action, the PCL chain diffusion and re-entanglement occurred. The small PCL crystals may act as “locks” over the interface to rebond the crack once they have cooled. In contrast to other healing techniques, this one does not use PCL as a healing agent, allowing you to keep on mending. Multiple healing is thus conceivable in this semi-IPN elastomer composite [180]. A summary of the results extracted from the studies of vitrimers based on the off the shelf materials is reported in Table 4.

4. Challenges and future perspective

3D printing is a very common technology today. With the rise of 4D printing technology, an innovative path for 3D printing formulation toward physical intelligence has been opened. However, there are other difficulties that have restricted the use of these methods for preparing various polymer compounds in the creation of 4D printing resins. These difficulties include the following:

- How to dissolve some polymers to prepare printing formulations
- How to create an efficient mechanism to create shape morphing properties in printed polymers
- How to create a reprocessable mechanism in polymer network for printed thermostats
- How to create a self-healing mechanism in polymer networks to prepare smart polymers

Research has employed a variety of approaches, including the utilization of nanoparticles, mechanical recycling of polymers, polymer mixing, change of surface characteristics, functionalization of polymers, and two other techniques. Vitrimerization provides a technological answer to these problems. Dynamic covalent bonds can be added with permanent covalent connections by utilizing the prevalent chemistry in vitrimers. So, capabilities like shape memory, reprocessing, self-healing, recyclability, and other smart and advanced features may be generated into the polymer network by activating these dynamic bands by a stimulus like temperature, heat, light, and other well-known stimuli. The breaking and re-forming of bonds are in competition after the induction of these properties due to the dynamic nature of the types of bonds in the network, and their control with a catalyst, temperature, light, and other factors can also maintain the product’s final properties.

Among all vitrimer categories, the usage of vat photopolymerization-based printing processes, such as DLP and SLA, has been more prevalent.

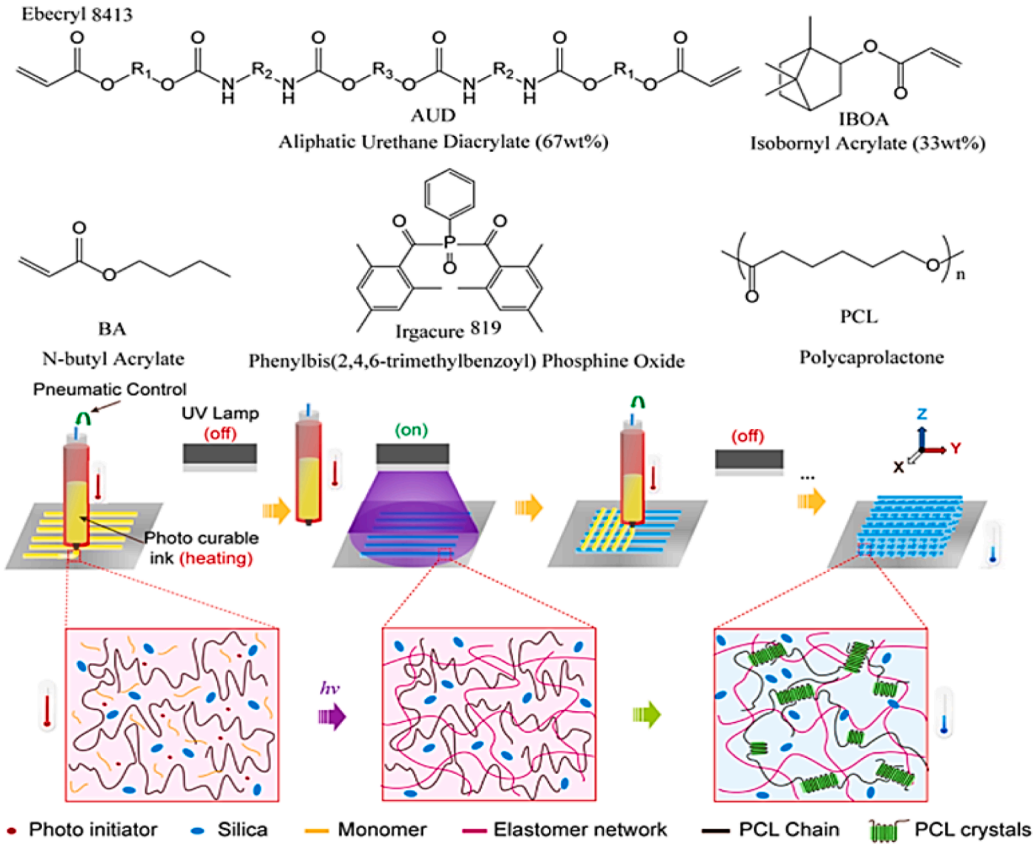

Fig. 23. Chemical structure of used monomers, oligomer, and other components for ink preparation and printing process (Reproduced from [180] with permission of American Chemical Society).

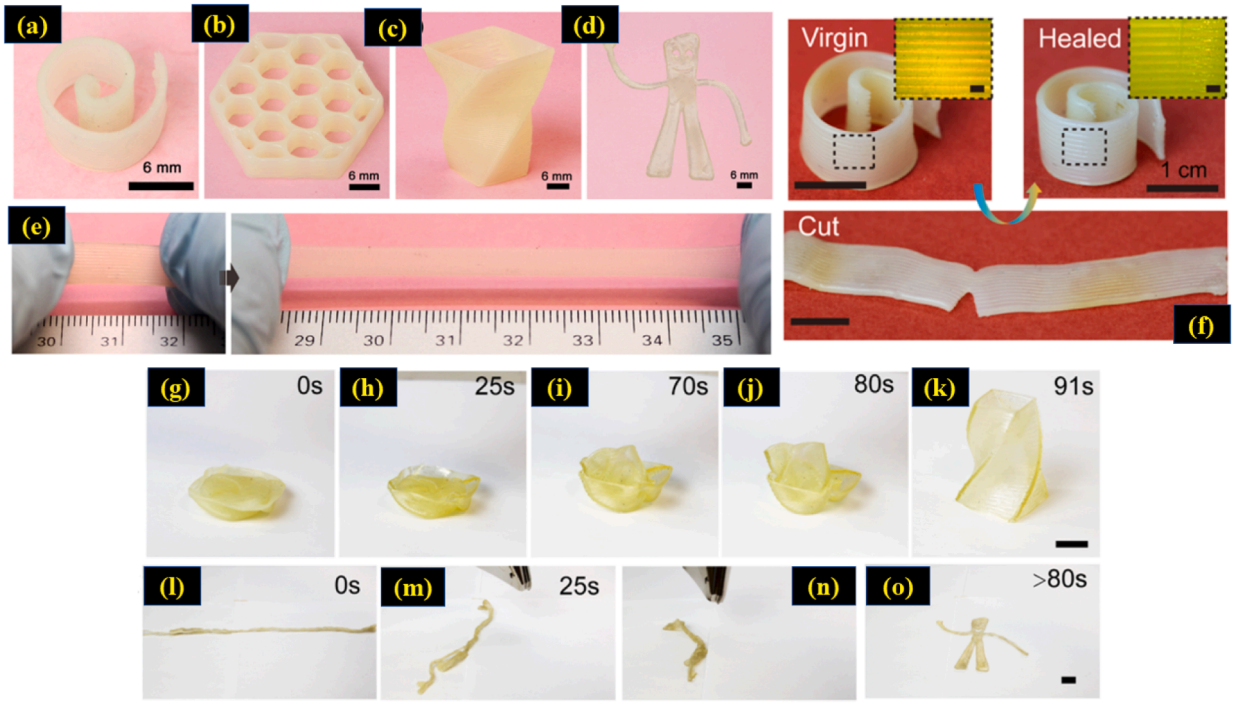

Fig. 24. 3D structures by DIW-based printing: (a) Archimedean spiral, (b) Honeycomb, (c) Hollow vase, (d) Gumby model, (e) Stretching a printed Archimedean spiral up to 300% strain, (f) Self-healing ability of printed Archimedean spiral structure, (g-k) Shape recovery of a compressed plate to its standing hollow vase original shape, (l-o) Long string recovers to its original shape of Gumby toy (Reproduced from [180] with permission of American Chemical Society).

Table 4
Summary of the studies and results from off the shelf materials-based vitrimer based 3D/4D printing formulations.

Category of vitrimer	Material	Type of Printing	Result	Application
Acrylate-Based [116]	HPPA, TPO, bisphenol A glycerolate monomer, $Zn(acac)_2$ [116]	DLP [116]	Reproducibly printed with good mechanical properties, Repairing properties, good printing ability [116]	3D/4D printing of structures with good mechanical properties, Repairing properties, good printing ability [116]
Acrylate-Based [160]	2-hydroxy-2-methylpropiophenone, 1,4-butanediol dimethacrylate, TPO, bisphenol A glycerolate dimethacrylate [160]	SLA [160]	High strength, stiffness, shape recovery ratio, recovery stress, and good recycleability, good printing ability, and reprocessing properties [160]	Multifunctional lightweight architectures [160]
Epoxy-Based [46]	DEGBA, thiol based curing agents, EDDET, Epikure 3253 [46]	DIW [46]	Self-healing and programmable shape [46]	Print flexible smart electronics (PFSE) [46]
Epoxy-Based [162]	aliphatic urethane diacrylate (Ebecryl 8402), BA, DGEBA, 2, 4, 6-tris-dimethylaminomethyl phenol, TPO [162].	DIW [162]	Shape memory, shape recovery ratio, cyclic stability and high shape constant ratio [162]	3D/4D printing of Composite structures [162]
Epoxy-Based [163]	EPS25 monomer, EDDET, PETMP, 4-DMAP, iron oxide micro-particles (Fe_3O_4) [163]		Magneto-responsive, Shape reconfiguration, increase in temperature and the activation of the bond exchange reaction, the flowability of the composite has also increased, magnetic gradient can induce dramatic and irreversible shape change, self-healing properties [163]	Design of remotely controllable soft robots, magnetically responsive soft composite [163]
Thiol-Based [168]	Trimethylolpropane triacrylate, Miramer A99, $Zn(acac)_2$, HPPA, GDGDA, Sudan II, BAPO, TPP, TBD [168]	DLP [164]	Quality of the print and the capabilities of the vitrimers prepared in 3D printing with a size below 50 μm, shape memory property, and repairing ability [168]	3D/4D printing of structures with facilitate exchange reaction [168]
Acrylonitrile Butadiene Styrene Terpolymer-Based [172]	ABS, Cysteamine, AIBN, glutaraldehyde, and octylamine [172]	FDM™ [172]	Reprocessing, reprintability, printing ability [172]	3D/4D printing of structures with Reprocessing, reprintability properties, thermoset recycling [172]
Polycaprolactone-Urethane Acrylate-Based [180]	AUD, isononyl acrylate, BA, PCL, Irgacure 819, fumed SiO_2 [180]	DIW [176]	self-healing, shape memory, highly stretchable, and good printing ability [180]	3D/4D printing of semi-IPN elastomer composite [180]

This can be due to the great speed and accuracy of these techniques, as well as other factors, such as the wide range of photoresists that can be applied in these processes. Furthermore, it can be inferred from the findings that using innovative vitrimerization chemistry confers advantageous features on the polymer network. In order to make this approach general, it is hoped that it will be used more frequently to prepare precious materials from polymer waste, thermosets, and thermoplastics.

5. Conclusion

In this review article, the types of chemistry of vitrimers for the design of vitrimerization reaction to introduce dynamic covalent bonds into the polymer network were presented. The latest research in the field of 4D printing with advanced properties such as shape memory, shape recovery, shape programming, high elasticity, recyclability, reprocessing, reprinting and other similar properties were discussed and reported in detail. After introducing the generalities of each research, the available formulations for synthesizing resins that can be used in various 3D printing techniques, such as FDM™, DLP, SLA, DIW, etc., were listed in detail. These mentioned recipes include the synthesis of oligomers, polymers, and modification of polymers. Besides, the descriptions on how to prepare 4D printing resins was introduced. At the end, the reported results with the desired properties and their relationship with Vitrimer chemistry was overviewed. By applying the formulations provided, it is expected that readers of this review article will be able to take a step toward the synthesis and manufacture of their desired formulation with specific properties to be used in various 3D/4D printing applications.

Declaration of Competing Interest

The authors declare that they have no known competing financial interests or personal relationships that could have appeared to influence the work reported in this paper.

Data availability

Data will be made available on request.

References

[1] R. Balu, N.K. Dutta, N.R. Choudhury, Plastic Waste Upcycling: A Sustainable Solution for Waste Management, Product Development, and Circular Economy, Polymers 14 (2022) 4788, https://doi.org/10.3390/polym14224788.
[2] Z.O.G. Schyns, M.P. Shaver, Mechanical Recycling of Packaging Plastics: A Review, Macromol. Rapid Commun. 42 (2021) 2000415, https://doi.org/10.1002/marc.202000415.
[3] J.A. Verschoor, H. Kusumawardhani, A.F. Ram, J.H. De Winde, Toward microbial recycling and upcycling of plastics: prospects and challenges, Front. Microbiol. 13 (2022), 821629, https://doi.org/10.3389/fmicb.2022.821629.
[4] M. La, F. Paolo, Polymer mechanical recycling: Downcycling or upcycling? Prog. Rubber Plast. Recycl. Technol. 20 (2004) 11–24, https://doi.org/10.1177/147776060402000102.
[5] S.C. Kosloski-Oh, Z.A. Wood, Y. Manjarrez, J.P.D.L. Rios, M.E. Fieser, Catalytic methods for chemical recycling or upcycling of commercial polymers, Mater. Horiz. 8 (2021) 1084–1129, https://doi.org/10.1039/d0mh01286f.
[6] X. Zhang, S. Xu, J. Tang, L. Fu, H. Karimi-Maleh, Sustainably Recycling and Upcycling of Single-Use Plastic Wastes through Heterogeneous Catalysis, Catalysts 12 (2022) 818, https://doi.org/10.3390/catal12080818.
[7] L. Yue, V.S. Bonab, D. Yuan, A. Patel, V. Karimkhani, I. Manas-Zloczower, Vitrimerization: A novel concept to reprocess and recycle thermoset waste via dynamic chemistry, Global Chall. 3 (2019) 1800076, https://doi.org/10.1002/gch2.201800076.
[8] P. Chakma, D. Konkolewicz, Dynamic covalent bonds in polymeric materials, Angew. Chem. Int. Ed. 58 (2019) 9682–9695, https://doi.org/10.1002/anie.201813525.
[9] S. Huang, X. Kong, Y. Xiang, X. Zhang, H. Chen, W. Jiang, Y. Niu, W. Xu, C. Ren, An overview of dynamic covalent bonds in polymer material and their applications, Eur. Polym. J. 141 (2020), 110094, https://doi.org/10.1016/j.eurpolymj.2020.110094.
[10] T. Maeda, H. Otsuka, A. Takahara, Dynamic covalent polymers: Reorganizable polymers with dynamic covalent bonds, Prog. Polym. Sci. 34 (2009) 581–604, https://doi.org/10.1016/j.progpolymsci.2009.03.001.
[11] R.T. Sanderson, Multiple and single bond energies in inorganic molecules, J. Inorg. Nucl. Chem. 30 (1968) 375–393, https://doi.org/10.1016/0022-1902(68)80464-6.
[12] J. Zheng, Z.M. Png, S.H. Ng, G.X. Tham, E.I. Ye, S.S. Goh, X.J. Loh, Z. Li, Vitrimers: Current research trends and their emerging applications, Mater. Today 51 (2021) 586–625, https://doi.org/10.1016/j.mattod.2021.07.003.

[13] C.N. Bowman, C.J. Kloxin, Covalent adaptable networks: reversible bond structures incorporated in polymer networks, Angew. Chem. Int. Ed. 18 (2012) 4272–4274, https://doi.org/10.1002/anie.201200708.

[14] C.J. Kloxin, T.F. Scott, B.J. Adzima, C.N. Bowman, Covalent adaptable networks (CANs): a unique paradigm in cross-linked polymers, Macromolecules 43 (2010) 2643–2653, https://doi.org/10.1021/ma902596s.

[15] W. Denissen, J.M. Winne, F.E. Du Prez, Vitrimers: permanent organic networks with glass-like fluidity, Chem. Sci. 7 (2016) 30–38, https://doi.org/10.1039/C5SC02223A.

[16] C.J. Kloxin, C.N. Bowman, Covalent adaptable networks: smart, reconfigurable and responsive network systems, Chem. Soc. Rev. 42 (2013) 7161–7173, https://doi.org/10.1039/C3CS60046G.

[17] G.M. Scheutz, J.J. Lessard, M.B. Sims, B.S. Sumerlin, Adaptable crosslinks in polymeric materials: resolving the intersection of thermoplastics and thermosets, J. Am. Chem. Soc. 141 (2019) 16181–16196, https://doi.org/10.1021/jacs.9b07922.

[18] D. Montarnal, M. Capelot, F. Tournilhac, L. Leibler, Silica-like malleable materials from permanent organic networks, Science 334 (2011) 965–968, https://doi.org/10.1126/science.1212648.

[19] T.D. Ngo, A. Kashani, G. Imbalzano, K.TQ. Nguyen, D. Hui, Additive manufacturing (3D printing): A review of materials, methods, applications and challenges, Compos. B Eng. 143 (2018) 172–196, https://doi.org/10.1016/j.compositesb.2018.02.012.

[20] J.V.G. González, M.I.S. Martínez, O.G.B. González, V.G. Ramos, A.K.G. Garza, M. G.F. Herrada, R.J.S. Aguilar, M.A.G. Ramírez, Multifunctional cube-like system for biomedical applications featuring 3D printing by dual deposition, scanner, and UV engraving, In Laser 3D Manufacturing. SPIE 10095 (2017) 78–81, https://doi.org/10.1117/12.2251588.

[21] P. Wu, J. Wang, X. Wang, A critical review of the use of 3-D printing in the construction industry, Autom. Constr. 68 (2016) 21–31, https://doi.org/10.1016/j.autcon.2016.04.005.

[22] B. Berman, 3-D printing: The new industrial revolution, Bus. Horiz. 55 (2012) 155–162, https://doi.org/10.1016/j.bushor.2011.11.003.

[23] J.W. Stansbury, M.J. Idacavage, 3D printing with polymers: Challenges among expanding options and opportunities, Dent. Mater. 32 (2016) 54–64, https://doi.org/10.1016/j.dental.2015.09.018.

[24] D. Raviv, W. Zhao, C. McKnelly, A. Papadopoulou, A. Kadambi, B. Shi, S. Hirsch, et al., Active printed materials for complex self-evolving deformations, Sci. Rep. 4 (2014) 1–8, https://doi.org/10.1038/srep07422.

[25] S. Tibbits, 4D printing: multi-material shape change, Archit. Des. 84 (2014) 116–121, https://doi.org/10.1002/ad.1710.

[26] F. Momeni, X. Liu, J. Ni, A review of 4D printing, Mater. Des. 122 (2017) 42–79, https://doi.org/10.1016/j.matdes.2017.02.068.

[27] S.K. Leist, J. Zhou, Current status of 4D printing technology and the potential of light-reactive smart materials as 4D printable materials, Virtual and Physical Prototyping 11 (4) (2016) 249–262, https://doi.org/10.1080/17452759.2016.1198630.

[28] G.A. Sydney, E.A. Matsumoto, R.G. Nuzzo, L. Mahadevan, J.A. Lewis, Biomimetic 4D printing.“, Nat. Mater. 15 (2016) 413–418, https://doi.org/10.1038/nmat4544.

[29] A. Subash, B. Kandasubramanian, 4D printing of shape memory polymers, Eur. Polym. J. (2020) 134 109771, https://doi.org/10.1016/j.eurpolymj.2020.109771.

[30] H. Wei, Q. Zhang, Y. Yao, L. Liu, Y. Liu, J. Leng, Direct-write fabrication of 4D active shape-changing structures based on a shape memory polymer and its nanocomposite, ACS Appl. Mater. Interfaces 9 (2017) 876–883, https://doi.org/10.1021/acsami.6b12824.

[31] J. Zhang, Z. Yin, L. Ren, Q. Liu, L. Ren, X. Yang, X. Zhou, Advances in 4D printed shape memory polymers: from 3D printing, smart excitation, and response to applications, Advanced Materials Technologies. 7 (2022) 2101568, https://doi.org/10.1002/admt.202101568.

[32] X. Wang, Y. He, Y. Liu, J. Leng, Advances in shape memory polymers: Remote actuation, multi-stimuli control, 4D printing and prospective applications, Mater. Sci. Eng. R. Rep. 151 (2022), 100702, https://doi.org/10.1016/j.mser.2022.100702.

[33] M.L. Williams, R.F. Landel, J.D. Ferry, The temperature dependence of relaxation mechanisms in amorphous polymers and other glassforming liquids, The Journal of the American Chemical Society. 77 (1995) 3701–3707, https://doi.org/10.1021/ja01619a008.

[34] Y. Nishimura, J. Chung, H. Muradyan, Z. Guan, Silyl ether as a robust and thermally stable dynamic covalent motif for malleable polymer design, J. Am. Chem. Soc. 139 (2017) 14881–14884, https://doi.org/10.1021/jacs.7b08826.

[35] M. Podgórski, B.D. Fairbanks, B.E. Kirkpatrick, M. McBride, A. Martinez, A. Dobson, N.J. Bongiardina, C.N. Bowman, Toward stimuli-responsive dynamic thermosets through continuous development and improvements in covalent adaptable networks (CANs), Adv. Mater. (2020) 32 1906876, https://doi.org/10.1002/adma.201906876.

[36] N. Sowan, H.B. Song, L.M. Cox, J.R. Patton, B.D. Fairbanks, Y. Ding, C. N. Bowman, Light-Activated Stress Relaxation, Toughness Improvement, and Photoinduced Reversal of Physical Aging in Glassy Polymer Networks, Adv. Mater. 33 (2021) 2007221, https://doi.org/10.1002/adma.202007221.

[37] T.F. Scott, A.D. Schneider, W.D. Cook, C.N. Bowman, Photoinduced plasticity in cross-linked polymers, Science 308 (2005) 1615–1617, https://doi.org/10.1126/science.1110505.

[38] J.F. Xu, Y.Z. Chen, L.Z. Wu, C.H. Tung, Q.Z. Yang, Dynamic covalent bond based on reversible photo [4+ 4] cycloaddition of anthracene for construction of double-dynamic polymers, Org. Lett. 15 (2013) 6148–6151, https://doi.org/10.1021/ol403015s.

[39] M. Abdallh, C. Yoshikawa, M.T. Hearn, G.P. Simon, K. Saito, Photoreversible smart polymers based on 2π+ 2π cycloaddition reactions: nanofilms to self-healing films, Macromolecules 52 (2019) 2446–2455, https://doi.org/10.1021/acs.macromol.8b01729.

[40] H. Frisch, D.E. Marschner, A.S. Goldmann, C.B. Kowollik, Wellenlängengesteuerte dynamische kovalente Chemie, Angew. Chem. 130 (2018) 2054–2064, https://doi.org/10.1002/anie.201709991.

[41] X. Qian, Q. Chen, Y. Yang, Y. Xu, Z. Li, Z. Wang, Y. Wu, Y. Wei, Y. Ji, Untethered recyclable tubular actuators with versatile locomotion for soft continuum robots, Adv. Mater. (2018) 30 1801103, https://doi.org/10.1002/adma.201801103.

[42] M.K. McBride, M. Hendrikx, D. Liu, B.T. Worrell, D.J. Broer, C.N. Bowman, Photoinduced Plasticity in Cross-Linked Liquid Crystalline Networks, Adv. Mater. 29 (2017) 1606509, https://doi.org/10.1002/adma.201606509.

[43] Y. Li, Y. Zhang, O. Rios, J.K. Keum, M.R. Kessler, Photo-responsive liquid crystalline epoxy networks with exchangeable disulfide bonds, RSC Adv. 7 (2017) 37248–37254, https://doi.org/10.1039/c7ra06343a.

[44] P.K. Shah, J.W. Stansbury, C.N. Bowman, Application of an addition–fragmentation-chain transfer monomer in di (meth) acrylate network formation to reduce polymerization shrinkage stress, Polym. Chem. 8 (2017) 4339–4351, https://doi.org/10.1039/C7PY00702G.

[45] B. T. Worrell, M. K. McBride, G. B. Lyon, L. M. Cox, C. Wang, S. Mavila, C. H. Lim et al, Bistable and photoswitchable states of matter, Nature communications. 2018, 9, 2804. https://doi.org/10.1038/s41467-018-05300-7.

[46] X. Kuang, Q. Mu, D.J. Roach, H.J. Qi, Shape-programmable and healable materials and devices using thermo-and photo-responsive vitrimer, Multifunctional Materials. 3 (2020), 045001, https://doi.org/10.1088/2399-7532/abbdc1.

[47] U. Haldar, K. Bauri, R. Li, R. Faust, P. De, Polyisobutylene-based pH-responsive self-healing polymeric gels, ACS Appl. Mater. Interfaces 7 (2015) 8779–8788, https://doi.org/10.1021/acsami.5b01272.

[48] C. Ding, M. Tian, R. Feng, Y. Dang, M. Zhang, Novel self-healing hydrogel with injectable, pH-responsive, strain-sensitive, promoting wound-healing, and hemostatic properties based on collagen and chitosan, ACS Biomater Sci. Eng. 6 (2020) 3855–3867, https://doi.org/10.1021/acsbiomaterials.0c00588.

[49] P. Zhang, F. Deng, Y. Peng, H. Chen, Y. Gao, H. Li, Redox-and pH-responsive polymer gels with reversible sol–gel transitions and self-healing properties, RSC Adv. 4 (2014) 47361–47367, https://doi.org/10.1039/C4RA08189G.

[50] Z. Guo, W. Ma, H. Gu, Y. Feng, Z. He, Q. Chen, X. Mao, J. Zhang, L. Zheng, pH-Switchable and self-healable hydrogels based on ketone type acylhydrazone dynamic covalent bonds, Soft Matter 13 (2017) 7371–7380, https://doi.org/10.1039/c7sm00916j.

[51] W. Denissen, J.M. Winne, F.E. Du Prez, Vitrimers: permanent organic networks with glass-like fluidity, Chem (2016) 30–38, https://doi.org/10.1039/c5sc02223a.

[52] M. Capelot, D. Montarnal, F. Tournilhac, L. Leibler, Metal-catalyzed transesterification for healing and assembling of thermosets, J. Am. Chem. Soc. 134 (2012) 7664–7667, https://doi.org/10.1021/ja302894k.

[53] M. Capelot, M.M. Unterlass, F. Tournilhac, L. Leibler, Catalytic control of the vitrimer glass transition, ACS Macro Lett. 1 (2012) 789–792, https://doi.org/10.1021/mz300239f.

[54] F.V. Lijsebetten, J.O. Holloway, J.M. Winne, F.E.D. Prez, Internal catalysis for dynamic covalent chemistry applications and polymer science, Chem. Soc. Rev. 49 (2020) 8425–8438, https://doi.org/10.1039/d0cs00452a.

[55] P. Taynton, H. Ni, C. Zhu, K. Yu, S. Loob, Y. Jin, H.J. Qi, W. Zhang, Repairable woven carbon fiber composites with full recyclability enabled by malleable polyimine networks, Adv. Mater. 28 (2016) 2904–2909, https://doi.org/10.1002/adma.201505245.

[56] C. He, S. Shi, D. Wang, B.A. Helms, T.P. Russell, Poly (oxime–ester) vitrimers with catalyst-free bond exchange, J. Am. Chem. Soc. 141 (2019) 13753–13757, https://doi.org/10.1021/jacs.9b06668.

[57] Y. Yang, Z. Pei, Z. Li, Y. Wei, Y. Ji, Making and remaking dynamic 3D structures by shining light on flat liquid crystalline vitrimer films without a mold, J. Am. Chem. Soc. 138 (2016) 2118–2121, https://doi.org/10.1021/jacs.5b12531.

[58] Z. Wang, Z. Li, Y. Wei, Y. Ji, Gold nanospheres dispersed light responsive epoxy vitrimers, Polymers 10 (2018) 65, https://doi.org/10.3390/polym10010065.

[59] Y. Yang, E. M. Terentjev, Y. Wei, Y. Ji, Solvent-assisted programming of flat polymer sheets into reconfigurable and self-healing 3D structures, Nature communications. 2018, 9, 1906. https://doi.org/10.1038/s41467-018-04257-x.

[60] J.M. Bolton, M.A. Hillmyer, T.R. Hoye, Sustainable thermoplastic elastomers from terpene-derived monomers, ACS Macro Lett. 3 (2014) 717–720, https://doi.org/10.1021/mz500269w.

[61] T. Liu, C. Hao, L. Wang, Y. Li, W. Liu, J. Xin, J. Zhang, Eugenol-derived biobased epoxy: shape memory, repairing, and recyclability, Macromolecules 50 (2017) 8588–8597, https://doi.org/10.1021/acs.macromol.7b01889.

[62] S. Zhang, T. Liu, C. Hao, L.I. Wang, J. Han, H. Liu, J. Zhang, Preparation of a lignin-based vitrimer material and its potential use for recoverable adhesives, Green Chem. 20 (2018) 2995–3000, https://doi.org/10.1039/c8gc01299g.

[63] F.I. Altuna, V. Pettarin, R.J.J. Williams, Self-healable polymer networks based on the cross-linking of epoxidised soybean oil by an aqueous citric acid solution, Green Chem. 15 (2013) 3360–3366, https://doi.org/10.1039/c3gc41384e.

[64] J. Wu, X. Yu, H. Zhang, J. Guo, J. Hu, M.H. Li, Fully biobased vitrimers from glycyrrhizic acid and soybean oil for self-healing, shape memory, weldable, and recyclable materials, ACS Sustain. Chem. Eng. 8 (2020) 6479–6487, https://doi.org/10.1021/acssuschemeng.0c01047.

[65] X. Yang, L. Guo, X. Xu, S. Shang, H. Liu, A fully bio-based epoxy vitrimer: Self-healing, triple-shape memory and reprocessing triggered by dynamic covalent bond exchange, Mater. Des. 186 (2020), 108248, https://doi.org/10.1016/j.matdes.2019.108248.

[66] J.P. Brutman, D.J. Fortman, G.X.D. Hoe, W.R. Dichtel, M.A. Hillmyer, Mechanistic study of stress relaxation in urethane-containing polymer networks, J. Phys. Chem. B 123 (2019) 1432–1441, https://doi.org/10.1021/acs.jpcb.8b11489.

[67] D. Zhang, H. Chen, Q. Dai, C. Xiang, Y. Li, X. Xiong, Y. Zhou, J. Zhang, Stimuli-Mild, Robust, Commercializable Polyurethane-Urea Vitrimer Elastomer via N, N′-Diaryl Urea Crosslinking, Macromol. Chem. Phys. 221 (2020) 1900564, https://doi.org/10.1002/macp.201900564.

[68] D.A. Bachmann, Ueber das Aldehydäthylchlorid und über das Verhalten von Acetalen zu Alkoholen in höherer Temperatur, Justus Liebigs Ann. Chem. 218 (1883) 38–56, https://doi.org/10.1002/jlac.18832180105.

[69] J.W. Hill, W.H. Carothers, Cyclic and Polymeric Formals1, J. Am. Chem. Soc. 57 (1935) 925–928, https://doi.org/10.1021/ja01308a045.

[70] Q. Li, S. Ma, S. Wang, W. Yuan, X. Xu, B. Wang, K. Huang, J. Zhu, Facile catalyst-free synthesis, exchanging, and hydrolysis of an acetal motif for dynamic covalent networks, J. Mater. Chem. A 7 (2019) 18039–18049, https://doi.org/10.1039/c9ta04073k.

[71] P. Taynton, K. Yu, R.K. Shoemaker, Y. Jin, H.J. Qi, W. Zhang, Heat-or water-driven malleability in a highly recyclable covalent network polymer, Adv. Mater. 26 (2014) 3938–3942, https://doi.org/10.1002/adma.201400317.

[72] W. Denissen, G. Rivero, R. Nicolaÿ, L. Leibler, J.M. Winne, F.E.D. Prez, Vinylogous urethane vitrimers, Adv. Funct. Mater. 25 (2015) 2451–2457, https://doi.org/10.1002/adfm.201404553.

[73] W. Denissen, M. Droesbeke, R. Nicolaÿ, L. Leibler, J.M. Winne, F.E.D. Prez, Chemical control of the viscoelastic properties of vinylogous urethane vitrimers, Nat. Commun. 8 (2017) 14857, https://doi.org/10.1038/ncomms14857.

[74] J.S.A. Ishibashi, J.A. Kalow, Vitrimeric silicone elastomers enabled by dynamic meldrum's acid-derived cross-links, ACS Macro Lett. 7 (2018) 482–486, https://doi.org/10.1021/acsmacrolett.8b00166.

[75] B.M.E.l. Zaatari, J.S.A. Ishibashi, J.A. Kalow, Cross-linker control of vitrimer flow, Polym. Chem. 11 (2020) 5339–5345, https://doi.org/10.1039/d0py00233j.

[76] M.M. Obadia, B.P. Mudraboyina, A. Serghei, D. Montarnal, E. Drockenmuller, Reprocessing and recycling of highly cross-linked ion-conducting networks through transalkylation exchanges of C-N bonds, J. Am. Chem. Soc. 137 (2015) 6078–6083, https://doi.org/10.1021/jacs.5b02653.

[77] J. Huang, L. Zhang, Z. Tang, S. Wu, B. Guo, Reprocessable and robust crosslinked elastomers via interfacial CN transalkylation of pyridinium, Compos. Sci. Technol. 168 (2018) 320–326, https://doi.org/10.1016/j.compscitech.2018.10.017.

[78] B. Hendriks, J. Waelkens, J.M. Winne, F.E.D. Prez, Poly (thioether) vitrimers via transalkylation of trialkylsulfonium salts, ACS Macro Lett. 6 (2017) 930–934, https://doi.org/10.1021/acsmacrolett.7b00494.

[79] Z. Tang, Y. Liu, Q. Huang, J. Zhao, B. Guo, L. Zhang, A real recycling loop of sulfur-cured rubber through transalkylation exchange of C-S bonds, Green Chem. 20 (2018) 5454–5458, https://doi.org/10.1039/c8gc02932f.

[80] O.R. Cromwell, J. Chung, Z. Guan, Malleable and self-healing covalent polymer networks through tunable dynamic boronic ester bonds, J. Am. Chem. Soc. 137 (2015) 6492–6495, https://doi.org/10.1021/jacs.5b03551.

[81] E. Zuckerkandl, L. Pauling, Evolutionary divergence and convergence in proteins, In Evolving genes and proteins. 1965, 97-166. https://doi.org/10.1126/science.aah5281.

[82] W.A. Ogden, Z. Guan, Recyclable, strong, and highly malleable thermosets based on boroxine networks, J. Am. Chem. Soc. 140 (2019) 6217–6220, https://doi.org/10.1021/jacs.8b03257.

[83] S. Delpierre, B. Willocq, G. Manini, V. Lemaur, J. Goole, P. Gerbaux, J. Cornil, P. Dubois, J.M. Raquez, Simple approach for a self-healable and stiff polymer network from iminoboronate-based boroxine chemistry, Chem. Mater. 31 (2019) 3736–3744, https://doi.org/10.1021/acs.chemmater.9b00750.

[84] Y. Yang, L. Huang, R. Wu, W. Fan, Q. Dai, J. He, C. Bai, Assembling of reprocessable polybutadiene-based vitrimers with high strength and shape memory via catalyst-free imine-coordinated boroxine, ACS applied materials & 12 (interfaces.2020,) 33305–33314, https://doi.org/10.1021/acsami.0c09712.

[85] C.A. Tretbar, J.A. Neal, Z. Guan, Direct silyl ether metathesis for vitrimers with exceptional thermal stability, J. Am. Chem. Soc. 141 (2019) 16595–16599, https://doi.org/10.1021/jacs.9b08876.

[86] S. Gao, Y. Liu, S. Feng, Z. Lu, Reprocessable and degradable thermoset with high T g cross-linked via Si–O–Ph bonds, J. Mater. Chem. A 7 (2019) 17498–17504, https://doi.org/10.1039/c9ta04951g.

[87] I. Azcune, I. Odriozola, Aromatic disulfide crosslinks in polymer systems: Self-healing, reprocessability, recyclability and more, Eur. Polym. J. 84 (2016) 147–160, https://doi.org/10.1016/j.eurpolymj.2016.09.023.

[88] S. Nevejans, N. Ballard, J.I. Miranda, B. Reck, J.M. Asua, The underlying mechanisms for self-healing of poly (disulfide) s, PCCP 18 (2016) 27577–27583, https://doi.org/10.1039/c6cp04028d.

[89] L. De, A. Ruiz, R. Martin, N. Markaide, A. Rekondo, G. Cabañero, J. Rodríguez, I. Odriozola, Epoxy resin with exchangeable disulfide crosslinks to obtain reprocessable, repairable and recyclable fiber-reinforced thermoset composites, Mater. Horiz. 3 (2016) 241–247, https://doi.org/10.1039/c6mh00029k.

[90] P. Yan, W. Zhao, B. Zhang, L. Jiang, S. Petcher, J.A. Smith, D.J. Parker, A. I. Cooper, J. Lei, T. Hasell, Inverse vulcanized polymers with shape memory, enhanced mechanical properties, and vitrimer behavior, Angew. Chem. Int. Ed. 59 (2020) 13371–13378, https://doi.org/10.1002/anie.202004311.

[91] A. Tsuruoka, A. Takahashi, D. Aoki, H. Otsuka, Fusion of different crosslinked polymers based on dynamic disulfide exchange, Angew. Chem. 132 (2020) 4324–4328, https://doi.org/10.1002/anie.201913430.

[92] F. Fan, S. Ji, C. Sun, C. Liu, Y. Yu, Y. Fu, H. Xu, Wavelength-controlled dynamic metathesis: a light-driven exchange reaction between disulfide and diselenide bonds, Angew. Chem. Int. Ed. 57 (2018) 16426–16430, https://doi.org/10.1002/anie.201810297.

[93] H. Gao, Y. Sun, M. Wang, Z. Wang, G. Han, L. Jin, P. Lin, Y. Xia, K. Zhang, Mechanically robust and reprocessable acrylate vitrimers with hydrogen-bond-integrated networks for photo-3D printing, ACS Appl. Mater. Interfaces 13 (2020) 1581–1591, https://doi.org/10.1021/acsami.0c19520.

[94] Q. Shi, K. Yu, X. Kuang, X. Mu, C.K. Dunn, M.L. Dunn, T. Wang, H.J. Qi, Recyclable 3D printing of vitrimer epoxy, Mater. Horiz. 4 (2017) 598–607, https://doi.org/10.1039/C7MH00043J.

[95] Y. Liu, Z. Tang, Y. Chen, C. Zhang, B. Guo, Engineering of β-hydroxyl esters into elastomer–nanoparticle interface toward malleable, robust, and reprocessable vitrimer composites, ACS Appl. Mater. Interfaces 10 (2018) 2992–3001, https://doi.org/10.1021/acsami.7b17465.

[96] X. Cao, H. Liu, X. Yang, J. Tian, B. Luo, M. Liu, Halloysite nanotubes@polydopamine reinforced polyacrylamide-gelatin hydrogels with NIR light triggered shape memory and self-healing capability, Compos. Sci. Technol. 191 (2020), 108071, https://doi.org/10.1016/j.compscitech.2020.108071.

[97] Z. Tang, Y. Liu, B. Guo, L. Zhang, Malleable, mechanically strong, and adaptive elastomers enabled by interfacial exchangeable bonds, Macromolecules 50 (2017) 7584–7592, https://doi.org/10.1021/acs.macromol.7b01261.

[98] M. Liu, Z. Jia, D. Jia, C. Zhou, Recent advance in research on halloysite nanotubes-polymer nanocomposite, Prog. Polym. Sci. 39 (2014) 1498–1525, https://doi.org/10.1016/j.progpolymsci.2014.04.004.

[99] Z. Tang, J. Huang, B. Guo, L. Zhang, F. Liu, Bioinspired engineering of sacrificial metal–ligand bonds into elastomers with supramechanical performance and adaptive recovery, Macromolecules 49 (2016) 1781–1789, https://doi.org/10.1021/acs.macromol.5b02756.

[100] N. Bitinis, M. Hernández, R. Verdejo, J.M. Kenny, M.A.L. Manchado, Recent advances in clay/polymer nanocomposites, Adv. Mater. 23, no. 5229–5236 (2011), https://doi.org/10.1002/adma.201101948.

[101] X. Zhou, B. Guo, L. Zhang, G.H. Hu, Progress in bio-inspired sacrificial bonds in artificial polymeric materials, Chem. Soc. Rev. 46 (2017) 6301–6329, https://doi.org/10.1039/C7CS00276A.

[102] J. Liu, S. Wang, Z. Tang, J. Huang, B. Guo, G. Huang, Bioinspired engineering of two different types of sacrificial bonds into chemically cross-linked cis-1, 4-polyisoprene toward a high-performance elastomer, Macromolecules 49 (2016) 8593–8604, https://doi.org/10.1021/acs.macromol.6b01576.

[103] E. Filippidi, T.R. Cristiani, C.D. Eisenbach, J.H. Waite, J.N. Israelachvili, B.K. Ahn, M.T. Valentine, Toughening elastomers using mussel-inspired iron-catechol complexes, Science 358 (2017) 502–505, https://doi.org/10.1126/science.aao0350.

[104] S. Seo, D.W. Lee, J.S. Ahn, K. Cunha, E. Filippidi, S.W. Ju, E. Shin, et al., Significant performance enhancement of polymer resins by bioinspired dynamic bonding, Adv. Mater. 29 (2017) 1703026, https://doi.org/10.1002/adma.201703026.

[105] J. Liu, C.S.Y. Tan, Z. Yu, Y. Lan, C. Abell, O.A. Scherman, Biomimetic supramolecular polymer networks exhibiting both toughness and self-recovery, Adv. Mater. 29 (2017) 1604951, https://doi.org/10.1002/adma.201604951.

[106] A. Liguori, S. Subramaniyan, J.G. Yao, M. Hakkarainen, Photocurable extended vanillin-based resin for mechanically and chemically recyclable, self-healable and digital light processing 3D printable thermosets, Eur. Polym. J. 178 (2022), 111489, https://doi.org/10.1016/j.eurpolymj.2022.111489.

[107] Y. Xu, K. Odelius, M. Hakkarainen, Photocurable, thermally reprocessable, and chemically recyclable vanillin-based imine thermosets, ACS Sustain. Chem. Eng. 8 (2020) 17272–17279, https://doi.org/10.1021/acssuschemeng.0c06248.

[108] J.F.I. Stanzione, J.M. Sadler, J.J.L. Scala, K.H. Reno, R.P. Wool, Vanillin-based resin for use in composite applications, Green Chem. 14 (2012) 2346–2352, https://doi.org/10.1039/C2GC35672D.

[109] S. Grauzeliene, M. Kastanauskas, V. Talacka, J. Ostrauskaite, Photocurable Glycerol-and Vanillin-Based Resins for the Synthesis of Vitrimers, ACS Applied Polymer Materials. 4 (2022) 6103–6110, https://doi.org/10.1021/acsapm.2c00914.

[110] S. Kasetaite, J. Ostrauskaite, V. Grazuleviciene, J. Svediene, D. Bridziuviene, Photocross-linking of glycerol diglycidyl ether with reactive diluents, Polym. Bull. 72 (2015) 3191–3208, https://doi.org/10.1007/s00289-015-1461-x.

[111] S. Kasetaite, J. Ostrauskaite, V. Grazuleviciene, D. Bridziuviene, E. Rainosalo, Biodegradable glycerol-based polymeric composites filled with industrial waste materials, J. Compos. Mater. 51 (2017) 4029–4039, https://doi.org/10.1177/00219983176978.

[112] S. Kasetaite, J. Ostrauskaite, V. Grazuleviciene, D. Bridziuviene, R. Budreckiene, E. Rainosalo, Biodegradable photocross-linked polymers of glycerol diglycidyl ether and structurally different alcohols, React. Funct. Polym. 122 (2018) 42–50, https://doi.org/10.1016/j.reactfunctpolym.2017.11.005.

[113] C. Zhang, M. Yan, E.W. Cochran, M.R. Kessler, Biorenewable polymers based on acrylated epoxidized soybean oil and methacrylated vanillin, Mater. Today Commun. 5 (2015) 18–22, https://doi.org/10.1016/j.mtcomm.2015.09.003.

[114] A. Navaruckiene, D. Bridziuviene, V. Raudoniene, E. Rainosalo, J. Ostrauskaite, Influence of vanillin acrylate-based resin composition on resin photocuring kinetics and antimicrobial properties of the resulting polymers, Materials. 14 (2021) 653, https://doi.org/10.3390/ma14030653.

[115] A. Navaruckiene, D. Bridziuviene, V. Raudoniene, E. Rainosalo, J. Ostrauskaite, Vanillin acrylate-based thermo-responsive shape memory antimicrobial photopolymers, Express Polym Lett 16 (2022) 279–295, https://doi.org/10.3144/expresspolymlett.2022.22.
[116] B. Zhang, K. Kowsari, A. Serjouei, M.L. Dunn, Q. Ge, Reprocessable thermosets for sustainable three-dimensional printing, Nat. Commun. 2018 (1831) 9, https://doi.org/10.1038/s41467-018-04292-8.
[117] X. Kuang, J. Wu, K. Chen, Z. Zhao, Z. Ding, F. Hu, D. Fang, H. J. Qi, Grayscale digital light processing 3D printing for highly functionally graded materials, Science advances. 2019, 5, eaav5790. 10.1126/sciadv. aav5790.
[118] T. Wu, P. Jiang, Z. Ji, Y. Guo, X. Wang, F. Zhou, W. Liu, 3D Printing of High-Performance Isocyanate Ester Thermosets, Macromol. Mater. Eng. 305 (2020) 2000397, https://doi.org/10.1002/mame.202000397.
[119] Z.X. Zhou, Y. Li, J. Zhong, Z. Luo, C.R. Gong, Y.Q. Zheng, S. Peng, L.M. Yu, L. Wu, Y. Xu, High-performance cyanate ester resins with interpenetration networks for 3D printing, ACS Appl. Mater. Interfaces 12 (2020) 38682–38689, https://doi.org/10.1021/acsami.0c10909.
[120] T.J. Wallin, L.E. Simonsen, W. Pan, K. Wang, E. Giannelis, R.F. Shepherd, Y. Mengüç, 3D printable tough silicone double networks, Nat. Commun. 11 (2020) 4000, https://doi.org/10.1038/s41467-020-17816-y.
[121] X. Kuang, Z. Zhao, K. Chen, D. Fang, G. Kang, H.J. Qi, High-speed 3D printing of high-performance thermosetting polymers via two-stage curing, Macromol. Rapid Commun. 39 (2018) 1700809, https://doi.org/10.1002/marc.201700809.
[122] Z. Chen, M. Yang, M. Ji, X. Kuang, H.J. Qi, T. Wang, Recyclable thermosetting polymers for digital light processing 3D printing, Mater. Des. 197 (2021), 109189, https://doi.org/10.1016/j.matdes.2020.109189.
[123] Z. Fang, Y. Shi, Y. Zhang, Q. Zhao, J. Wu, Reconfigurable polymer networks for digital light processing 3D printing, ACS Appl. Mater. Interfaces 13 (2021) 15584–15590, https://doi.org/10.1021/acsami.0c23107.
[124] M.T. Sabatini, L.T. Boulton, H.F. Sneddon, T.D. Sheppard, A green chemistry perspective on catalytic amide bond formation, Nat. Catal. 2 (2019) 10–17, https://doi.org/10.1038/s41929-018-0211-5.
[125] R. Baruah, A. Kumar, R.R. Ujjwal, S. Kedia, A. Ranjan, U. Ojha, Recyclable thermosets based on dynamic amidation and aza-michael addition chemistry, Macromolecules 49 (2016) 7814–7824, https://doi.org/10.1021/acs.macromol.6b01807.
[126] C.E. Hoyle, A.B. Lowe, C.N. Bowman, Thiol-click chemistry: a multifaceted toolbox for small molecule and polymer synthesis, Chem. Soc. Rev. 39 (2010) 1355–1387, https://doi.org/10.1039/B901979K.
[127] C. C. Cook, E. J. Fong, J. J. Schwartz, D. H. Porcincula, A. C. Kaczmarek, J. S. Oakdale, B. D. Moran et al, Additive Manufacturing: Highly Tunable Thiol-Ene Photoresins for Volumetric Additive Manufacturing (Adv. Mater. 47/2020), Advanced Materials. 2020, 32, 2070355. https://doi.org/10.1002/adma.202070355.
[128] Y. Huang, G. Ye, J. Yang, Synthesis and properties of UV-curable acrylate functionalized tung oil based resins via Diels-Alder reaction, Prog. Org. Coat. 78 (2015) 28–34, https://doi.org/10.1016/j.porgcoat.2014.10.011.
[129] D.M. Patil, G.A. Phalak, S.T. Mhakse, Boron-containing UV-curable oligomer-based linseed oil as flame-retardant coatings: Synthesis and characterization, Iran. Polym. J. 27 (2018) 795–806, https://doi.org/10.1007/s13726-018-0652-3.
[130] V.S.D. Voet, J. Guit, K. Loos, Sustainable photopolymers in 3D printing: a review on biobased, biodegradable, and recyclable alternatives, Macromol. Rapid Commun. 42 (2021) 2000475, https://doi.org/10.1002/marc.202000475.
[131] U. Biermann, U. Bornscheuer, M.A.R. Meier, J.O. Metzger, H.J. Schäfer, Oils and fats as renewable raw materials in chemistry, Angew. Chem. Int. Ed. 50 (2011) 3854–3871, https://doi.org/10.1002/anie.201002767.
[132] B.K. Ahn, J. Sung, N. Kim, S. Kraft, X.S. Sun, UV-curable pressure-sensitive adhesives derived from functionalized soybean oils and rosin ester, Polym. Int. 62 (2013) 1293–1301, https://doi.org/10.1002/pi.4420.
[133] E. Sharmin, F. Zafar, D. Akram, M. Alam, S. Ahmad, Recent advances in vegetable oils based environment friendly coatings: A review, Ind. Crop. Prod. 76 (2015) 215–229, https://doi.org/10.1016/j.indcrop.2015.06.022.
[134] J. Tang, J. Zhang, J. Lu, J. Huang, F. Zhang, Y. Hu, C. Liu, et al., Preparation and properties of plant-oil-based epoxy acrylate-like resins for UV-curable coatings, Polymers 12 (2020) 2165, https://doi.org/10.3390/polym12092165.
[135] S. Rengasamy, V. Mannari, Development of soy-based UV-curable acrylate oligomers and study of their film properties, Prog. Org. Coat. 76 (2013) 78–85, https://doi.org/10.1016/j.porgcoat.2012.08.012.
[136] J. Dai, X. Liu, S. Ma, J. Wang, X. Shen, S. You, J. Zhu, Soybean oil-based UV-curable coatings strengthened by crosslink agent derived from itaconic acid together with 2-hydroxyethyl methacrylate phosphate, Prog. Org. Coat. 97 (2016) 210–215, https://doi.org/10.1016/j.porgcoat.2016.04.014.
[137] B. C. Gross, J. L. Erkal, S. Y. Lockwood, C. Chen, D. M. Spence, Evaluation of 3D printing and its potential impact on biotechnology and the chemical sciences, 2014, 3240-3253. https://doi.org/10.1021/ac403397r.
[138] S.C.L. Auer, M. Schwentenwein, C. Gorsche, J. Stampfl, R. Liska, Toughening of photo-curable polymer networks: a review, Polym. Chem. 7 (2016) 257–286, https://doi.org/10.1039/C5PY01631B.
[139] A.B. Lowe, Thiol-ene "click" reactions and recent applications in polymer and materials synthesis, Polym. Chem. 1 (2010) 17–36, https://doi.org/10.1039/B9PY00216B.
[140] O. Türünç, M.A.R. Meier, The thiol-ene (click) reaction for the synthesis of plant oil derived polymers, Eur. J. Lipid Sci. Technol. 115 (2013) 41–54, https://doi.org/10.1002/ejlt.201200148.
[141] U. Shaukat, B. Sölle, E. Rossegger, S. Rana, S. Schlögl, Vat Photopolymerization 3D-Printing of Dynamic Thiol-Acrylate Photopolymers Using Bio-Derived Building Blocks, Polymers 14 (2022) 5377, https://doi.org/10.3390/polym14245377.
[142] W. Niu, Z. Zhang, Q. Chen, P.F. Cao, R.C. Advincula, Highly recyclable, mechanically isotropic and healable 3D-printed elastomers via polyurea vitrimers, ACS Materials Letters. 3 (2021) 1095–1103, https://doi.org/10.1021/acsmaterialslett.1c00132.
[143] J.J. Lessard, L.F. Garcia, C.P. Easterling, M.B. Sims, K.C. Bentz, S. Arencibia, D. A. Savin, B.S. Sumerlin, Catalyst-free vitrimers from vinyl polymers, Macromolecules 52 (2019) 2105–2111, https://doi.org/10.1021/acs.macromol.8b02477.
[144] W. Denissen, I.D. Baere, W.V. Paepegem, L. Leibler, J. Winne, F.E.D. Prez, Vinylogous urea vitrimers and their application in fiber reinforced composites, Macromolecules 51 (2018) 2054–2064, https://doi.org/10.1021/acs.macromol.7b02407.
[145] B.E. Kelly, I. Bhattacharya, H. Heidari, M. Shusteff, C.M. Spadaccini, H.K. Taylor, Volumetric additive manufacturing via tomographic reconstruction, Science 363 (2019) 1075–1079, https://doi.org/10.1126/science.aau7114.
[146] H. Wang, C. He, H. Luo, W. Huang, Z. Yang, X. Chen, J. He, Method for 3D printing of polymer in condensed state, China Patent Application. 24 (2019), https://doi.org/10.3390/polym12102330.
[147] L. Lei, L. Han, H. Ma, R. Zhang, X. Li, S. Zhang, C. Li, H. Bai, Y. Li, Well-Tailored Dynamic Liquid Crystal Networks with Anionically Polymerized Styrene-Butadiene Rubbers toward Modulating Shape Memory and Self-Healing Capacity, Macromolecules 54 (2021) 2691–2702, https://doi.org/10.1021/acs.macromol.0c02741.
[148] J. Choi, S. Kim, J. Yoo, S.H. Choi, K. Char, Self-healable antifreeze hydrogel based on dense quadruple hydrogen bonding, Macromolecules 54 (2021) 6389–6399, https://doi.org/10.1021/acs.macromol.1c00295.
[149] X. Li, J. Li, W. Wei, F. Yang, M. Wu, Q. Wu, T. Xie, Y. Chen, Enhanced mechanochemiluminescence from end-functionalized polyurethanes with multiple hydrogen bonds, Macromolecules 54 (2021) 1557–1563, https://doi.org/10.1021/acs.macromol.0c02622.
[150] B.A.G. Lamers, J.J.B.V.D. Tol, K.M. Vonk, B.F.M.D. Waal, A.R.A. Palmans, E. W. Meijer, G. Vantomme, Consequences of Molecular Architecture on the Supramolecular Assembly of Discrete Block Co-oligomers, Macromolecules 53 (2020) 10289–10298, https://doi.org/10.1021/acs.macromol.0c02237.
[151] J. Scavuzzo, S. Tomita, S.h. Cheng, H. Liu, M. Gao, J.P. Kennedy, S. Sakurai, S.Z. D. Cheng, L. Jia, Supramolecular elastomers: self-assembling star–blocks of soft polyisobutylene and hard oligo (β-alanine) segments, Macromolecules 48 (2015) 1077–1086, https://doi.org/10.1021/ma502322n.
[152] A. Gasperini, G.J.N. Wang, F.M. Lopez, H.C. Wu, J. Lopez, J. Xu, S. Luo, et al., Characterization of hydrogen bonding formation and breaking in semiconducting polymers under mechanical strain, Macromolecules 52 (2019) 2476–2486, https://doi.org/10.1021/acs.macromol.9b00145.
[153] K. Cao, G. Liu, Low-molecular-weight, high-mechanical-strength, and solution-processable telechelic poly (ether imide) end-capped with ureidopyrimidinone, Macromolecules 50 (2017) 2016–2023, https://doi.org/10.1021/acs.macromol.7b00156.
[154] J. Chen, Y. Wen, L. Zeng, X. Wang, H. Chen, W.M. Huang, Y. Bai, W. Yu, K. Zhao, P. Hu, Room-Temperature Solid-State UV Cross-Linkable Vitrimer-like Polymers for Additive Manufacturing, Polymers 14 (2022) 2203, https://doi.org/10.3390/polym14112203.
[155] J. Joe, J. Shin, Y.S. Choi, J.H. Hwang, S.H. Kim, J. Han, B. Park, et al., A 4D Printable Shape Memory Vitrimer with Repairability and Recyclability through Network Architecture Tailoring from Commercial Poly (ε-caprolactone), Adv. Sci. 8 (2021) 2103682, https://doi.org/10.1002/advs.202103682.
[156] Z. Jiao, B. Luo, S. Xiang, H. Ma, Y. Yu, W. Yang, 3D printing of HA/PCL composite tissue engineering scaffolds, Adv Ind Eng Polym Res. 2 (2019) 196–202, https://doi.org/10.3390/polym14245460.
[157] Z. Meng, J. He, Z. Cai, F. Wang, J. Zhang, L. Wang, R. Ling, D. Li, Design and additive manufacturing of flexible polycaprolactone scaffolds with highly-tunable mechanical properties for soft tissue engineering, Mater. Des. 189 (2020), 108508, https://doi.org/10.1016/j.matdes.2020.108508.
[158] Y. Zhou, J.G.P. Goossens, R.P. Sijbesma, J.P.A. Heuts, Poly (butylene terephthalate)/glycerol-based vitrimers via solid-state polymerization, Macromolecules 50 (2017) 6742–6751, https://doi.org/10.1021/acs.macromol.7b01142.
[159] X. Li, Y. Yang, Y. Zhang, T. Wang, Z. Yang, Q. Wang, X. Zhang, Dual-method molding of 4D shape memory polyimide ink, Mater. Des. 191 (2020), 108606, https://doi.org/10.1016/j.matdes.2020.108606.
[160] A. Li, A. Challapalli, G. Li, 4D printing of recyclable lightweight architectures using high recovery stress shape memory polymer, Scientific reports. 2019, 9, 1-13. | https://doi.org/10.1038/s41598-019-44110-9.
[161] J. Deng, X. Kuang, R. Liu, W. Ding, A.C. Wang, Y.C. Lai, K. Dong, et al., Vitrimer elastomer-based jigsaw puzzle-like healable triboelectric nanogenerator for self-powered wearable electronics, Adv. Mater. 30 (2018) 1705918, https://doi.org/10.1002/adma.201705918.
[162] K. Chen, X. Kuang, V. Li, G. Kang, H.J. Qi, Fabrication of tough epoxy with shape memory effects by UV-assisted direct-ink write printing, Soft Matter 14 (2018) 1879–1886, https://doi.org/10.1039/C7SM02362F.
[163] G. Dong, Q. He, S. Cai, Magnetic vitrimer-based soft robotics, Soft Matter 18 (2022) 7604–7611, https://doi.org/10.1039/D2SM00893A.
[164] J. Canadell, H. Goossens, B. Klumperman, Self-healing materials based on disulfide links, Macromolecules 44 (2011) 2536–2541, https://doi.org/10.1021/ma2001492.

[165] Z. Song, Z. Wang, S. Cai, Mechanics of vitrimer with hybrid networks, Mech. Mater. 153 (2021), 103687, https://doi.org/10.1016/j.mechmat.2020.103687.
[166] M. Zhang, F. Zhao, W. Xin, Y. Luo, Room-Temperature Self-Healing and Reprocessable Waterborne Polyurethane with Dynamically Exchangeable Disulfide Bonds, ChemistrySelect 5 (2020) 4608–4618, https://doi.org/10.1002/slct.201904316.
[167] E. Rossegger, R. Höller, D. Reisinger, J. Strasser, M. Fleisch, T. Griesser, S. Schlögl, Digital light processing 3D printing with thiol–acrylate vitrimers, Polym. Chem. 12 (2021) 639–644, https://doi.org/10.1039/D0PY01520B.
[168] E. Rossegger, R. Höller, D. Reisinger, M. Fleisch, J. Strasser, V. Wieser, T. Griesser, S. Schlögl, High resolution additive manufacturing with acrylate based vitrimers using organic phosphates as transesterification catalyst, Polymer 221 (2021), 123631, https://doi.org/10.1016/j.polymer.2021.123631.
[169] M. Hayashi, R. Yano, Fair investigation of cross-link density effects on the bond-exchange properties for trans-esterification-based vitrimers with identical concentrations of reactive groups, Macromolecules 53 (2019) 182–189, https://doi.org/10.1021/acs.macromol.9b01896.
[170] W. Alabiso, S. Schlögl, The impact of vitrimers on the industry of the future: Chemistry, properties and sustainable forward-looking applications, Polymers 12 (2020) 1660, https://doi.org/10.3390/polym12081660.
[171] T.J.L. Korley, T.H. Epps III, B.A. Helms, A.J. Ryan, Toward polymer upcycling—adding value and tackling circularity, Science 373 (2021) 66–69, https://doi.org/10.1126/science.abg4503.
[172] S. Kim, M.A. Rahman, M.d. Arifuzzaman, D.B. Gilmer, B. Li, J.K. Wilt, E.L. Curzio, T. Saito, Closed-loop additive manufacturing of upcycled commodity plastic through dynamic cross-linking, Science, Advances 8 (2022) eabn6006, https://doi.org/10.1126/sciadv.abn6006.
[173] A. Rahimi, J.M. García, Chemical recycling of waste plastics for new materials production, Nat. Rev. Chem. 1 (2017) 0046, https://doi.org/10.1038/s41570-017-0046.
[174] M. Röttger, T. Domenech, R.V.D. Weegen, A. Breuillac, R. Nicolaÿ, L. Leibler, High-performance vitrimers from commodity thermoplastics through dioxaborolane metathesis, Science 356 (2017) 62–65, https://doi.org/10.1126/science.aah5281.
[175] N.J.V. Zee, R. Nicolaÿ, Vitrimers: Permanently crosslinked polymers with dynamic network topology, Prog. Polym. Sci. 104 (2020), 101233, https://doi.org/10.1016/j.progpolymsci.2020.101233.
[176] S. Dhers, G. Vantomme, L. Avérous, A fully bio-based polyimine vitrimer derived from fructose, Green Chem. 21 (2019) 1596–1601, https://doi.org/10.1039/C9GC00540D.
[177] B.R. Elling, W.R. Dichtel, Reprocessable cross-linked polymer networks: are associative exchange mechanisms desirable? ACS Cent. Sci. 6 (2020) 1488–1496, https://doi.org/10.1021/acscentsci.0c00567.
[178] E.D. Rodriguez, X. Luo, P.T. Mather, Linear/network poly (ε-caprolactone) blends exhibiting shape memory assisted self-healing (SMASH), ACS Appl. Mater. Interfaces 3 (2011) 152–161, https://doi.org/10.1021/am101012c.
[179] X. Luo, P.T. Mather, Shape memory assisted self-healing coating, ACS Macro Lett. 2 (2013) 152–156, https://doi.org/10.1021/mz400017x.
[180] X. Kuang, K. Chen, C.K. Dunn, J. Wu, V.C.F. Li, H.J. Qi, 3D printing of highly stretchable, shape-memory, and self-healing elastomer toward novel 4D printing, ACS Appl. Mater. Interfaces 10 (2018) 7381–7388, https://doi.org/10.1021/acsami.7b18265.